AN INVESTIGATION INTO IN SITU BIODEGRADTION UNDER SULPHATE-REDUCING CONDITIONS IN A PETROLEUM CONTAMINATED SHALLOW AQUIFER

A Dissertation Presented to The Academic Faculty

By

Dean William McCormick
BSc (Hons) Environmental and Geographical Science,
University of Cape Town

Submitted in Partial Fulfilment of the requirements for the degree of
Master of Science in Environmental Geochemistry

Department of Geological Sciences

DEDICATION

This thesis is dedicated to the memory of Beresford Reader and Charles McCormick

ABSTRACT

The accidental contamination of shallow aquifers as a result of leaking underground storage tanks is common and poses serious environmental problems. Because of their toxicity and relative solubility, the benzene, toluene, ethylbenzene, and xylene (BTEX) components of petroleum products are of particular concern. For this reason mechanisms that assist in removing BTEX from contaminated environments have been the focus of numerous studies.

The stimulation of microbial growth is a relatively nonobtrusive and cost effective strategy for the natural attenuation of petroleum contaminated sites. Previous studies have shown that BTEX compounds are able to degrade when coupled to SO_4^{2-} reduction.

In this study tracer experiments conducted on sediment samples extracted from a petroleum contaminated shallow sandy aquifer, showed that relative to *in situ* rates, sulphate reduction rates (SRR's) increased upon addition of varying concentrations of sulphate added under laboratory conditions,. These experiments were also useful in confirming that the availability of SO_4^{2-} as a terminal electron acceptor was limiting SRR's. Moreover, via Monod kinetics, calculated half saturation constants predicted sulphate concentrations to optimise microbial growth rates and hence sulphate reduction rates.

Sulphide amendment experiments showed inhibition to the SRR, relative to the *in situ* rates. However, iron and sulphate incubation experiments conducted over a 72-hour period hinted that iron sulphide precipitation was more than likely buffering the system against the toxic effects of elevated sulphide concentrations.

Based on these findings it is postulated that SO_4^{2-} additions could act as an effective strategy in removing BTEX from the petroleum contaminated aquifer.

ACKNOWLEDGEMENTS

The author would sincerely like to thank the following people for their contributions and support to this thesis:

Dr Alakendra Roychoudhury for his patience, assistance and advice throughout this project

Professor Anton le Roux for his understanding during difficult periods

Patrick Sieas for his assistance in the lab

Ross Holland his time spent assisting with sampling in the field

Andrew Kerr for also willingly helping with sampling as well as for the graphics

Paul Aucamp for allowing me access to equipment and data

My friends and family for their encouragement and support during an extremely testing and difficult year

TABLE OF CONTENTS

LIST OF TABLES

LIST OF FIGURES

ABBREVIATIONS

BTEX	Benzene, toluene, ethylbenzene, xylene isomers
SRB	Sulphate reducing bacteria
SRR	Sulphate reduction rate
TEA	Terminal electron acceptor

CHAPTER 1 – INTRODUCTION

1.1 Introduction

Contamination of soil, sediment and groundwater systems with petroleum via leaks in underground storage tanks, improper disposal techniques or inadvertent spills are widespread and frequently reported. Petroleum fuels are crude distillates, which in addition to many other hydrocarbon constituents, contains benzene, toluene, ethyl benzene and xylene isomers (BTEX). These are chemicals of environmental concern as they are relatively soluble, toxic, carcinogenic, and are reported to be very mobile in the environment (Loveley, 1997; Johnson *et al.*, 2003; Villatoro-Monzón *et al.*, 2003). As a result, there is substantial interest in the mechanisms designed to remove BTEX from contaminated environments.

The emergence of intrinsic (or natural) bioremediation as a strategy for reducing the concentration of contaminants in subsurface environments has, in the last two decades, been well documented. Remediation via natural attenuation is seen as a nonobtrusive and cost-effective solution for reducing the concentration of contaminants in subsurface environments. During the attenuation process intramolecular bonds of organic molecules tend to break, resulting in the alteration of toxicity and transport properties of these compounds (Madsen, 1991). Under aerobic conditions, microbes facilitate the oxidation of energy rich hydrocarbons to carbon dioxide and water or other innocuous end products, using molecular oxygen as the terminal electron acceptor (TEA; Englert *et al.*, 1993). In subsurface environments, where oxygen supply is either absent or limited, alternative TEA's are sought. The sequence of alternative TEA's used for biodegradation is governed by availability and thermodynamic principles (Stumm and Morgan, 1996). Under anoxic conditions, the theoretical sequence is denitrification, followed by manganese reduction, iron reduction, sulphate reduction, and methanogenesis. Although the use of TEA's tends to be sequential, simultaneous usage can occur (Ward *et al.,* 1995).

Generally speaking the depletion of terminal electron acceptors is considered to be the primary factor that limits the rate of *in situ* BTEX biodegradation (Godsey *et al.*, 2004). Enhanced intrinsic bioremediation is technology that aims to stimulate contaminant degradation by supplementing subsurface microbial populations with nutrients and/or electron acceptors that may be limiting.

Traditional *in situ* treatment schemes for BTEX contaminated plumes involve the injection of oxygen as the terminal electron acceptor. Following oxygen enrichment, BTEX degradation is known to proceed rapidly (Edwards *et al.*, 1992). However the limitations of this technology, termed air sparging, is that oxygen consumption tends to be rapid, and the rate of recharge is generally slow due to the low solubility of oxygen in groundwater (Brown *et al.*, 1994). Recent laboratory findings have concluded that electron acceptors that are highly water-soluble could replace oxygen in the anaerobic degradation of BTEX compounds.

Given that nitrate is highly water soluble, has low sorbtion, a high electron-accepting capacity for its mass, and is non toxic to micro organisms it could potentially be used as an additive to enhance intrinsic bioremediation (Ward *et al.*, 1995) Indeed, field and laboratory studies have demonstrated the complete mineralisation of toluene, ethylbenzene and xylene isomers with nitrate acting as the TEA (Barbaro *et al.*, 1992; Anid *et al.*, 1993). However, an important drawback to nitrate addition is that it is expensive and toxic to humans (Ward *et al.,* 1995). Additionally, nitrate is not naturally abundant, thus in many aquifers, microbial populations may not be adapted to utilizing nitrate as a TEA.

Iron (III) in the form of insoluble, amorphous iron oxides, is both widespread and common to aquifer environments (Anderson *et al.*, 1998). Benzene and toluene degradation has been reported following the addition of Fe (III) chelated to nitrilotriacetic acid, however this has only been explored at the bench-scale level (Lovley *et al.*, 1994). Furthermore, Fe (III) salts are only slightly soluble and for its mass have a relatively low electron accepting capacity. An advantage to Fe (III) is that its reduced form (Fe II) is non toxic, particularly at levels that would be expected during bioremediation (Ward *et al.,* 1995).

Sulphate has the potential to serve as an excellent additive to expedite the breakdown of BTEX compounds. It is highly water-soluble, has a high electron-accepting capacity for its mass, and does not sorb appreciably. Furthermore, relative to nitrate, it is inexpensive and is non-toxic to microorganisms. It is also found in abundance, either dissolved in groundwater, or as mineral forms including barium sulphate and gypsum. Moreover, stoichiometric relationships to BTEX compounds make it highly effective in mineralising BTEX hydrocarbons. However, the toxic effects to both microorganisms and humans, caused by high sulphide concentration, the end product of sulphate reduction, have likely

contributed to a lack of interest in sulphate as a viable alternative TEA (Ward *et al.*, 1995).

1.2 Aims and objectives

Preliminary results from a petroleum contaminated shallow sandy aquifer in Kuils River, Western Cape, South Africa, indicate that sulphate and iron reduction are the dominant pathways for *in situ* mineralization of aromatic hydrocarbons (Roychoudhury and Merrett, in review). Furthermore incubation experiments conducted with contaminated aquifer sediments and inherent microbial assemblages, predict that BTEX oxidation is primarily occurring in winter and is coupled to sulphate reduction.

With this in mind, the main objective of this study was to assess the capacity of sulphate addition to act as an effective strategy in removing BTEX hydrocarbons from the contaminated aquifer.

Specifically this study will:

(1) Investigate the groundwater chemistry of the contaminant plume.
(2) Assess the impact of substrate addition on *in situ* biodegradation rates
(3) Quantify Monod kinetic parameters in order to understand the factors that control sulphate reduction
(4) Assess the toxicity effect of sulphide on the rates of sulphate reduction

1.3 Study area

1.3.1 Site location

The study site is situated in the town of Kuils River, a densely populated urban and industrial area located 23 km East North East of Cape Town, South Africa (Figure 1.1). The site overlies the extensively developed Cape Flats Aquifer near the coast in the Western Cape region.

1.3.2 Climate

The Western Cape, incorporating the Cape Peninsula and adjoining districts, experiences a typical Mediterranean climate with hot dry summers followed by cold winter months during which the majority of the rainfall occurs (SAWB, 1996). Highly localised microclimates exist due to the influence of geographical and topographical features. The average annual rainfall expected for the study site and its surrounds is approximately 600mm (SAWB, 1996).

The mean temperature fluctuates between 13 °C in winter and 21 °C in summer. This is in contrast to the diurnal and annual temperature means of inland areas, which vary from 2.2 °C in winter to 30.5 °C in summer (SAWB, 1996).

The prevailing winter winds alternate from the north and south, whereas in summer the winds prevail from the south and south-east (SAWB, 1996).

1.3.3 Geology and soils

The oldest geological formations in the vicinity of the area belong to the Malmesbury Group (Theron, 1992; Figure 1.1). The Malmesbury Group consists of low-grade metamorphic rocks such as phyllitic shale, quartz, and sericitic schist, siltstone, sandstone and greywacke (Meyer, 2001). Intruded into the Malmesbury Group throughout the south-western Cape are numerous plutons of the Cape Granite Suite (~540 Ma in age), of which the Cape Peninsula pluton is a significant number (Reid *et al.,* 1998). The Cape Granite and the Malmesbury Group meta-sedimentary rocks are unconformably overlain by the quartzites of the Table Mountain Group. The almost horizontal sandstones of the Peninsula Formation

have been linked to the same formation capping the Hottentots Holland Mountains on the eastern fringe of the Cape Flats (Reid *et al.,* 1998). This is an area of low topography, which separates the Peninsula from inland hills and was formed following post-Palaeozoic erosion of sandstones of the Table Mountain Group between False Bay and Table Bay (Reid *et al.,* 1998; Harris *et al.,* 1999)

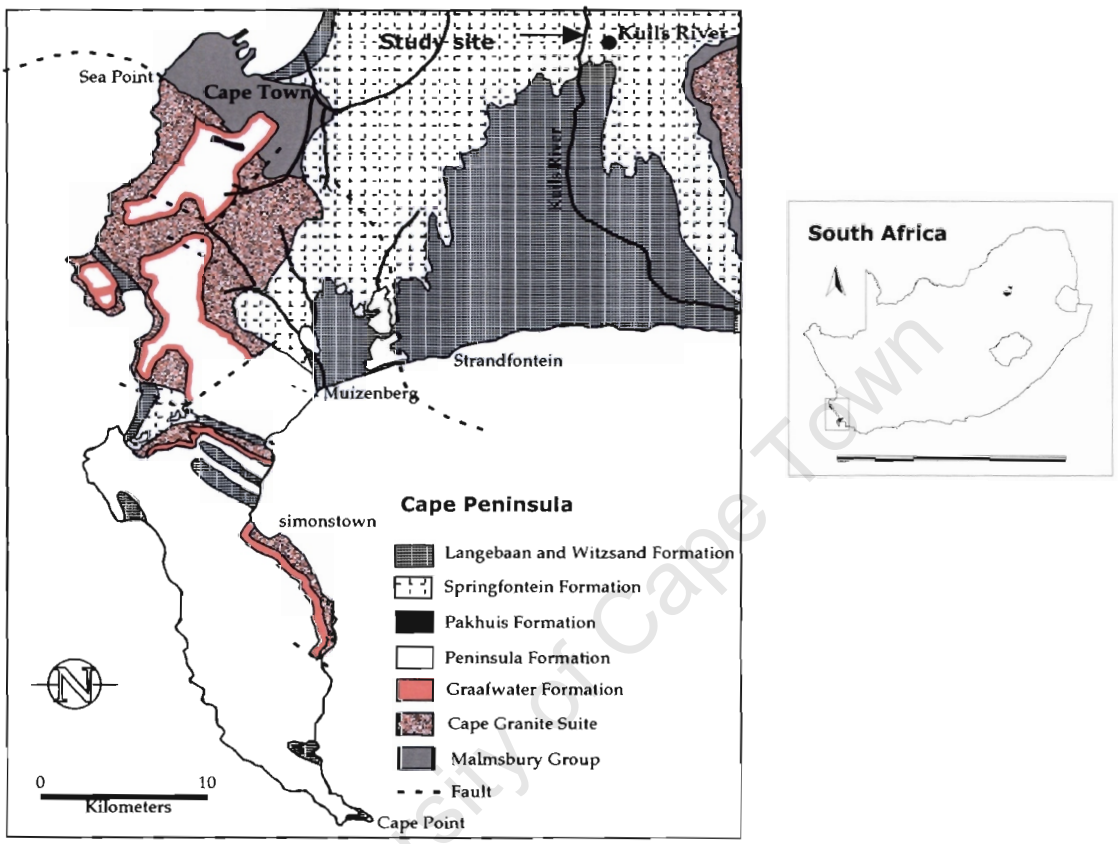

Figure 1.1: Location of the study area, incorporating the surrounding geology.

Sediments of the Cenozoic Sandveld Group overlie bedrock of much of the Cape Flats. The bedrock is made up primarily of the Malmesbury Group and Cape Granite (Reid *et al.,* 1998; Harris *et al.,* 1999). Table 1.1 depicts the stratigraphy of the Sandveld Group. Of special interest for this study is the Springfontein Formation, which is primarily an aeolian formation of fine to medium quartzose sand, which is exposed over large parts of the Cape Flats. It also forms the dominant part of the unconfined, Cape Flats Aquifer (Harris *et al.,* 1999). Surficial soils in the vicinity of the study area are yellow, red or brown and were formed *in situ* on the Malmesbury rocks during weathering. The soil is further described as clayey, with numerous small nodules of ferricrete and fragments of vein quartz and a variable quantity of sand grains (Theron *et al.,* 1992). The depth of the soil to the underlying bedrock is estimated to be approximately 10m (Theron *et al.,* 1992).

Table 1.1: Cenozoic Formations of the Western Cape (from Theron *et al.*, 1992)

Age			Lithology	Formation	
Quaternary	Holocene		Aeolian, calcareous, quertzose sand	Witzand	Sandveld Group
	Pleistocene		Aeolian, calcrete-capped calcareous sandstone	Langebaan	
			Littoral, calcrete-capped coquina	Velddrif	
			Fluvial gravel, marine clay and littoral sand	Milnerton	
			Aeolian quartzose sand with intermittent peaty layers	Springfontein	
Neogene	Pliocene		Quartzose and muddy sand, and shelly gravel, phosphate rich	Varswater	
	Miocene	Late	Conglomeratic sandy phosphorite	Saldanha	
		Middle	Angular quartzose gravely sand and peaty clays	Elandsfontyn	

1.3.4 Hydrogeology

The Cape Flats Aquifer unit consists of low-lying unconsolidated sands which were formed by deposition following river and wind erosion. It connects the Peninsula to the Tygerberg and Stellenbosch hills to the east, and is regarded as one of the most extensive unconsolidated to semi-consolidated intergranular aquifers in South Africa with groundwater occurring within the intergranuar interstices in a porous medium (Meyer, 2001). Although the average depth of the water table is 3.75 m, it is variable depending on the season. The shallow depth and the coarse-grained nature of the sands have opened the aquifer to exploitation. Fresh water extracted from this aquifer is currently used for irrigation purposes (Maclear, 1995). Typical borehole yields for the study area range from 0.1 to 0.5 $l.s^{-1}$ (Meyer, 2000).

1.4 Land use and history of contamination

1.4.1 Land use

Land use in the immediate vicinity of the site is variable. The study area encompasses a petrol station, and a car dealership immediately to the south, and a magistrates court and police station to the north (Figure 1.2). West of the site, adjacent to Industry Road, is a workshop whilst apartment buildings exist directly opposite and adjacent to Van Riebeek Street to the East.

1.4.2 History of contamination

Between the 8th and 18th September 2000, following the rupture of a 14m^3 underground storage tank, 101,560 l of 97-octane petrol was released into the surrounding groundwater system. Shortly thereafter 45 PVC cased monitoring wells were put in place to monitor the flow of the contaminated plume. As at 22nd March 2001, 82,340 l (81% of the reported leakage) had been recovered using vacuum-enhanced extraction. Further attempts at vacuum extraction in April 2001 proved unsuccessful with the result that a significant volume of contaminant was left unattenuated. The lack of gradient at this site has confined the plume to an area of approximately 15 000m^2. Current concentrations (Appendix A) of BTEX compounds pose an unacceptable risk to human health with the result that the occupation houses and offices adjacent to the spill site had to be discontinued. The risk of ingestion is considered unlikely as no groundwater abstractions are currently taking place in the area. See Appendix A for an aerial overview of the site.

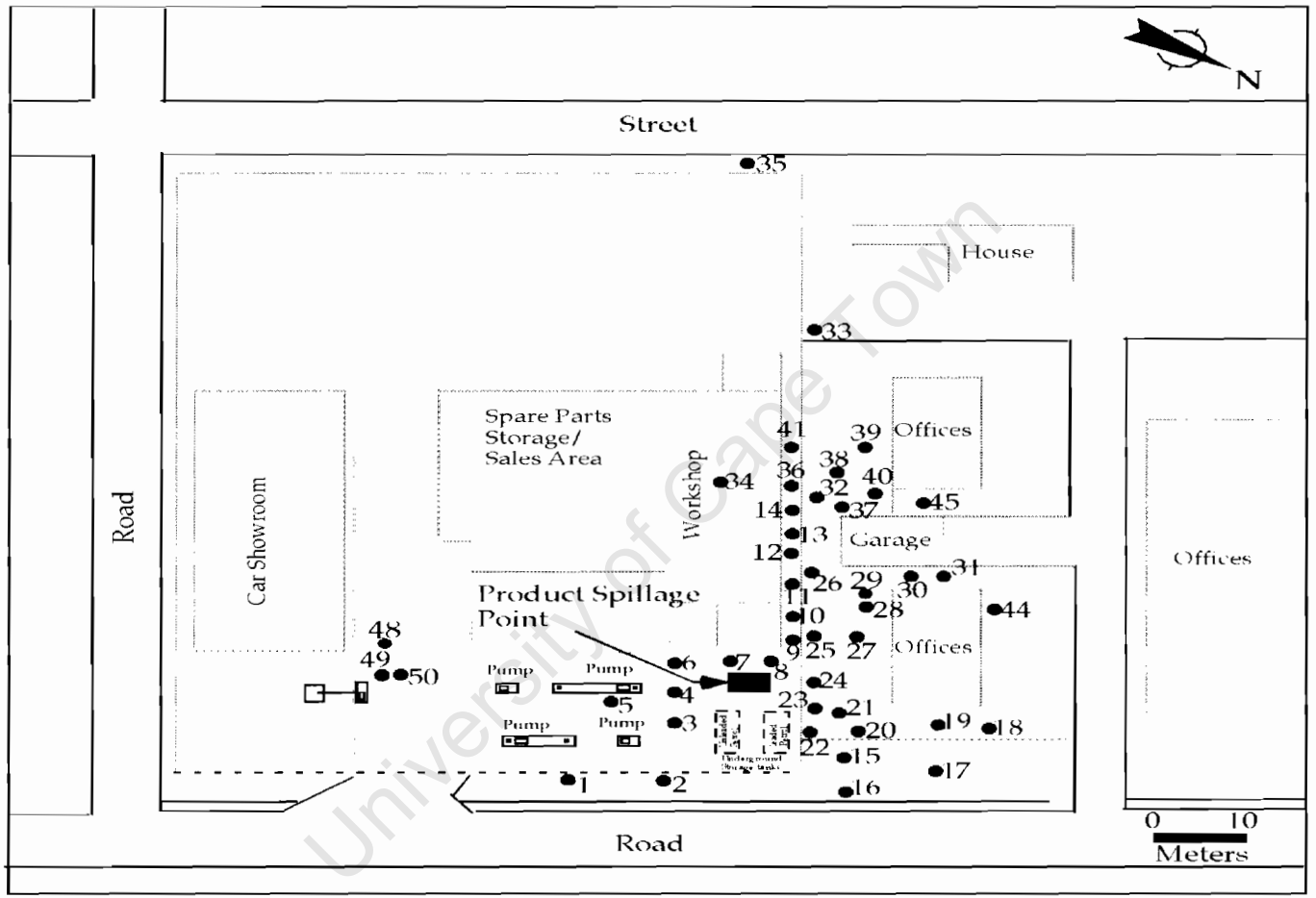

Figure 1.2: Plan of the study area depicting the position of the monitoring wells. (Taken from Roychoudhury and Merrett, (in review), adapted after Kantey & Templer Consulting Engineers).

CHAPTER 2 – LITERATURE REVIEW

2.1 Fundamental principles of bioremediation

Once released into groundwater systems, petroleum hydrocarbons are acted on by a combination of physical, chemical, and biological processes which disperse the contamination (Chapelle, 1993). Of these processes, only microbial degradation results in the mass loss of contaminants, and is therefore regarded as the predominant mechanism for natural attenuation at petroleum-contaminated sites (Gieg *et al.*, 1999).

The process of biodegradation begins when microbes assimilate hydrocarbons inside the membrane (Johnson *et al.,* 2003). These energy rich compounds are then mineralized via a chain of oxidation-reduction (redox) couples, where the energy required for microbial growth, is extracted by means of a stepwise oxidation of the organic molecule. It can only proceed if a relatively more oxidised chemical species is available, since electrons liberated during oxidation, cannot roam free (Stumm and Morgan, 1996). The compounds that act as a "sink" for the expelled electrons are termed terminal electron acceptors (TEA's).

During aerobic respiration, oxygen is the TEA of choice. However, many contaminated aquifer environments are anaerobic with the result that a number of less highly oxidised compounds serve as the TEA. The sequence is governed by thermodynamic principles (Stumm and Morgan, 1996), and follows the TEA with the highest energy yield downward. Possible TEA's include NO^{3-}, Fe^{3+}, Mn^{4+}, SO_4^{2-} and CO_2.

2.1.1 Redox potential

Given that TEA's are used in decreasing order of energy yield, by measuring the redox potential (E_h), the availability of a specific TEA is determined (Figure 2.1). The redox potential that supports oxygen-based metabolism is greater than that required for nitrate-based systems. Sulphate and methanogenic-based systems require the lowest redox potentials, and are strongly inhibited by oxygen (Anderson et al., 1995). A changing redox potential, indicative of TEA availability, is generally accompanied by a change in microbial community structure (Anderson et al., 1995).

Linberg and Runnels (1984) observed that redox processes occurring in natural waters are generally not at equilibrium. Moreover, they showed that redox potentials are mixed potentials that are impossible to relate to a single dominant redox couple. Because of this, redox potentials should be used as a qualitative indicator of the overall redox state as apposed to being an absolute indicator.

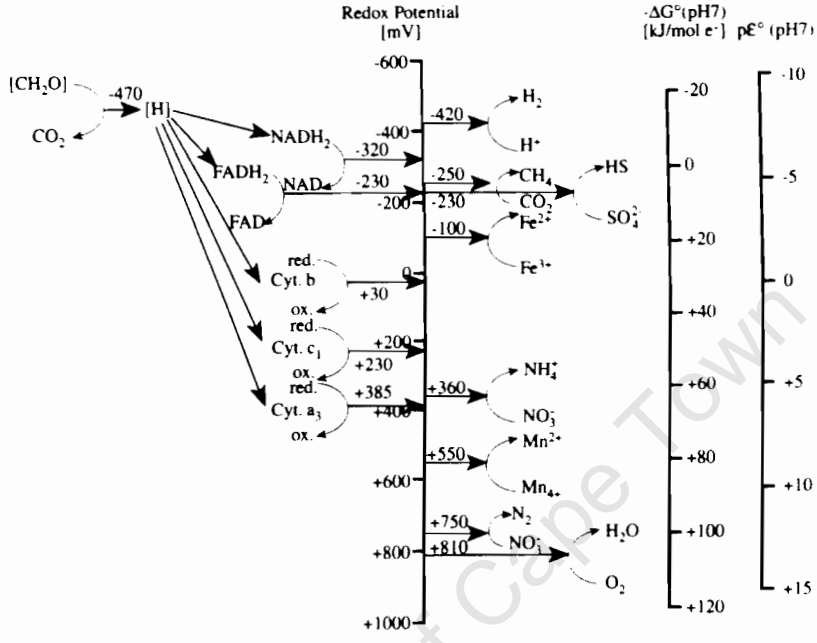

Figure 2.1: Oxidation-reduction potentials of microbial electron transfer reactions (Zhender and Stumm, 1988)

2.2 Review of BTEX biodegradation via sulphate reduction

Since sulphate reduction is believed to be a dominant process taking place at the site, a review of previous work linking sulphate reduction to BTEX biodegradation is deemed necessary.

The sulphate-reducing bacteria (SRB) are nearly ubiquitously distributed and are a unique physiological group of prokaryotes in that they have the capability of using inorganic sulphate as a terminal electron acceptor during respiration (Barton and Tomei, 1995; Fauque, 1995). This respiratory process, occurring under anaerobic conditions, is undertaken by SRB for the purpose of generating high-energy compounds for biosynthetic reactions involved in their growth and maintenance (Akagi, 1995). Anaerobic microbial processes that involve sulphate reduction play an important role in the degradation of a wide variety of

substrates, including saturated hydrocarbons and a variety of aromatic and xenobiotic compounds (Stackerbrandt and Devereux, 1995). Indeed, the number of undesirable compounds amenable to biodegradation under sulphate reducing conditions has increased dramatically (Ensley and Suflita, 1995).

Perusal of literature suggests that to some or other degree, BTEX compounds can degrade with sulphate acting as the primary terminal electron acceptor. For example, the anaerobic destruction of toluene and xylene isomers coupled to sulphate reduction has been noted with several types of inocula. Haag *et al.* (1991) showed via column microcosms established with aquifer material obtained from a petroleum spill that toluene and *p*-xylene was degraded following the addition of sulphate. In this study, sulphate was the only detectable electron acceptor in the microcosms. In later studies Edwards *et al.* (1992) and Bellar *et al.* (1992) confirmed via ^{14}C-labeled substrates, the complete mineralization of toluene and *o*-xylene to $^{14}CO_2$. In both cases, the stoichiometries of loss of both aromatic hydrocarbons and the reduction of sulphate were consistent with sulphate serving as the sole electron acceptor for oxidation. A similar study, involving a combination of field and laboratory work, was carried out along a groundwater flow path in the sulphate reduction zone of a petroleum contaminated aquifer in Hanahan, South Carolina (Chapelle *et al.*, 1996). In this instance, rates of toluene loss, coupled to sulphate reduction, were consistent with measured rates of toluene destruction estimated by the injection of ^{14}C-labeled toluene into laboratory incubations of aquifer sediments. Toluene degradation was also detected in sulphate-reducing enrichments inoculated with marine sediments (Rabus *et al.*, 1993).

Anaerobic ethylbenzene degradation and biotransformation under sulphate-reducing conditions has also been observed. Reinhard *et al.* (1997) demonstrated via an *in situ* study that ethylbenzene can be oxidised in the presence of SRB, however the rates of degradation were significantly slower than those measured for toluene, *o*-xylene and *m*-xylene. These findings were later confirmed by Phelps *et al.* (1999). More recently Nakagawa *et al.* (2002) demonstrated the depletion of ethylbenzene by sulphate reducing enrichments inoculated with polluted marine sediments retrieved from Tokyo Bay, Japan. The study was further able to characterize the microbial community structure and the successive changes in the ethylbenzene-degrading sulphate reducing conditions.

Until recently, benzene was believed to be completely recalcitrant to microbial attack under anaerobic conditions. However several workers have observed benzene degradation under sulphate reducing conditions. Lovely *et al.* (1995) confirmed, via highly reduced marine sediments, that benzene could be oxidized, in the absence of O_2, to carbon dioxide and that benzene oxidation was coupled to sulphate reduction. Earlier findings by Edwards and Grbić-Galić (1992) showed that 90% of ^{14}C-labeled benzene was converted to $^{14}CO_2$ by aquifer derived microorganisms inoculated into an anaerobic medium containing sulphate as the potential electron acceptor. However they could not confirm that sulphate served as the terminal electron acceptor. Following an investigation into BTEX biodegradation under a range of redox conditions, Reinhard *et al.* (1997) concluded that benzene was only associated with sulphate reduction, although its removal was only pronounced at certain depths. More recently, Anderson and Lovely (2000) observed the complete loss of benzene following sulphate addition to a petroleum-contaminated aquifer. However Weiner and Lovley (1998) cautioned that not all petroleum-contaminated aquifers contained the appropriate benzene-degrading microorganisms. They concluded that benzene was likely to persist even following sulphate addition under certain conditions.

2.3 Implications of sulphide accumulation on microbial activity

While laboratory and field studies, described above, have demonstrated the mineralization potential of BTEX compounds in the presence of sulphate, concerns regarding sulphide toxicity have resulted in a general lack of interest in the use of sulphate as a solution to BTEX removal (Ward *et al.*, 1995). The following text describes the potential problems associated with free sulphide accumulation. This is an important consideration when assessing the potential for a system to effectively demonstrate BTEX removal following sulphate amendments.

When SRB consume aromatic hydrocarbons, the process leads to the production of sulphide (defined here as the sum of H_2S, HS^- and S^{2-}), which by its chemical properties and physiological effects is a far more conspicuous substance than the substrate itself (Widdel, 1988). Sulphide, in the form of H_2S, is chemically reactive and even at low concentrations, (>0.2 ppm), is known to be toxic to both humans and microorganisms (Widdel, 1988; Ward *et al.*, 1995).

It is generally assumed that the neutral undissociated H_2S molecule is the agent of toxicity, since it is membrane permeable only in this form (Speece, 1983, Olezskiewicz *et al.*, 1989). O'Flaherty *et al.*, (1998) later suggested toxicity was pH dependant, with observed inhibition related to undissociated H_2S concentration between pH 6.8 - 7.2, whereas above pH 7.2, inhibition was related to the total sulphide concentration. Inhibition casued by total sulphide concentrations at higher pH of was also earlier reported by Koster *et al.* (cited in Olezskiewicz *et al.*, 1989).

Research has indicated that at relatively high H_2S concentrations, microbial activity decreases, thus inhibiting the potential for BTEX biodegradation when coupled to SO_4^{2-} reduction. However there appears to be inconsistencies as to the H_2S concentration thresholds that SRB's are able to tolerate. For example, Edwards *et al.* (1992) observed that toluene and xylene degradation concomitant with sulphate reduction was significantly reduced following the addition of 1 mM Na_2S. Furthermore, mineralization was shown to completely cease after 5 mM Na_2S amendments. Similar observations were made by Klemps *et al.* (1985). Interestingly, Reis *et al.*, (1992) reported only marked inhibition in the growth rates of SRB following exposure to H_2S concentrations of 16 mM.

The fate of H_2S is believed to be extremely complex (Chapelle, 1993). Sulphide can diffuse into the aerobic zone of groundwater systems where it is oxidised back to sulphur. Indeed, Chapelle (1993) reports a number of microorganisms which use H_2S as their sole energy source, and in so doing mediate the oxidative process. More commonly however, H_2S is precipitated out of solution by readily reacting with metals, especially iron, to form iron sulphides such as FeS or FeS_2. Sediments with an abundance of ferrous iron are excellent buffers at free sulphide accumulation. Bellar *et al.* (1992) has indicated that the problems associated with sulphide toxicity can be overcome in the presence of ferric iron. The study showed that following the addition of millimolar concentrations of amorphous $Fe(OH)_3$, toluene degradation in subsurface soils contaminated with aviation fuel, was greatly accelerated. Indeed Edwards *et al.* (1992) corroborated these findings following the addition of $FeSO_4$. Both studies concluded that the addition of ferric or ferrous iron probably accelerated BTEX transformation by removing free H_2S from the solution, thereby preventing the inhibitory effects of sulphide toxicity.

The periodic injection of nitrate is also believed to be useful in preventing sulphide accumulations. Research conducted to address the souring of natural oil reserves showed that nitrate addition curbed souring by stimulating sulphide oxidizing bacteria and thereby reducing S^{2-} concentrations (McInerney *et al.*, 1992).

2.4 Organic substrate

Alkanes, alkylaromatics and aromatics are the predominant chemicals comprising most petroleum products and are rich in carbon (Englert *et al.*, 1993). Their potential degradability can generally be estimated on their structure and is directly proportional to molecular weight (Rosenberg and Ron, 1996). For example, alkanes of intermediate chain length (C_{10} – C_{24}) are rapidly degraded, whereas long chains are resistant, and after exceeding a molecular weight of 500-600 $g.mol^{-1}$ they cease to serve as carbon sources (Englert *et al.*, 1993). Branching structures typical of monocyclic aromatics, such as BTEX, generally reduce the biodegradation rate, since branching creates tertiary and quaternary carbon atoms that constitute a hindrance to beta oxidation (Englert *et al.*, 1993).

The crucial biochemical step in the breakdown of BTEX compounds is the oxidization of the aromatic rings by oxygenase enzymes, of which 0.1 to 1.0 % of microbes possess (Dineen *et al.*, 1993). The specificity of the process is generally related to the genetic potential of the particular microorganism to introduce molecular oxygen into the hydrocarbon (Rosenberg and Ron, 1996). Moreover, the specific genetic capacity is expressed in the hydrocarbon substrate specificity of the oxygenase and in the ability of the carbon source to induce the various enzyme activities involved in biodegradation (Rosenberg and Ron, 1996). This is what sets the various microbial communities apart and results in affinities for various carbon sources by phylogentecally different microbes.

These affinities have been demonstrated among BTEX compounds. For example, in studies where mixtures of aromatic hydrocarbon were tested for anaerobic biodegradability, sequential utilization of compounds has been reported. In most cases, toluene is the substrate of choice for resident microbial communities (Haag *et al.*, 1991). The sequence thereafter is not as clear. For example, in a study on landfill leachate, Reinhard *et al.* (1984) reported that, under methanogenic conditions, *o*-xylene was degraded more rapidly compared to *m*-xylene, *p*-xylene,

and ethylbenzene. Conversely however, Khun *et al.,* (1985) observed *m*-xylene, and *p*-xylene, removal prior to *o*-xylene in conditions that were reported to be denitrifying. Under the same conditions, Battermann and Werner (cited in Haag *et al.*, 1991), found xylenes degraded only after concentrations of benzene, toluene, and ethylbenzene were reduced.

Substrate affinities by microbial organisms have also been linked to sulphate reduction. Edwards *et al.* (1992) observed that *o*-xylene degradation was always preceeded by *m*-xylene, *p*-xylene and toluene. Moreover, in the presence of simpler organic compounds, such as lactate, glucose and yeast extract, the degradation of toluene and xylene isomers ceased altogether, at least until all preferred substrates were consumed.

An assessment of substrate preferences can therefore serve as a proxy to the type of microbial community present. Furthermore, by amending sediments with a mixture of high and low molecular weight organic substrates, an evolutionary account of the microbial community can be inferred. For example, SRB with a preference towards higher molecular weight compounds are more closely related to more modern sulphate reducers, whereas those with affinities towards low molecular weight substrates tend to be less evolved (Roychoudhury, 2004). Lactate, a high molecular weight organic acid is reportedly the most generic carbon source for SRB (Kleikemper *et al.*, 2002).

2.5 Approaches to estimating *in situ* biodegradation

Obtaining reliable estimates for biodegradation rates of is imperative in terms of assessing the efficiency of intrinsic bioremediation (Chapelle *et al.*, 1996). Generally speaking, evidence confirming *in situ* biodegradation is achieved by comparing microbial and geochemical signatures of a contaminated area with those in an uncontaminated reference area (Gieg *et al.*, 1999). Currently a number of approaches can be adopted to assess whether intrinsic bioremediation is occurring, however each is subject to interpretational constraints.

An approach frequently used to measure biodegradation rates, is to collect aquifer sediments and construct static or flow-through microcosms in the laboratory (Chapelle *et al.*, 1996). The disappearance of a particular organic compound is then measured (Wilson *et al.*, 1994 b). Alternatively the production

of $^{14}CO_2$ from radio labelled compounds can also be measured (Bellar *et al.*, 1992; Edwards and Grbić-Galić, 1992; Edwards *et al.*, 1992). The advantage to these methods is that they are applicable to a wide variety of hydrologic systems, and that abiotic controls can be used to separate biotic from nonbiotic effects (Chapelle *et al.*, 1996). However, Madsen (1991) highlights uncertainties in due to sediment disturbance and difficulties in reproducing *in situ* conditions as obstacles that need to be overcome when adopting the laboratory approach.

Leahy and Colwell (1990) suggested that *in situ* biodegradation reflects a delicate balance of nutritional, physical and biological relationships that act dynamically in response to environmental factors such as oxygen, water, pH, and nutrients. Thus when a water, soil, or sediment sample is removed from the field, it should not be assumed that the physiological status of the accompanying microorganisms is unaltered (Madsen 1991). Indeed Chapelle and Lovley (1990) reported that the rates of microbial metabolism in some groundwater systems were grossly overestimated as a result of laboratory methods.

Another widely used approach is to measure the decrease in electron acceptors such as O_2, NO_3^-, Fe^{3+}, and SO_4^{2-}, and increases in the concentrations of Fe^{2+}, S^{2-}, CO_2, or CH_4 in a contaminated region relative to a reference area (Gieg *at al.*, 1999). The measured values can then be used to estimate the amount of contamination biodegraded based on stoichiometric calculations (Anderson, 1995).

Table 2 lists the stoichiometric relationship between BTEX and the respective TEA. It is noted that SO_4^{2-} is stoichiometrically the most effective at BTEX removal, however, thermodynamically speaking it remains the least favoured.

Gieg eta al. (1999) notes that while indicative of *in situ* responses to contamination, geochemical changes related to resident TEA's do not necessarily attest to contaminant loss. Furthermore, there are often uncertainties with respect to separating the effects from microbial processes from abiotic processes such as sorption (Chapelle, 1996).

Table 2.1: Various redox reactions possibly involved in BTEX degradation, associated free energy change, and stoichiometric relationship between BTEX and terminal electron acceptors (TE), respectively.

Redox pathways for BTEX degradation	$\Delta_r G°$ [1] (kJ.mol^{-1})	mol BTEX/ mol TE [2]
Benzene		
$C_6H_6 + 7.5O_2 + 3H_20 \rightarrow 6H^+ + 6HCO_3^-$	-3066	0.13
$C_6H_6 + 6NO^-_3 \rightarrow 6HCO_3^- + 3N_2$	-3002	0.17
$C_6H_6 + 30FeOOH + 54H^+ \rightarrow 42H_20 + 6HCO_3^- + 30Fe^{2+}$	-1370	0.03
$C_6H_6 + 3.75SO_4^{2-} + 3H_20 \rightarrow 2.25H^+ + 6HCO_3^- + 3.75HS^-$	-105	0.27
Toluene		
$C_7H_8 + 9O2 + 3H_20 \rightarrow 7H^+ + 7HC0_3^-$	-3670	0.11
$C_7H_8 + 7.2NO_3^- + 0.2H^+ \rightarrow 0.6H_20 + 7HCO_3^- + 3.6N_2$	-3593	0.14
$C_7H_8 + 36FeOOH + 65H^+ \rightarrow 51H_20 + 7HCO_3^- + 36Fe^{2+}$	-1635	0.03
$C_7H_8 + 4.5SO_4^{2-} + 3H_20 \rightarrow 7.5H^+ + 7HCO_3^- + 4.5HS^-$	-118	0.22
Ethyl benzene/Xylene		
$C_8H_{10} + 10.5O_2 + 3H_20 \rightarrow 8H^+ + 8HCO_3^-$	-4291/-4307	0.10
$C_8H_{10} + 8.4N0_3^- + 0.4H^+ \rightarrow 1.2H_20 + 8HCO_3^- + 4.2N_2$	-4201/-4217	0.12
$C_8H_{10} + 42FeOOH + 76H^+ \rightarrow 60H_20 + 8HCO_3^- + 42Fe^{2+}$	-1917/-1933	0.02
$C_8H_{10} + 5.2SO_4^{2-} + 3H_20 \rightarrow 2.75H^+ + 8HCO_3^- + 5.25HS^-$	-146/-162	0.19

[1] Thermodynamic data taken from Roychoudhury and Merritt (in review)
[2] TE = Terminal electron

2.6 Quantification of sulphate reduction

The approach adopted in this study was to indirectly determine the rate of BTEX removal in terms of the loss of SO_4^{2-} concentration. Thus sulphate reduction rates (SRR) were quantified. While the interpretational constraints, highlighted above, are acknowledged, restrictions imposed by finances, resources, and time dictated this decision.

While the review thus far has indicated that SRB are able to mineralize organic BTEX compounds, they are also known to use a wide variety of electron acceptors (NO_3^-, O_2 to name a few), either in the absence, or sometimes in the presence of sulphate (Widdel, 1988). Thus, given their metabolic diversity, the mere presence of SRB does not necessarily imply that sulphate reduction will take place (Ulrich *et al.*, 1997). Moreover, while the loss of SO_4^{2-} and the production of S^{2-} are indicative of sulphate reduction, the absence of changes in these chemical species should not be taken as evidence to exclude this process. For example, the oxidation and/or precipitation of aqueous H_2S as metal sulphides can modify pool

sizes, such that increases in sulphide concentration may be undetectable (Ulrich *et al.*, 1997). It is therefore imperative that in assessing sulphate reduction rates, these individual sulphur species are accurately quantified.

Previous methods at quantification, involving high-temperature combustion and oxidation of sulphur species, failed in their ability to distinguish pyrite sulphur from organic sulphur (Canfield *et al.*, 1986). Radiotracer experiments involving $^{35}SO_4^{2-}$ have proved far more successful in determining SRR. The technique involves the incubation of $^{35}SO_4^{2-}$ with sediments, followed by the extraction and quantification of the produced ^{35}S-sulphides, including H_2S^{35} , $H^{35}S^-$, $Fe^{35}S$, and $Fe^{35}S_2$. By heating sediment samples with a solution of Cr^{2+} and HCl during a distillation, reduction of the total inorganic sulphur is achieved, thus excluding organic sulphur. The liberated sulphide, in the form of H_2S, is then trapped in a solution of zinc acetate. The reduced radiolabelled (^{35}S-sulphides) fraction can then be quantified via a liquid scintillation counter and then SRR's quantified (Ulrich *et al.*, 1997). The chromium reduction technique was adopted in this study and is further described in section 3.3.

2.7 Basic theory of liquid scintillation counting

The above review has shown that by introducing radioactive $^{35}S0_4^{2-}$ into isolated sediment samples, the rate at which labelled sulphide is produced, accurate sulphate reduction rates to be calculated. This has previously been demonstrated by Jørgensen (1978). In calculating the SRR, radioactive disintegrations need to be counted, and is achieved by means of liquid scintillation counters. A brief overview of the theory behind liquid scintillation is therefore warranted.

2.7.1 Liquid scintillation

During liquid scintillation, radioactive decay is detected and counted (Beckman Instruments, 1988). The radioactive sample to be counted is mixed with a "scintillation cocktail" which usually contains a solvent, an emulsifier, and fluor. The cocktail serves to convert the energy of the particle emitted during the radioactive decay process into light which is detected by the liquid scintillation counter (LS counter). LS counters measure the alpha particles (a positively charged helium nucleus), beta particles (an electron), a positron (a positively charged electron), Auger electrons, conversion electrons, and Compton electrons.

Molecules in the solvent are able to absorb part of the energy emitted during radioactive decay, causing them to become excited. The number of excited solvent molecules is proportional to the energy of the radioactive decay being measured. This energy is then transferred between solvent molecules since they are the predominant species in the cocktail. In a process occurring in less than 10^{-12} seconds, the excited solvent molecules transfer their energy to a fluor molecule. On returning to their ground state, each excited flour molecule emits one photon of light at a wavelength between 320 and 420 nm, depending on the fluor. The amount of light emitted is proportional to the energy of the particle. Therefore the higher the energy of the particle, the more solvent molecules it is able to excite (because it travels further in the solvent). The result is that more light is generated. This light is then directed to photomultiplier tubes in the LS counter, the purpose of which is to convert it into measurable electrical pulses. The amplitude of each pulse is proportional to the energy of the particle. These pulses are then analysed by the LS counter, converted into digital form, and stored in the appropriate channel of the multichannel analyser, corresponding to the particle energy. During sample measurement, the multichannel analyser accumulates the number of pulses (or counts) in each channel. This data is then used to determine the energy of the particles in the sample, and the rate (counts per minute, or CPM) of the radioactive decay in the sample. The CPM is the total number of pulses in the channels of the multichannel analyser divided by the total time in minutes of obtaining the count.

Tracer experiments that follow (see section) are used to determine the CPM values that are necessary to calculate microbially mediated reduction rates (see section).

2.8 Kinetics of nutrient-limited microbial growth

To survive, microorganisms must transform environmentally available nutrients to forms that are useful for incorporation into cells and synthesis of cell polymers (Norris *et al.*, 1994). Any limitations in nutrient supply would therefore impede growth and development, and as a result the goal of establishing an effective bioremediation strategy would be severely compromised. A brief overview of the Monod equation (Monod, 1949), which explores the kinetics of nutrient limited microbial growth, is therefore necessary.

2.8.1 The Monod equation

Although microbial growth biochemistry tends to be complex, it often follows simple rate equations (Brezonik, 1993). The basis for most microbial growth models is expressed in terms of the empirically derived, hyperbolic, Monod equation (Monod, 1949).

$$R = \frac{R_{max}[S]}{K_s + [S]}$$

where R is the specific growth rate, R_{max} is the maximum rate where nutrient concentrations, $[S]$, is not limiting and K_s is the half saturation constant for nutrient limited growth and corresponds to the concentration at which R is one-half of its maximum.

By determining the specific rate of microbial growth, as a function of limiting substrate concentration, the above serves as a proxy to establishing the effectiveness of bioremediation in removing unwanted contaminants. Since one of the aims of this project is to look at the role that sulphate reducers play in removing BTEX compounds, sulphate reduction rates will be modelled as a function of limiting sulphate concentration. Given that the rate is also dependant on the speed at which nutrients, like sulphate and organic hydrocarbons are carried across the cell membrane, the Monod equation is said to be transport limited (Roychoudhury, 2004).

2.8.2 Determination of K_s and R_{max} values

By calculating K_s, the concentration of nutrient supply at which microbial growth is maximized, can be quantified. Therefore the theoretical maximum rate at which contaminants like BTEX, can be removed from the system, is established.

In order to calculate K_s and R_{max}, the Monod equation is linearised to yield Lineweaver-Burk plots (Roels, 1983). These are plots depicting the reciprocal of the nutrient reduction rates (1/NRR) as a function of the reciprocal of varying nutrient concentrations (1/C). They are thus described as double reciprocal plots.

R_{max} is calculated by taking the reciprocal of the intercept of slope of the straight line, and K_s established by substituting the calculated R_{max} for the slope of the straight-line equation.

CHAPTER 3 - METHODOLOGY

3.1 Groundwater sample collection and analysis

Groundwater chemistry data can be used to deduce a great deal about the zonation, extent, and rates of microbial processes in groundwater systems (Chapelle, 1993). To this end, the first phase of the study involved groundwater sampling from an extensive network of PVC cased monitoring wells. Sampling took place in September 2004, near the end of the winter rainfall period. Given the limited resources available, sampling took several days to complete.

It should be noted that the naming convention applied to all sampled wells is based on the letters 'MW' (representing the word 'monitoring well') prefixed to the well number. The well number is taken from a pre-existing plan, (Figure 1.2), as supplied by Kantey and Templer Consulting Engineers.

3.1.1 Field measurements and sample collection procedure

Of the 45 PVC cased and capped monitoring wells, 32 were used for groundwater sample collection, as the others were dry. The location of the wells is illustrated in Figure 1.2. Three monitoring wells (MW 48, MW 49, and MW 50) were positioned up gradient from the contaminated plume to serve as background samples. Prior to sampling the volume of groundwater occupying each monitoring well was calculated. Thereafter, using Teflon® bailers, each well was purged of approximately three well volumes to remove groundwater equilibrated with the atmosphere, and thus ensuring that the analysis of groundwater samples are truly reflective of the *in situ* conditions. Following each purge, measurements of pH, temperature, electrical conductivity, and dissolved oxygen were made using a WTW® Multi 340i Set. Additionally, Eh was measured using a Sentek portable electrode. Only once Eh, temperature and electrical conductivity stabilised was purging discontinued and the parameters measured. In order to record consistent measurements, the instruments were calibrated prior to commencing field work each day, as well as at random intervals while in the field.

Teflon® bailers were used to collect the groundwater samples. To minimize the introduction of oxygen into the sample through splashing, the bailer was carefully lowered into the monitoring well. Once removed, the content of the bailer was

poured into a glass beaker to measure the field parameters described above. Although it is recognised that this method will almost certainly result in the loss of H_2S as well as leading to inaccurate dissolved oxygen readings, it was deemed the most appropriate given time and cost constraints.

Additionally water from each monitoring well was poured into 50ml VWR® brand centrifuge vials. Each vial was acidified to a pH <2 using concentrated HCl for further cation analyses. Thereafter the vials were capped without leaving any headspace and kept on ice in the field. Upon returning to the laboratory the vials were transferred to a fridge maintained at 4°C until further analysis.

For the analyses of Fe^{2+}, alkalinity, ΣH_2S, and SO_4^{2-}, samples were fixed in the field to avoid equilibration with the atmosphere. All samples were placed on ice and transported back to the laboratory to determine concentrations. For a more in-depth discussion relating to the analytical techniques performed on the above, the reader is referred to sections 3.1.2. to 3.1.5.

BTEX concentrations were supplied and are published with the kind permission of Kantey & Templer Consulting Engineers. Analysis was performed by Inspectorate M&L (PTY) Ltd, Consulting Industrial Chemists, Analysts and Samplers and involved using the purge and trap method.

3.1.2 Determination of alkalinity

Alkalinity concentrations were determined using the method of Sarazin *et al.* (1999). The advantages of this method are its accuracy, rapidity and the small sample volume required (Sarazin *et al.*, 1999). This method uses a weak acid ($HCHO_2$) and a pH sensitive dye (Bromophenol-Blue) to neutralise all basic species taken into account in the alkalinity expression. The product of the neutralisation reaction is a colour complex with an absorbance at 590 nm as a function of the original alkalinity of the sample.

The colour reagent was prepared by mixing 25 ml of Bromophenol-Blue solution (500 $mg.l^{-1}$) and 25 ml of 0.1 M formic acid in a 250 ml volumetric flask. Furthermore alkalinity standards of 2, 4, 6, 8, 10, and 12 mM were prepared from a stock solution of 0.1 M sodium carbonate ($NaHCO_3$).

Prior to groundwater sampling, 15 ml VWR® Brand centrifuge vials were precharged with the 2 ml of the colour reagent. While in the field, 2 ml of filtered sample was pipetted into the vials. Similarly, 2 ml of each standard was added to the reagent to prepare the calibration curve. Using a spectrophotometer, the absorbance of the standards and the samples was measured at 590 nm. This was performed following each day of sampling. A second order polynomial is applied to the calibration curve in order to calculate the alkalinity of the samples.

3.1.3 Determination of sulphate

The turbidimetric method described by Tabatabai (1974) was followed in order to calculate sulphate concentrations. This procedure utilises the turbidity of barium sulphate ($BaSO_4$) colloids. These form following the reaction of $BaCl_2.2H_2O$, maintained in suspension by gelatine, with sediment pore waters containing sulphate ions. The concentrations are then measured in a spectrophotometer at 420 nm after a constant reaction time.

A stock gelatine solution was prepared by first measuring a slight excess over 500 ml of de-ionised water into an Erlenmeyer flask and heating it to 70 °C on a hot plate. Thereafter 1.5 g of gelatine was added and stirred slowly to dissolution. The solution was left to cool before placing it in a refrigerator for a minimum of 16 hours.

In order to prepare the reagent, the stock gelatine solution was removed from the fridge and allowed to warm to room temperature. Thereafter 50 ml of the stock solution was pipetted into an Erlenmeyer flask to which 0.5 g barium chloride ($BaCl_2.2H_2O$) was added. To dissolve, the solution was stirred using a magnetic stirrer for 1 hour. Once complete, the solution was left to stand for a further 1 hour before returning it to the fridge. The Barium-Gelatine solution is then ready for use the next day.

Additionally a 0.01 M K_2SO_4 stock solution was prepared from which standards with concentrations of 250, 500, 750, 1000, 1500, and 2000 µM were diluted.

Prior to entering the field 15 ml VWR® Brand centrifuge vials were precharged with 1000 µL 0.05 M HCl. To each vial 1000 µL of filtered sample was added. On returning to the laboratory each day, 250 µL of the Barium-Gelatine solution was

added to each vial at 1 minute intervals. Each vial was then thoroughly mixed with the aid of a Vortex Genie. This was carefully done so as to avoid the solution from touching the interior of the vial cap. Following exactly 30 minutes of reaction time, and at 1-minute intervals, the absorbance of the standards and samples was measured at 420 nm. The concentration of the samples was calculated from the calibration curve.

3.1.4 Determination of sulphide

The analysis for sulphide concentration was carried out using the method described by Cline (1969). This method reportedly measures only soluble suphides.

The mixed diamine reagent, for expected sulphide concentrations in the range of 3 to 40 μM, was prepared by dissolving 2 g of N,N-dimethyl-p-phenylenediamine sulphate and 3 g ferric chloride ($FeCl_3.6H_20$) in 500 ml of cool 50% (v/v) reagent grade HCl. For the preparation of the standards, oxygen free water was prepared by purging 2 l of de-ionised water with nitrogen for 1 hour. From this, a 0.01 M $Na_2S.9H_20$ stock solution was prepared and thereafter 5, 10, 20, 30, and 40 μM dilutions were made to determine the calibration curve.

While in the field 500 ml of filtered sample was pipetted into 15 ml VWR® Brand centrifuge vials. To each sample, five drops of 20% (w/v) zinc acetate solution was added in order to trap the sulphide. On returning to the laboratory, the samples were thoroughly shaken, and thereafter 3 ml of the fixed solution was pipetted into 15 ml VWR® Brand centrifuge vials. To each vial 400 μl of mixed diamine reagent was added. Following 20 minutes reaction time, the absorbance was determined at 620 nm using a spectrophotometer. The same methodology was performed on the standards. The sulphide concentration for each sample is then calculated from the calibration curve. As mentioned in section 3.1.1 calculated sulphide concentrations may not accurately reflect true values given the described methodology of sample collection. This should be borne in mind during the analysis of results.

3.1.5 Fe^{2+} Determination

For the determination of Fe^{2+} concentrations in the samples, the ferrozine method, modified after Stookey (1970) was used.
To prepare the ferrozine buffer, approximately 0.2 g ferrozine and 12 g Hepes was weighed out into a 1 l volumetric flask and then made up to 1 l using de-ionised water. Furthermore, a stock solution of 0.01 M ferrous sulphate ($FeSO_4^{2-}.7H_20$) was prepared. From the stock solution, dilutions of 50, 100, 250, 500, 750 and 1000 µM were made up and used to prepare the standards for the calibration curve.

While in the field, sufficient sample for the determination of Fe^{2+}, alkalinity, and sulphide was collected in a syringe, and filtered into a 50 ml glass beaker using a 0.45 µm flow-through PTFE filter. In order to fix Fe^{2+} in the field, 250 µl of the filtered sample was disbursed (Eppendorf® auto pippete), into 15 ml VWR® Brand centrifuge vials that were precharged with 5 mL of ferrozine.

Following each sampling session, a new calibration curve was determined in the laboratory by linear regression analysis of the prepared standards. The Fe^{2+} concentrations for each sample were then determined from the calibration curve. The absorbance of the samples and standards was measured at 562 nm using a spectrophotometer.

3.2 Sediment collection and analyses

All sediment samples were excavated using a hand held auger from the groundwater/sediment interface, at a depth of approximately 2.5 m. To avoid oxidation at the surface, the samples were immediately double bagged and preserved in a portable chamber. Anaerobic conditions were maintained with the aid of Anaerocult® A packs. The chambers were then placed on ice before being transported back to the laboratory and immediately transferred to an anaerobic chamber with an automatic airlock. This procedure was adopted for all sediment collected in sections 3.2.1 – 3.2.4.

3.2.1 Determination of *in situ* sulphate reduction rates

In situ SRR's were determined in order to establish a point of reference for controlled experiments involving SO_4^{2-}, S^{2-} and organic substrate additions. This was deemed necessary given the aims and objectives of this study.

The four sampling points chosen were based on variable SO_4^{2-} concentrations. The choice was limited, as only a small section of the monitored site was accessible to subsurface sediments. Thus sediment samples were retrieved close to MW 19, MW 24, MW 27 and MW 28 respectively. Sampling took place at the end November 2004 and all samples were subjected to the following experimental conditions.

While in the field, pre-weighed, triplicate VWR® Brand 15ml centrifuge vials, representing each sample point, were filled to approximately 4ml with the sediment sample, using a steel spatula. Thereafter 50 µl of carrier free $^{35}SO_4^{2-}$ (1μCi/μl) was carefully injected into each vial, followed by 2 ml of groundwater extracted from the purged wells. Finally, 5 ml of 20% (w/v) zinc acetate was added in order to inhibit further reduction. The vials were then capped and immediately frozen before being transported back to the laboratory. Upon arrival, the vials were transferred to a freezer. The samples are then ready for further analysis for measurements of ^{35}S incorporated in the reduced fraction using a one-step distillation process modified after Canfield *et al.* (1986). For a detailed description of this procedure, see section 3.3.

3.2.2 Sulphate amendment experiment

In this experiment sediments extracted from positions close to MW 27 and MW 28 were subjected to increasing SO_4^{2-} concentrations. The idea was to assess the impact that increased sulphate dilutions would have on SRR's relative to the *in situ* SRR's for corresponding sample sites. Furthermore this type of experiment allows half saturation constants (K_s) to be calculated, which are important variables in attempting to maximize microbial growth rates and hence increase SRR's. This has important implications in expediting BTEX removal. Sampling took place at the end of November 2004 and the following procedure was followed.

Two sets of 30 pre-weighed 15 ml VWR® Brand centrifuge vials were filled, using a steel spatula, to approximately 4ml with sample sediment extracted from close

to MW 27 and MW 28 respectively. The vials were then preserved in an anaerobic chamber for 24-hours. This time frame was assumed long enough for the resident SRB in the samples to completely reduce *in situ* SO_4^{2-} concentrations. Thereafter, triplicate vials were amended with 1 ml of 0.1, 0.25, 0.5, 1, 3, 5, 10, 15, 20, and 28 mM potassium sulphate (K_2SO_4) solution respectively. Immediately thereafter, 50µl of carrier free $^{35}SO_4^{2-}$ (1μCi/μl) was injected into each vial before being placed under incubation for a further 24-hours. Following incubation, further reduction was inhibited by pipetting 5 ml of 20% (w/v) zinc acetate into each vial before being placed in a freezer. The samples are then ready for further analysis (see section 3.3).

3.2.3 Sulphide amendment experiment

Sulphide toxicity and its inhibitory effects on microbial communities have already been discussed in the literature review (section 2.3.). Given its potential impact on SRR's, and given the specific aims and objectives of this study, experiments involving S^{2-} amendments on extracted sediment samples were deemed necessary. The decision to sample from MW 27, was based on work by Merrett (2003), who observed that SO_4^{2-} was being reduced at relatively high levels for this location. Sampling was conducted in late October 2004. All samples were subjected to the following experimental procedure.

Using sediment samples extracted close to MW 27 eighteen pre-weighed 15 ml VWR® Brand centrifuge vials were filled to approximately 4 ml with the aid of a steel spatula. Thereafter 2 ml of groundwater extracted from MW 27 was pipetted into each vial followed by 50 µl of carrier free $^{35}SO_4^{2-}$ (1μCi/μl). The tracer was injected longitudinally using a pipette while the pipette tip was slowly removed from the sediment. The vials were then incubated for 30 minutes. Triplicate vials were then amended with Na_2S such that their molar sulphide concentrations measured 0.5, 1, 3, 5, and 10 mM respectively. The remaining vials served to act as the control for the experiment and were therefore not amended with Na_2S. Following a further 2-hour incubation period, sediment samples were fixed with 5 ml of 20% (w/v) zinc acetate and immediately transferred to a freezer to terminate any microbial activity. The samples are then ready for further analysis (see section 3.3).

3.2.4 Organic substrate amendment experiments

The affinity that microbial populations have for certain organic compounds has been discussed in section 2.4. For most SRB, lactate is believed to be the organic salt of choice (Kleikemper et al., 2002). To test this, three simple organic salts, including lactate, were added to sediment extracted next to MW 27. These were then compared to *in situ* rates, to assess affinities for these compounds by the resident microbial population. MW 27 was selected for sampling, as sulphate reduction was known to be taking place at this location (Merrett, 2003). The samples were retrieved in late November 2004 and were subjected to the following experimental procedure.

Using a steel spatula, three sets of pre-weighed triplicate 15 ml® VWR Brand centrifuge vials were filled to approximately 4 ml with the extracted sediment. To each vial 2 ml of groundwater extracted from MW 27 was pipetted, followed by the injection of 50µl of carrier free $^{35}SO_4^{2-}$ (1μCi/μl). The vials were then incubated for 30 minutes. Thereafter each set of triplicates was amended with 1 mM concentrations of sodium acetate (CH_2COONa), sodium formate (HCOONa), and sodium lactate ($CH_3CHOHCOONa$) respectively. The vials were then stored anaerobically for a further 2 hours. Finally 5 ml of 20% (w/v) zinc acetate was pipetted into each vial, before placing them in a freezer, until further use (see section 3.3)

3.3 Determination of sulphate reduction rates

Sulphate reduction rates for samples amended with sulphate (section 3.2.2), sulphide (section 3.2.3) and organic substrates (3.2.4), in addition to *in situ* rates for the four monitoring wells (3.2.1) were determined by following the chromium reduction technique, modified after Canfield *et al.* (1985). This technique has proven to be highly suited for the routine analysis of reduced inorganic sulphur in modern and ancient sediments (Canfield *et al.*, 1985). See section 2.6 for a more in depth discussion.

3.3.1 Experimental apparatus

The experimental apparatus consists of a digestion flask which attaches to a condenser (Figure 3.1). A section of tubing connects from the top of the condenser to a glass test tube which acts as the trapping vessel for liberated sulphide. A series of 6 flasks operate simultaneously, with tank nitrogen being

distributed via entry points to each flask. Both the prepared sample sediment and the reagent mixture are added via a separate entry point to the digestion flask. All connection points are then well sealed with silicon lubricant to prevent the escape of the reduced inorganic sulphur. The apparatus is then ready for use.

3.3.2 Preparation of chromium solution

Approximately 500 g of zinc pellets were weighed out into a glass bottle, to which 125 ml of 2 M HCl was added. Once bubbling ceased, the HCl solution was decanted and a solution of 61.61 g chromium (III) chloride hexahydrate ($CrCl_3.6H_2O$), dissolved in 250 ml of 0.5 M HCl, was poured over the zinc pellets. Nitrogen gas was then bubbled through the solution for approximately 2 hours or until such time that the solution turned blue in colour. Thereafter 60 ml syringes, marked at 16 ml intervals, were filled with the reduced chromium solution. These were then preserved in a refrigerator until further use. Due to atmospheric oxidation, the reduced chromium solution was prepared every 3 days (Canfield *et al.*, 1985)

3.3.3 Preparation of sediment sample

For each distillation, 6 preserved sediment samples (see sections 3.2.1 – 3.2.4) were removed from the freezer and allowed to defrost. After centrifuging the samples for 5 minutes at 5000 rpm, 100 µl of the supernatant was pipetted into marked scintillation vials each precharged with 5 ml scintillation liquid. The remaining supernatant was decanted from the centrifuge vials. The weight of the remaining sediment was then calculated from the difference between the total weight of the centrifuge vial, including the remaining sediment, and preweighed empty vials (see sections 3.2.1 – 3.2.4). Thereafter the sediment in each vial was thoroughly homogenised using a steel spatula, before weighing out approximately 1 g of each sample into the digestion vessels (Figure 3.1).

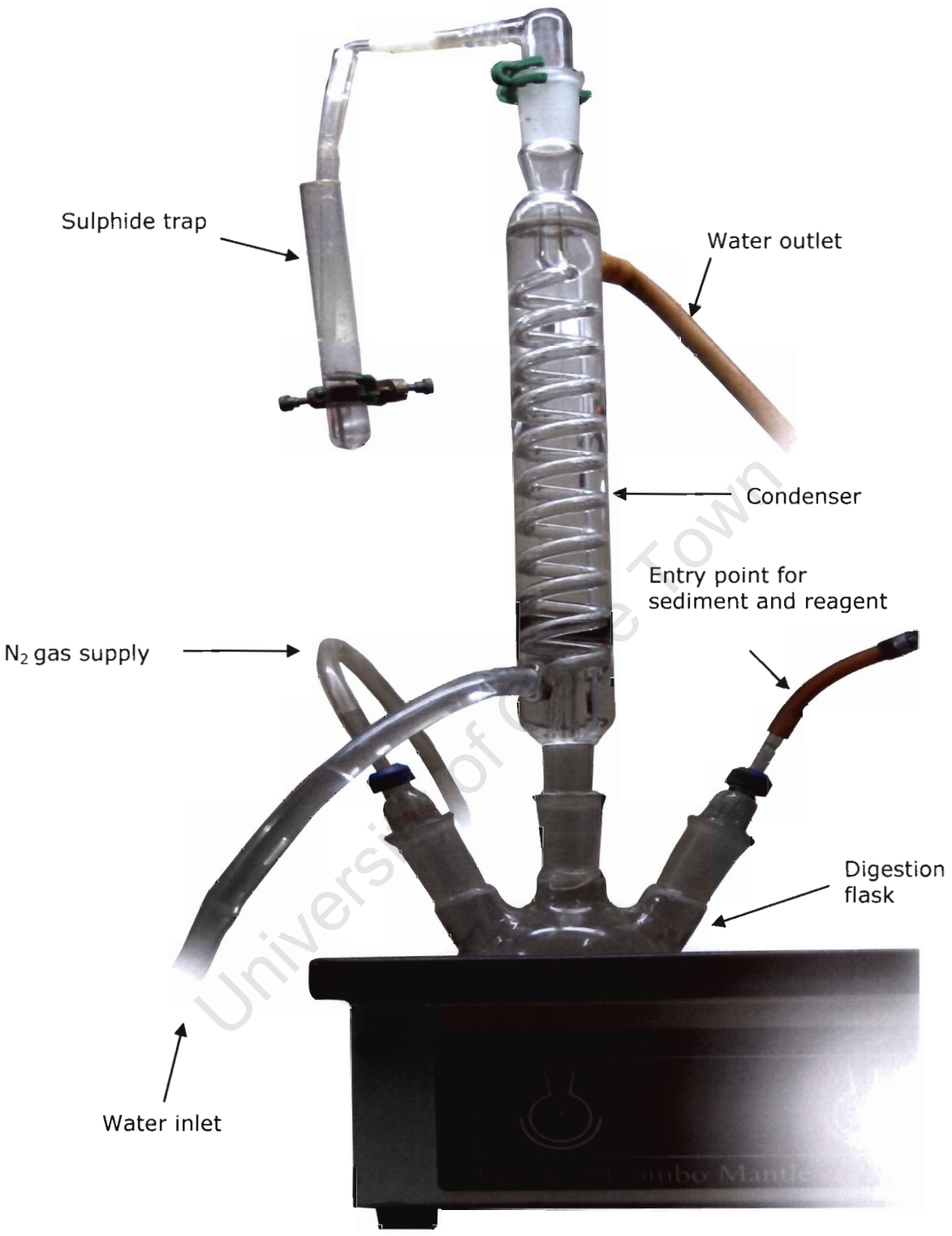

Figure 3.1: Distillation device used to determine sulphate reduction rates. (Graphic courtesy of Andrew Kerr).

3.3.4 Preparation of sulphide trapping vessels

A solution of 5% (w/v) zinc acetate was prepared of which 10 ml was pipetted into 6 separate clean, glass test tubes followed by a single drop of silicon anti-foaming agent. Each test tube was then connected to the gas line to act as trapping vessels for the liberated sulphide (Figure 3.1.). Zinc is preferred to other metals, as ZnS is not known to cause quenching during scintillation counting (section 3.3.4) of the sulphide radioactivity (Jørgenson, 1978)

3.3.5 Distillation procedure and liquid scintillation counts

To remove atmospheric oxygen the system was initially flushed for approximately 10 minutes with N_2 gas. Thereafter 16 ml of the reagent mixture, together with 8 ml of concentrated HCl was added to each digestion flask. The flasks were then heated to boiling point and N_2 gas bubbled through the system at a rate of 2-3 bubbles per second. The liberated H_2S was collected in the zinc acetate trapping vessels. Following 1-hour reaction time the contents of the trapping vessels were poured into marked scintillation vessels, each precharged with 10 ml scintillation liquid. Thereafter the radioactivity of the both the distillate and supernatant (see section 3.3.2) was measured using a BECKMAN LS 5000 TD liquid scintillation counter at the Microbiology department at the University of Cape Town.

3.3.6 Calculation of sulphate reduction rates

SRR 's were calculated according the following equation (Jørgenson, 1978):

$$SRR = \frac{[SO_4^{2-}].(^{35}S - H_2S)..\alpha}{(^{35}S - SO_4^{2-}).t} \quad (\text{nm.cm}^{-3}\text{d}^{-1})$$

Where $[SO_4^{2-}]$ is the sulphate concentration in $nm.cm^{-1}$ of the sedmiment, ^{35}S-SO_4^{2-} (supernatant) and the ^{35}S-H_2S (distillate) are the total sulphate and sulphide radio activities, t, is the incubation time measured in days, and α is the isotope fractionation factor of the bacterial sulphate reduction.

3.4 Incubation experiments

The aim of the incubation experiments was primarily to establish *in situ* Fe^{3+}, and SO_4^{2-} reduction rates as well as to plot changes in extractable, solid phase Fe^{2+} concentrations. This data is useful in establishing whether concomitant Fe^{3+} and SO_4^{2-} reduction is taking place as well as to calculate *in situ* SRR's and Fe^{3+} reduction rates.

While it was hoped to generate results from samples collected at the end of the winter rainy season, this was not possible as several attempts at conducting the experiment failed. For this reason, the results presented are based on incubation experiments that were performed midway through summer, in early January 2005.

3.4.1 Determination of Fe^{3+} and SO_4^{2-} reduction

In accordance with the sampling procedure outlined in section 3.2, sediment was extracted at positions directly opposite MW 27 and MW 28. This decision was based on existing SO_4^{2-} and Fe^{2+} concentrations for groundwater samples taken from MW 27 and MW 28. Both sets of samples were subjected to the following experimental conditions.

Using a steel spatula, the sediment sample extracted was thoroughly homogenised inside the anaerobic chamber. Sixteen 50 ml VWR® Brand centrifuge vials were then filled with the sediment and capped without leaving any headspace. Thereafter duplicate vials, for each sampling point were sacrificed at 0, 1, 2, 6, 12, 24, 48, and 72 hours and immediately centrifuged at 5000 rpm for 5 minutes. The supernatant, representative of the sediment pore water, was then carefully pipetted out and filtered through a 0.45 μm filter. By following the methods outlined in section 3.1.3 and 3.1.5, the Fe^{2+} and SO_4^{2-} pore water concentrations for each duplicate were determined. These concentrations were then plotted against time in order to assess the rates of both iron and sulphate reduction.

3.4.2 Determination of Fe^{2+} extractions

During incubation experiments, the tandem reduction of Fe^{3+} and SO_4^{2-} is possible which may lead to the precipitation of Fe^{2+} in the sediments. In order to measure solid phase Fe^{2+} concentrations, the top portion of the sediments in the 50 ml vials used for the incubation was discarded in case any oxidation had occurred. Thereafter, approximately 1 g of sediment was weighed out into a 15 ml VWR brand centrifuge tube, precharged with 10 ml of 0.5 M HCl. The vials were then placed on a shaker at a speed of 125 rpm for 1 hour. On completion, the vials were centrifuged at a speed of 5000 rpm for 2.5 minutes. Without filtering, 100 µl of the supernatant was pipetted off the top and the Fe^{2+} concentration determined by using the ferrozine method (Stookey, 1970) outi;ined in section 3.1.5. The above procedure was performed on incubated samples extracted from both MW 27 and MW 28.

3.4.3 BTEX concentrations

All BTEX concentrations (Appendix C) are presented with permission of Kantey & Templer Consulting Engineers. The analysis was performed by Inspectorate M&L (PTY) Ltd, Consulting Industrial Chemists, Analysts and Samplers and involved using the purge and trap method.

CHAPTER 4 – RESULTS

4.1 Groundwater Analysis

For the results of all of the analyses carried out on groundwater samples the reader is referred to Appendix B. Table 4.1 tabulates the both the mean and range for anion and cation concentrations, together with the mean and range for all geochemical measurements taken in the field. MW 48, MW 49 and MW 50 represent background samples whereas all other boreholes are representative of the contaminated plume.

The pH of the groundwater sampled from background boreholes has a narrow neutral range (7.0 – 7.1), whereas the contaminant plume is slightly acidic to neutral (6.6 – 7.2). The highest measured pH of 7.2 was recorded at MW 27. Generally speaking contaminant plume EC values are greater than those recorded at background sampling points. The highest measured EC within the plume is 2.16 $mS.cm^{-1}$. Temperature readings are variable, with the lowest (17.5 °C) and highest (22.0 °C) recorded temperature found in the contaminant plume. The temperature range for background samples is 18.1 °C at MW 49 to 19.9 °C at MW 48. All redox potential (Eh) values for contaminant plume samples are negative with recorded values that range between –57 mV at MW 37 and –302 mV at MW 24. This contrasts significantly with background water samples whose values are positive and range between 132 and 150 mV. The dissolved oxygen concentrations for the contaminant plume ranges between 0 and 1.95 $\mu g.l^{-1}$, and are generally lower than the concentrations measured at the background samples (1.15 – 2.23 $\mu g.l^{-1}$). No dissolved oxygen was recorded at MW 25. Alkalinity measurements within the contaminant plume are highly variable and range between 4.4 (MW 19) and 12.7 μM (MW 4). Background samples reveal a narrow alkalinity range between 7.6 μM and 9.2 μM.

SO_4^{2-} concentrations are, by comparison to the mean, significantly high at MW 27 (2825 μM). The range of background SO_4^{2-} concentrations is 681 μM at MW 50 to 934 μM at MW 48. Reduced sulphur concentrations, in the form of ΣH_2S appear to be insignificant for background samples. The highest calculated S^{2-} concentration is located at MW 26. Significantly, no Fe^{2+} is found to exist at the background sampling points, whereas all plume samples exhibited measurable concentrations. The highest measured value of 2,171 μM exists closest to the spill site at MW 4.

Table 4.1: Mean inorganic analyses in contaminated and uncontaminated groundwater

Parameter	Background samples [1]		Contaminated samples [2]	
	Average	Range	Average	Range
pH	7.1	7.0 – 7.1	6.8	6.6 - 7.2
EC (µS/cm)	1,006	911 – 1,182	1,239	288 – 2,160
Temperature (°C)	19.0	18.1 – 19.9	19.6	17.5 – 22.0
Eh (mV)	164	132 - 209	-162	(-57) – (-302)
DO (µg/L)	1.80	1.15 – 2.23	0.90	0 – 1.95
Salinity	0.4	0.4 – 0.5	0.6	0 – 1.1
Alkalinity (µM) [3]	8.2	7.6 – 9.2	8.5	4.4 – 12.7
SO_4^{2-} (µM)	772	681 - 934	499	97 – 2,825
Fe^{2+} (µM)	0	0	395	3 – 2,171
S^{2-} (µM)	0.2	0.1 – 0.3	8.9	0.2 - 60.2

[1] Mean values for inorganic parameters from uncontaminated water based on three monitoring wells (MW 48, MW 49 and MW 50).
[2] Mean values for inorganic parameters from contaminated water based on all other monitoring wells (n=28)
[3] Total alkalinity

4.2 Spatial variation of groundwater chemistry

To assist the reader in gaining a better visual perspective of the existing groundwater chemistry at the site, contour plots of the recorded Eh and dissolved oxygen concentrations, in addition to the measured concentrations of SO_4^{2-}, Fe^{2+}, S^{2-}, and BTEX were generated in Surfer® version 8. The contours were plotted based on the interpolation of spot measurements at each sampled well using Point Kriging with a linear drift. The results of the contouring are shown in Figures 4.1 (a – g).

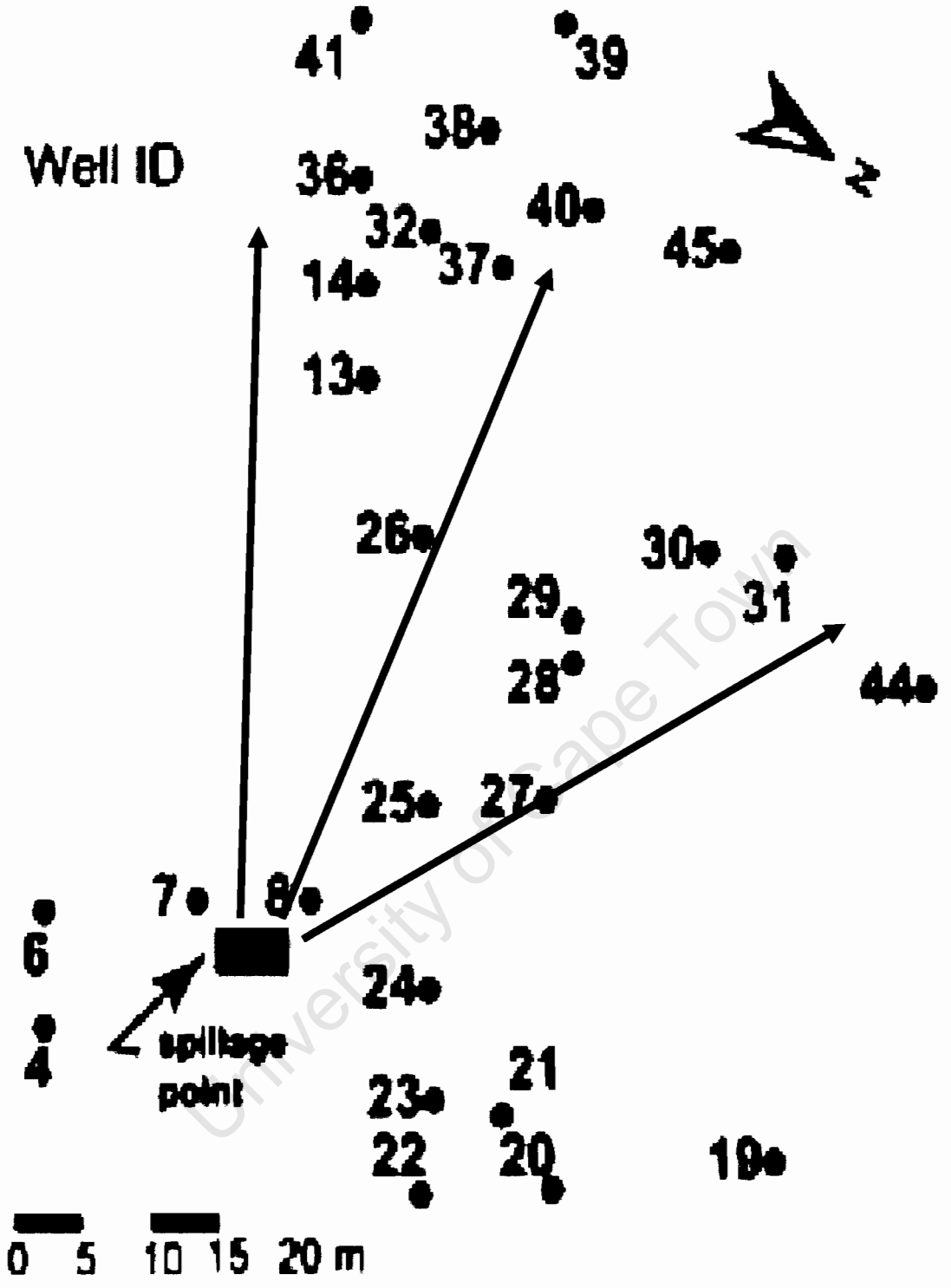

Figure 4.1a: Plot illustrating well positions and ID's. The dark arrows represent the predicted hydrological flow pattern.

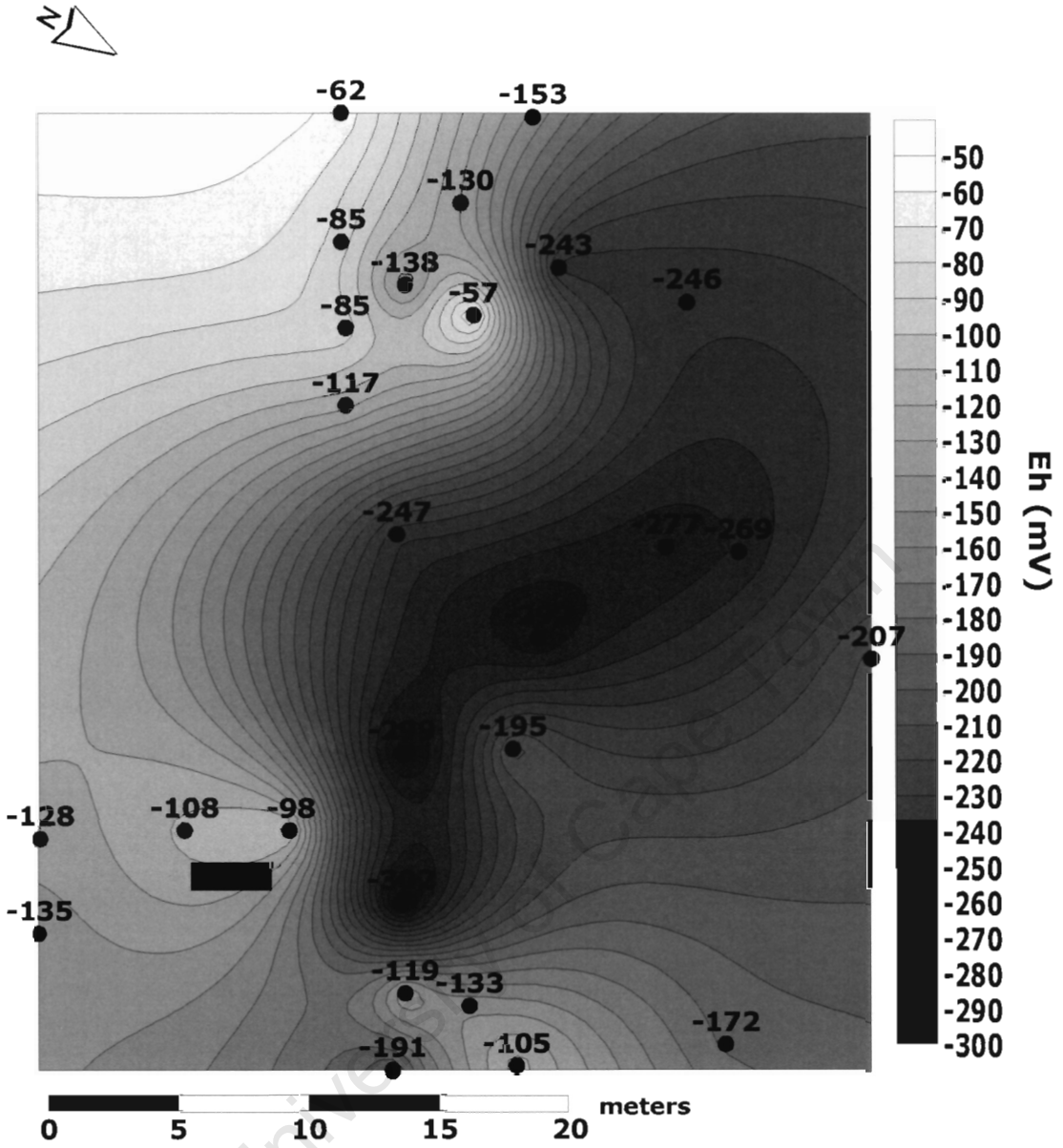

Figure 4.1b: Contour plot showing the spatial distribution of Eh measurements recorded across the contaminated site. The black rectangle denotes the point of discharge.

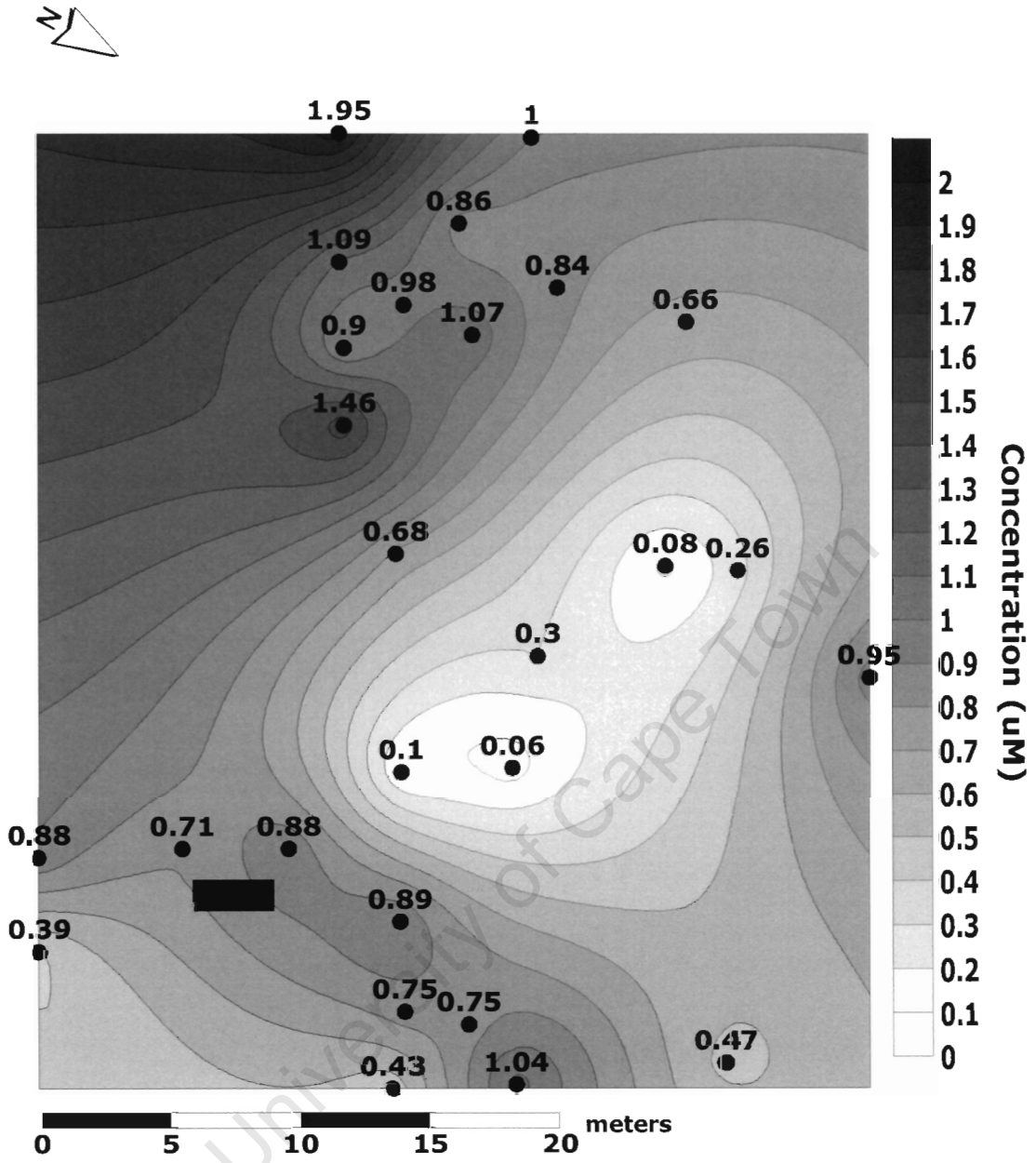

Figure 4.1c: Contour plot showing the spatial distribution of variable dissolved oxygen concentrations across the contaminated site. The black rectangle denotes the point of discharge.

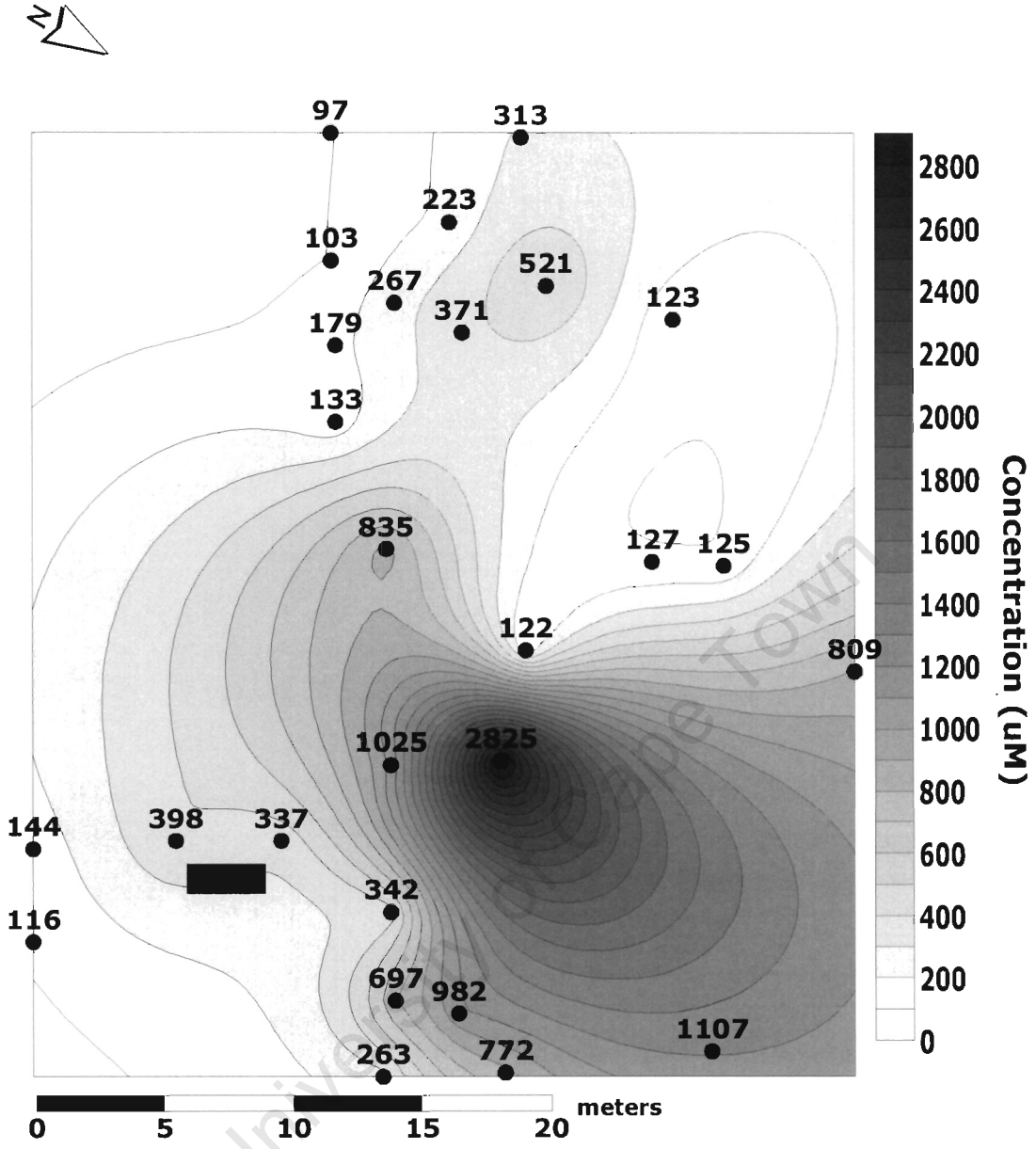

Figure 4.1d: Contour plot showing the spatial distribution of SO_4^{2-} concentrations measured across the contaminated site. The black rectangle denotes the point of discharge. Note that whilst it is acknowledged that the spatial distribution of sampling points between MW27 (2825 uM) and MW19 (1107 uM) is insufficient to be able to approximate SO_4^{2-} concentrations in between these sampling points, the presence of a building made the sinking of additional sampling wells difficult. Thus interpolated values based on only two sampling points are used and should be considered in the review of results.

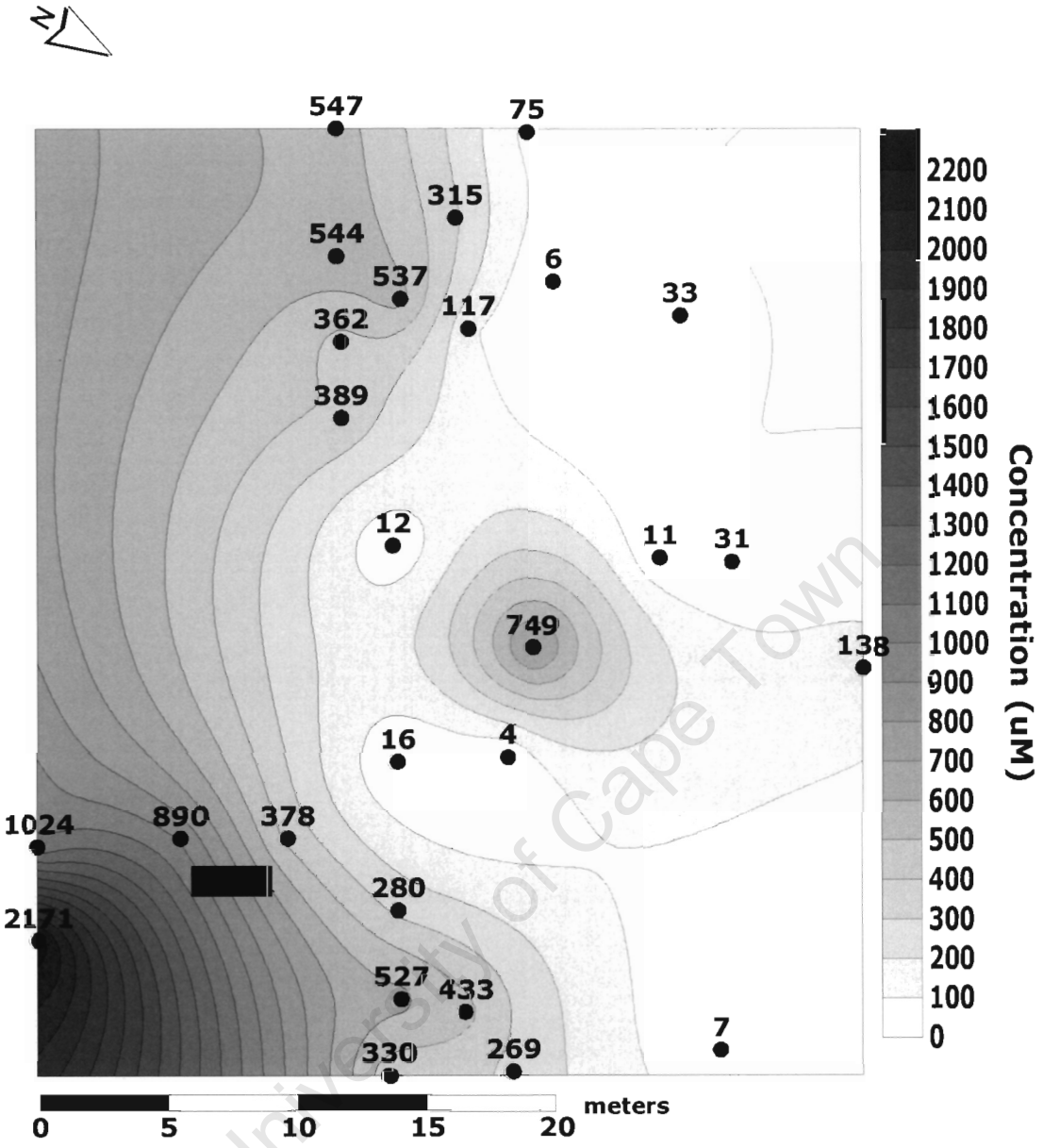

Figure 4.1e: Contour plot showing the spatial distribution of Fe^{2+} concentrations measured across the contaminated site. The black rectangle denotes the point of discharge.

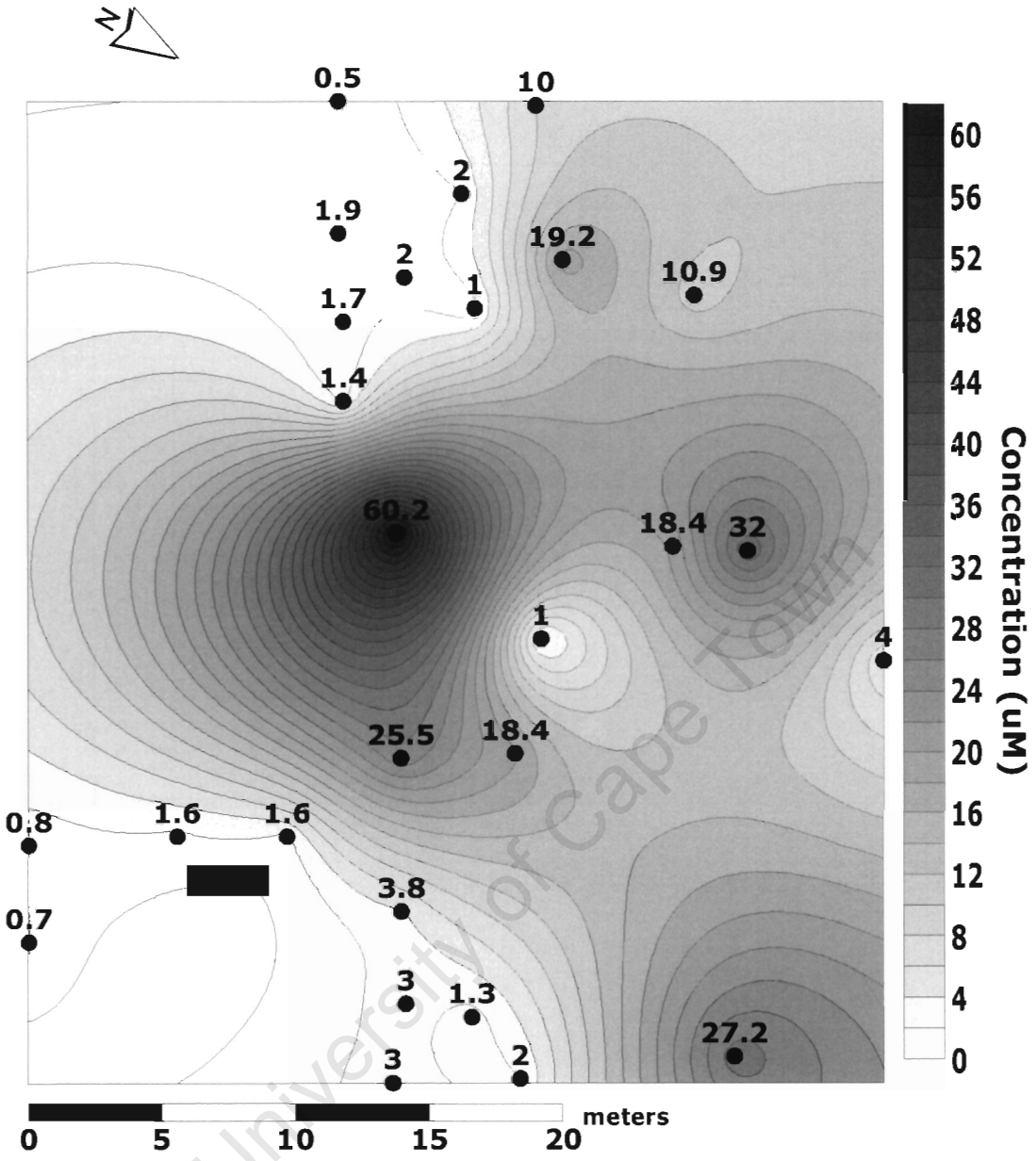

Figure 4.1f: Contour plot showing the spatial distribution of S^{2-} concentrations measured across the contaminated site. The black rectangle denotes the point of discharge.

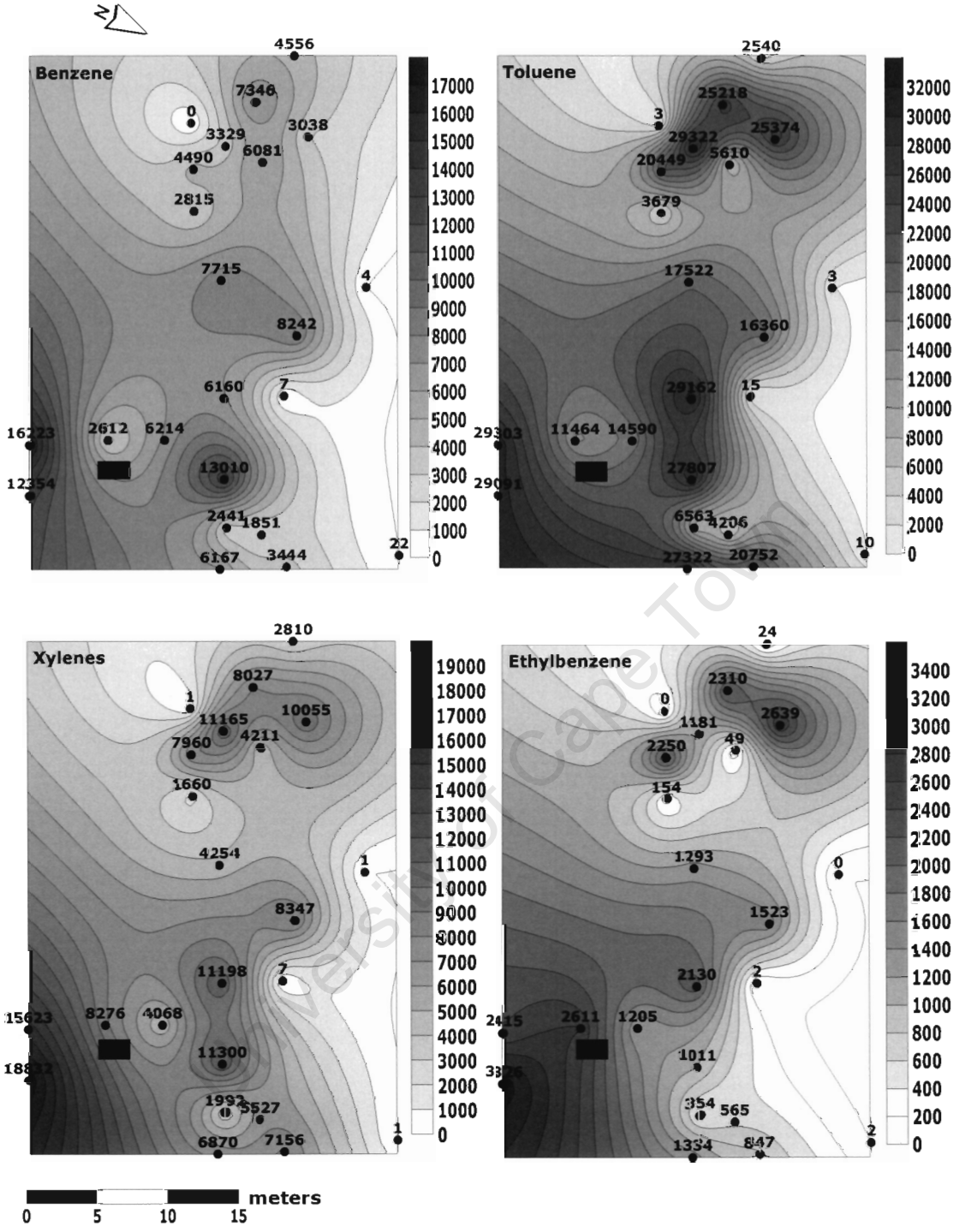

Figure 4.1g: Contour plot showing the spatial distribution of BTEX concentrations measured across the contaminated site. All concentrations reported as $\mu g.l^{-1}$. The black rectangle denotes the point of discharge.

4.2 BTEX concentrations

For the most part, the different BTEX compounds appear to be concentrated nearest the spillage point (Figure 4.1f). Further west of this area, near MW 38, and MW 32, a second elevated concentration zone is observed, particularly for the TEX components. Moreover, concentrations of xylene isomers, together with Toluene, are significant near MW 25 and MW 24. For Benzene, the distribution appears more uniform in its distribution pattern. Interestingly, MW 19, MW 27, MW 30, and MW 36 all show concentrations of BTEX which are significantly reduced, or below detectable concentrations. Moreover, MW 19, MW 27, and MW 30 are positioned north, north west of the point of discharge.

4.3 Sulphate reduction rates using radiotracer experiments

The ensuing text describes the results for sulphate reduction rates (SRR), which were calculated, based on the radiotracer experiments. It should be noted that the SRR's reported are based on the average rate calculated for triplicate vials.

4.3.1 *In situ* sulphate reduction rates determined using the radiotracer technique

In situ SRR's for MW 24 (233 ± 66 $nm.cm^{-3}.d^{-1}$; ±1σ, n = 3) and MW 28 (116 ± 31 $nm.cm^{-3}.d^{-1}$; ±1σ, n = 3) are the lowest recorded for the 4 wells sampled (Figure 4.2). MW 27 is observed to have the highest calculated SRR at 6,360 ± 6,166 $nm.cm^{-3}.d^{-1}$; ±1σ, n = 3, followed by MW 19, at 1,950 ± 273 $nm.cm^{-3}.d^{-1}$ (±1σ, n = 3).

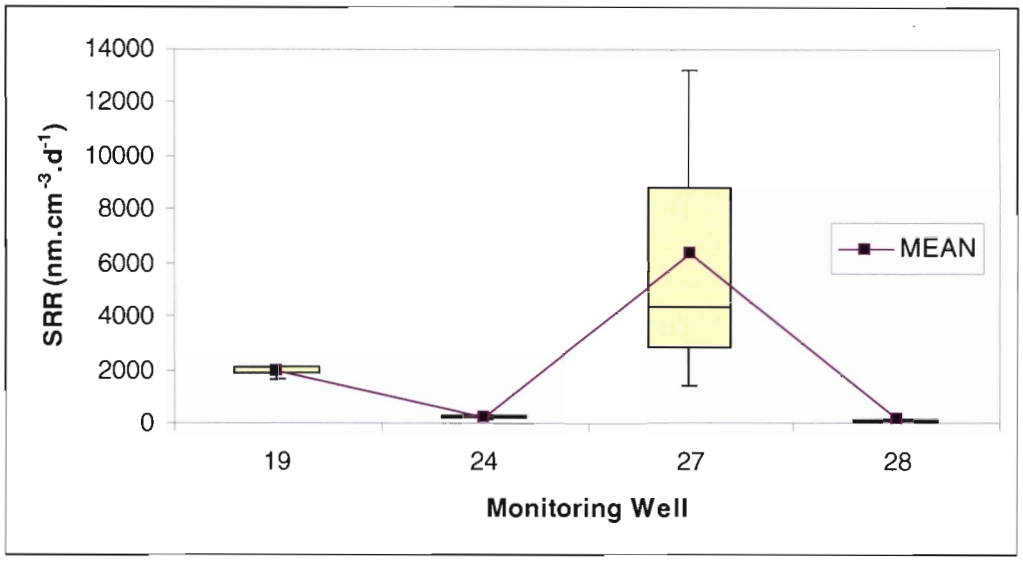

Figure 4.2: *In situ* sulphate reduction rates calculated samples extracted from MW 19, MW, 24, MW 27, and MW 28.

4.3.2 Sulphate reduction rates following sulphate amendments using the radiotracer technique

Calculated SRR's for MW 27 consistently increased following sulphate amendments (Figure 4.3). The addition of 0.1 mM K_2SO4 resulted in the lowest recorded SRR of 316 ±146 $nm.cm^{-3}.d^{-1}$ (±1σ, n = 3), whereas the highest recorded SRR of 95,482 ± 24,868 $nm.cm^{-3}.d^{-1}$ (±1σ, n = 3) was calculated following the addition of 28 mM K_2SO4.

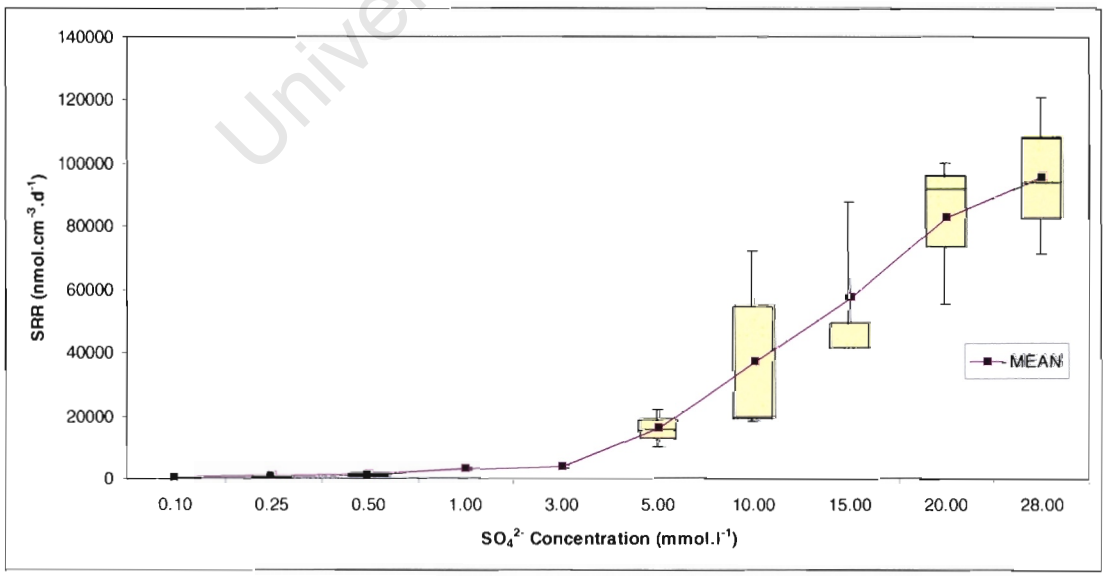

Figure 4.3: Plot showing sulphate reduction rates for MW 27 following sulphate amendment experiments.

Generally speaking, SRR's increase following sulphate amendments to samples extracted from MW 28 (Figure 4.4). The trend is however inconsistent, with a observed spike evident following 1 mM K_2SO_4 additions. Moreover, calculated mean SRR's appear to peak at 84,347 ± 26,794 nm.cm^{-3}.d^{-1} (±1σ, n = 3) after increasing sulphate concentrations to 15 mM. A comparison of calculated SRR's for corresponding SO_4^{2-} additions shows that MW 28 tends to be higher than those calculated for MW 27.

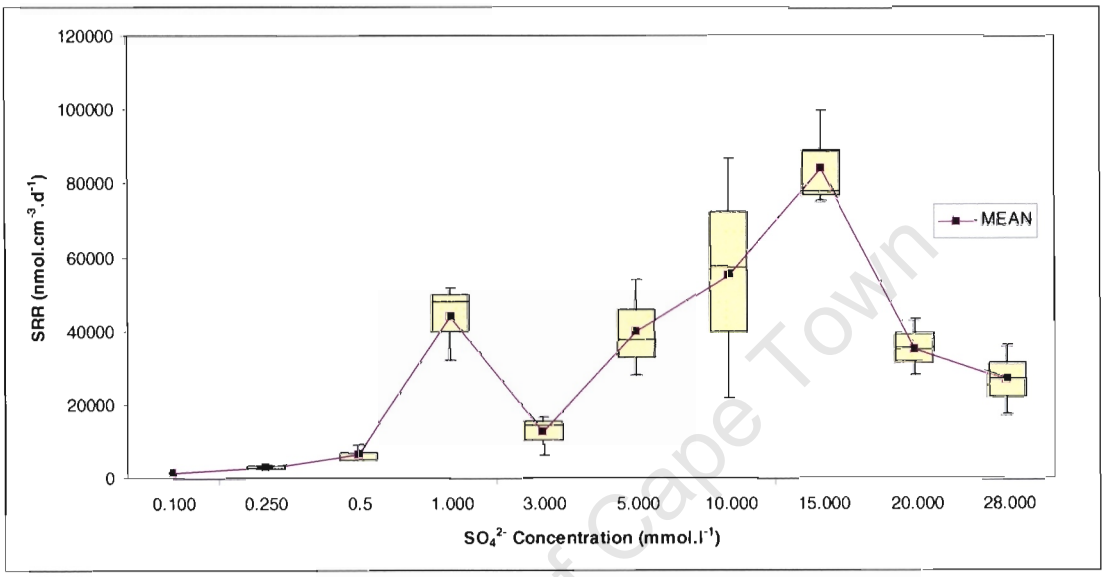

Figure 4.4: Plot showing sulphate reduction rates for MW 28 following sulphate amendment experiments.

4.3.2.1 Monod kinetic constants

Using the linearized form of the Monod equation (Lineweaver-Burke plots), the half saturation constants, K_s, and the R_{max} values for MW 27 and MW 28 were determined (Figures 4.5 and 4.6). For MW 27 an R_{max} of 25,000 nmol.cm^{-3}.d^{-1} and a K_s of 7.5 mM was determined. By contrast, the calculated R_{max} and K_s calculated for MW 28 are 50,000 nmol.cm^{-3}.d^{-1} and 3.5 mM respectively.

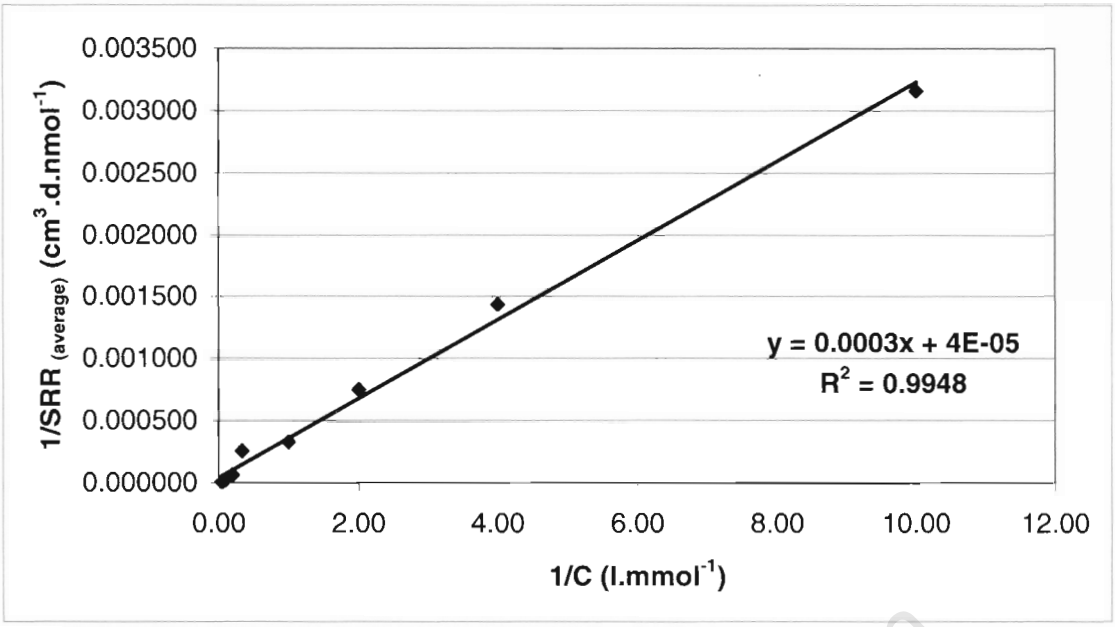

Figure 4.5: Lineweaver-Burke plot for MW 27 following sulphate amendment experiments.

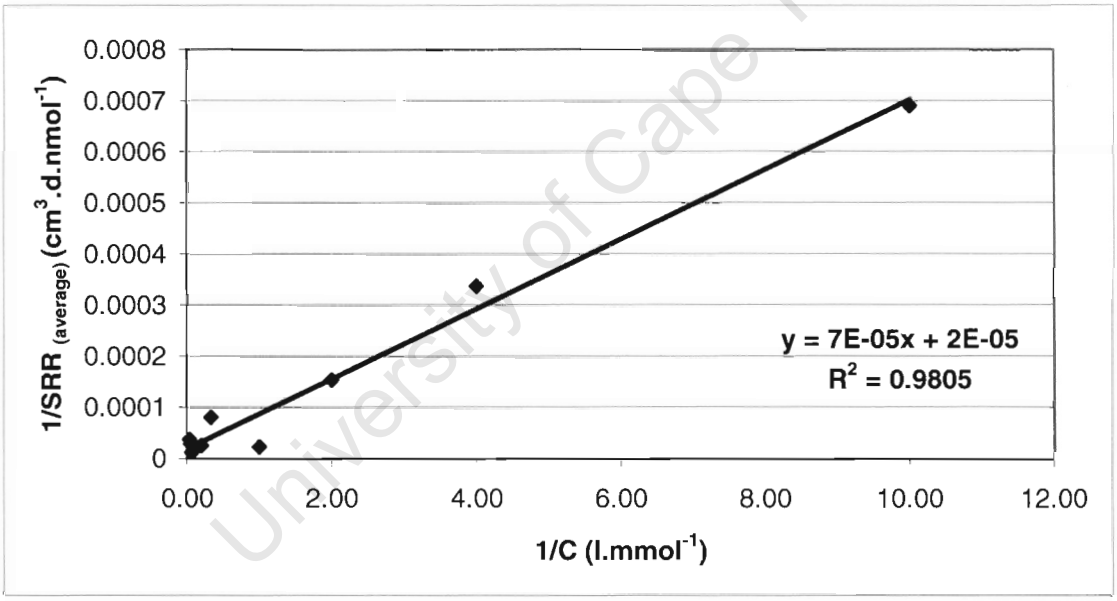

Figure 4.6: Lineweaver-Burke plot for MW 28 following sulphate amendment experiments.

4.3.3 Sulphate reduction rates following sulphide amendments using the radiotracer technique

The average SRR following sulphide amendments on sediment samples extracted next to MW 27 appear to be constant (Figure 4.7). The average SRR's range between 3,508 nmol.cm^{-3}.d^{-1} (n = 3) and 5,150 nmol.cm^{-3}.d^{-1} (n = 3). These values correspond to 0.5 mM and 3 mM Na_2S concentrations respectively. The mean *in situ* rate (7,325 nmol.cm^{-3}.d^{-1}), is significantly higher than the calculated

rates for samples amended with $Na_2S.6H_20$. It should be noted that the mean values were calculated by averaging the SRR results and thereafter subtracting the calculated mean control SRR (4,511 nmol.cm^{-3}.d^{-1}; n = 3). This should be considered when verifying the results in Table B5 (Appendix B).

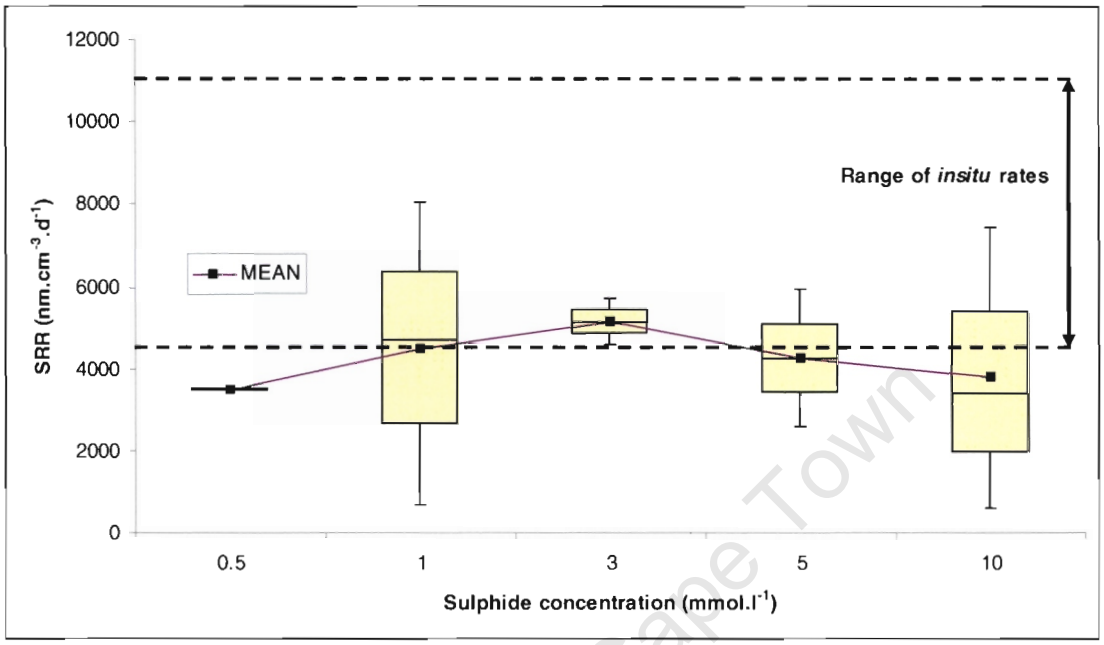

Figure 4.7: Plot showing SRR's following amendment of samples extracted from MW 27 with varying sulphide concentrations.

4.3.4 Sulphate reduction rates following organic salt additions suing the radiotracer technique

The effects of SRR following the addition of simple organic acids to samples extracted from MW 27 were variable (Figure 4.8). By comparison to the calculated *in situ* rate 7,352 nm.cm^{-3}.d^{-1}, sodium lactate addition appeared to increase the average SRR (10,139 nmol.cm^{-3}.d^{-1}). Calculated SRR's following amendments with sodium formate and sodium acetate were lower (5,504 and 4,311 nmol.cm^{-3}.d^{-1} respectively). Significantly, these rates fell below the *in situ* rate.

It should be noted that the averaged SRR for formate was based on duplicate vials, as the first sample, Formate (a), cracked following centrifuging. Moreover, CPM distillate counts for the third acetate sample, Acetate (c), was deemed too low to truly reflect the SRR and as such were excluded from the calculations. Moreover , as per the sulphide experiments in 4.3.3 above, the mean SRR's were calculated and thereafter the averaged SRR (4,484 ± 354 nm.cm^{-3}.d^{-1} (±1σ, n =

3) for the control was subtracted. This accounts for the discrepancies between the above reported values and those tabulated in Table B6 (Appendix B).

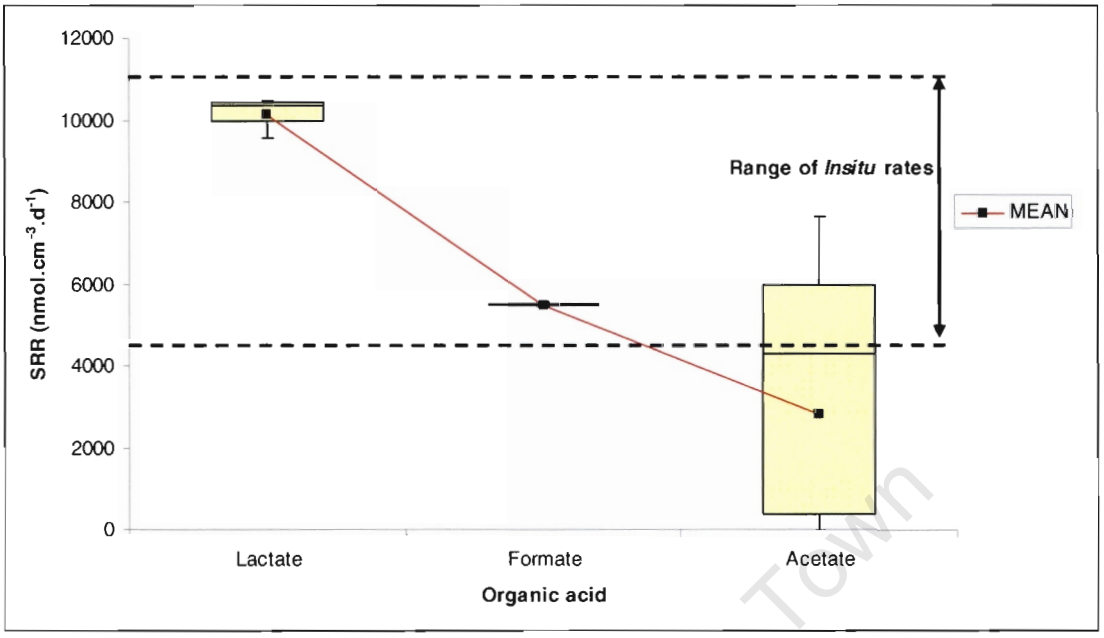

Figure 4.8: SRR calculated for MW 27 following the addition of simple organic salts.

4.3.5 Sediment incubations experiments

4.3.5.1 Pore water Fe^{2+} concentrations

Pore water concentrations for samples extracted from MW 27 fluctuated considerably over the 72-hour incubation period (Figure 4.9). The concentration peaked at t=48 (29,846 ± 8,987 nM (±1σ, n = 2). It should be noted that the mean pore water concentration at t =0 (7,535 ± 2,598 μM (±1σ, n = 2) for sample MW 27 differed significantly to the groundwater concentration (4 μM).

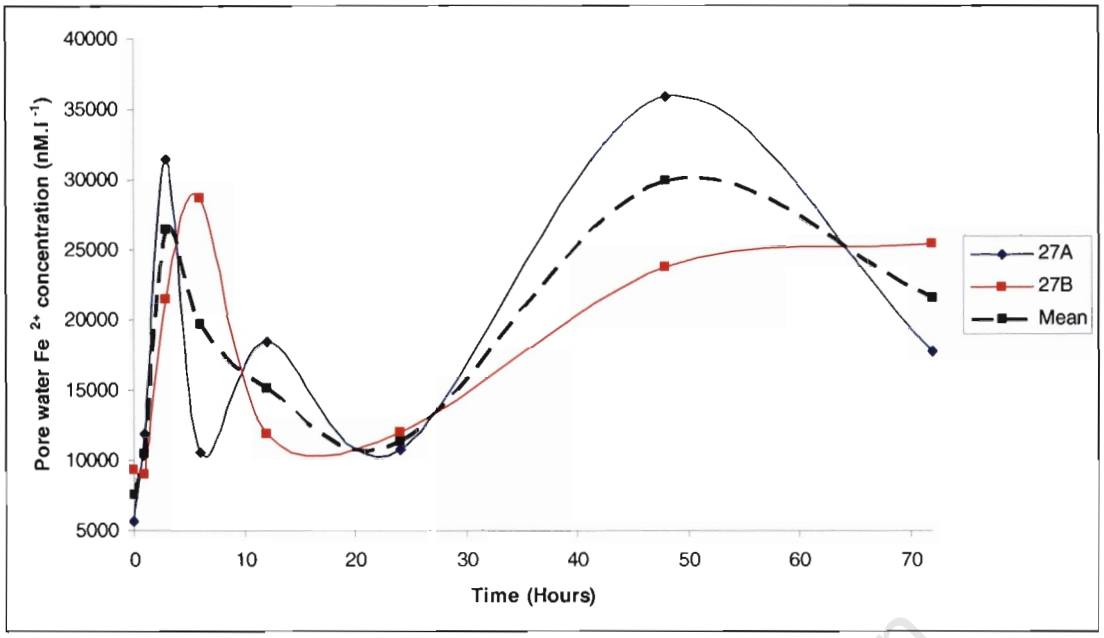

Figure 4.9: Pore water Fe^{2+} concentrations measured over a 72-hour incubation period for sediment extracted from MW 27.

Pore water concentrations for MW 28 show fluctuations within the first 3 hours of incubation (Figure 4.10). Thereafter the mean concentration levels off between t=6 and t=48. It should be noted that the concentration at t=24 could not be determined as the vials sacrificed cracked after centrifuging. A further increase in the mean Fe^{2+} concentration is noticed at t=72 (112,811 ± 182 nM (±1σ, n = 2). As per MW 27, mean pore water concentrations at t=0 (17,047 ± 5,561 nM; ±1σ, n = 2) significantly differ to the calculated groundwater concentration (570 μM).

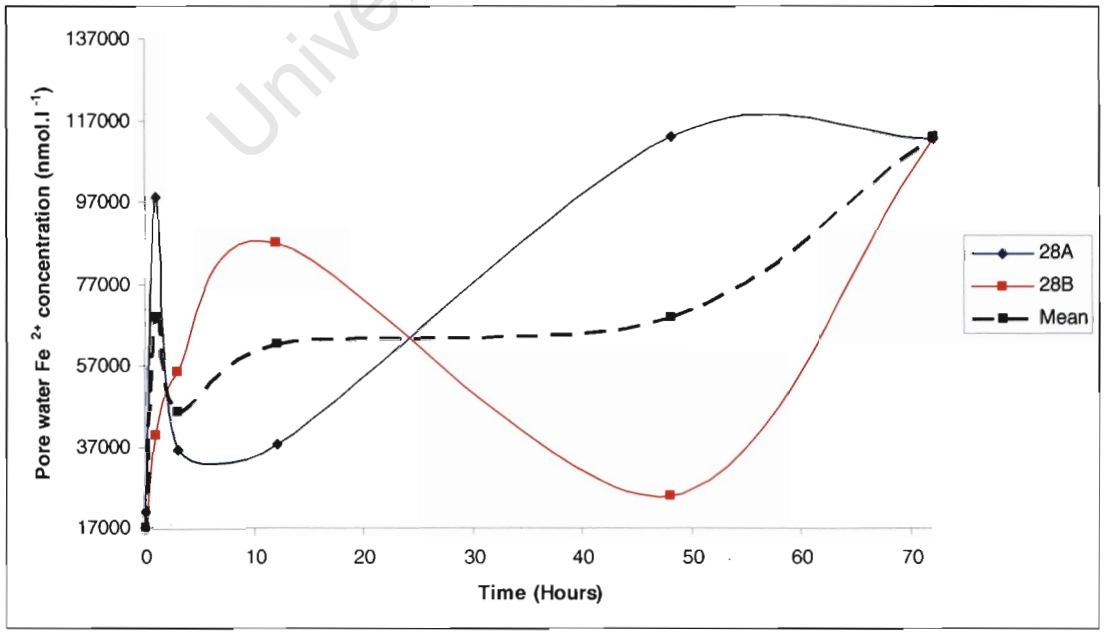

Figure 4.10: Pore water Fe^{2+} concentrations measured over a 72-hour incubation period for sediment extracted from MW 28.

4.3.5.2 Pore water SO_4^{2-} concentrations

For incubated sediment extracted from MW 27, mean pore water SO_4^{2-} concentration (2,792 ± 162 µM; ±1σ, n = 2) peaks at t=1 (Figure 4.11). Between t=1 and t=12, SO_4^{2-} concentration declines rapidly, and thereafter the rate of SO_4^{2-} reduction slows. The first hour aside, overall, SO_4^{2-} concentrations decline during the 72-hour incubation experiment. It should be noted that the groundwater concentration (2,910 µM) measured for MW 27 shows similarities to the mean measured pore water concentration at t=0 (2,723 151 µM; ±1σ, n = 2).

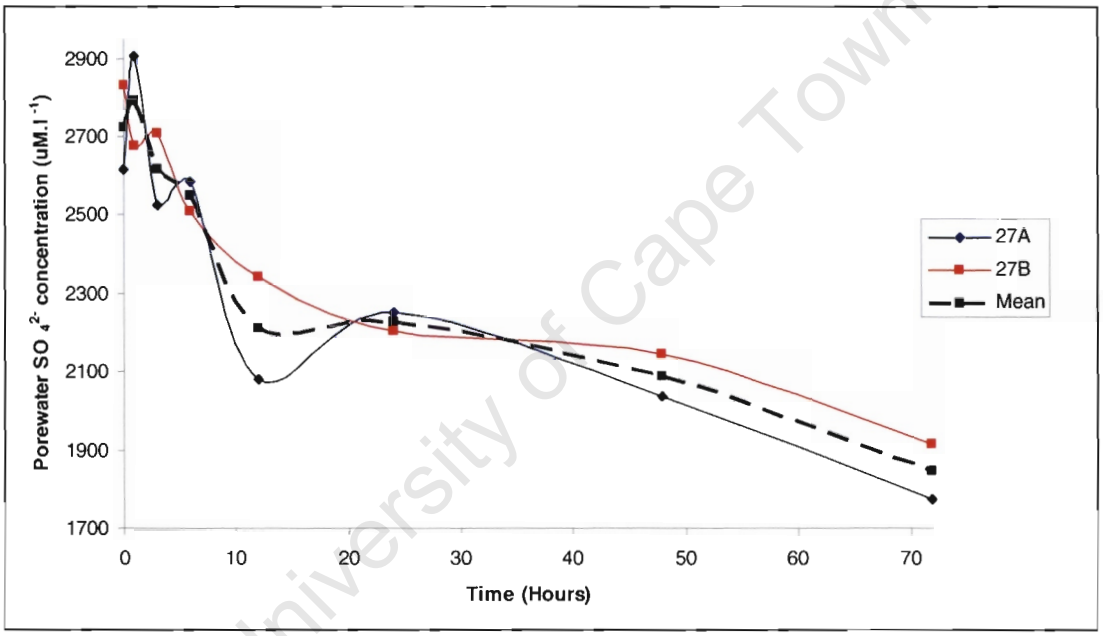

Figure 4.11: Pore water SO_4^{2-} concentrations measured over a 72-hour incubation period for sediment extracted from MW 27.

The results for MW 28 appear more consistent when compared to MW 27 (Figure 4.12). Average SO_4^{2-} concentration declines rapidly in the first hour of incubation. At t=0, SO_4^{2-} measured 4,335 ± 54 µM, (±1σ, n = 2) and at t=1, it measured 3,334 ±540 µM, (±1σ, n = 2). This was followed by an increase at t=3 (4,014 ± 313 µM; ±1σ, n = 2). Thereafter the concentration was observed to consistently decline, before tapering around t =24. It should be noted that results for t=6 were not possible as the vials sacrificed at this time cracked whilst in the centrifuge.

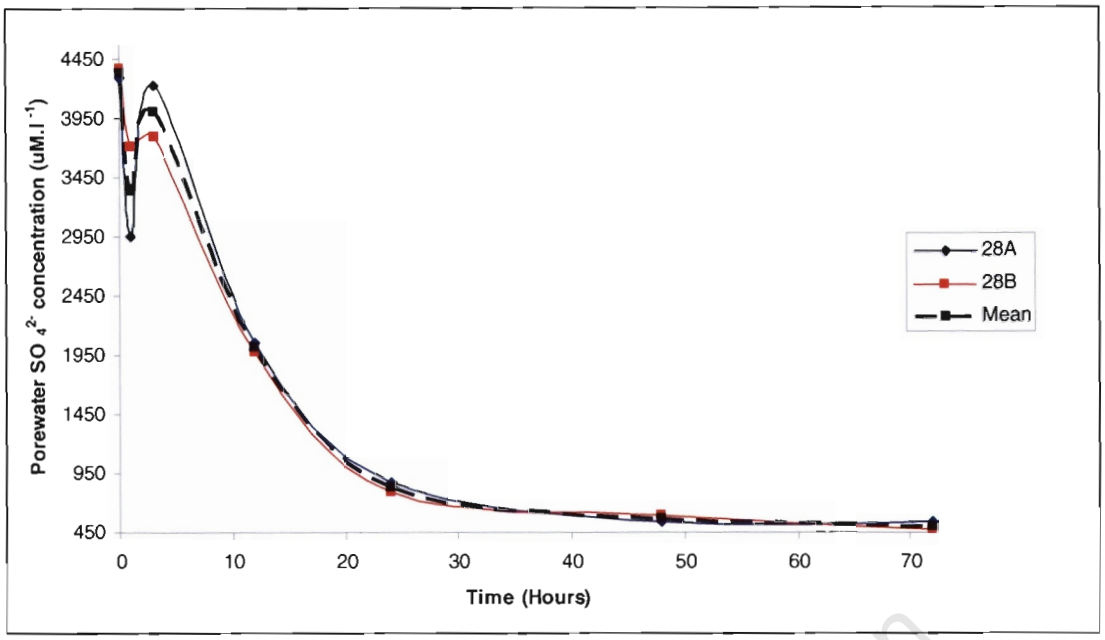

Figure 4.12: Pore water SO_4^{2-} concentrations measured over a 72-hour incubation period for sediment extracted from MW 28.

4.3.5.3 Solid phase Fe^{2+} extractions

Solid phase Fe^{2+} extracted from sediments fluctuate throughout incubation experiment for both MW 27 and MW 28 (Figure 4.13 and 4.14). The mean concentration ranges between 9,834 $nm.cm^{-3}$ (t=0) and 12,179 $nm.cm^{-3}$ (t=72) for MW 27, whereas for MW 28, the range is 4,640 $nm.cm^{-3}$ and 9,741 $nm.cm^{-3}$, measured at t=24 and t=72 respectively. Again it should be noted that for MW 28, the mean concentration for t=6 could not be determined as the vials cracked following centrifuging.

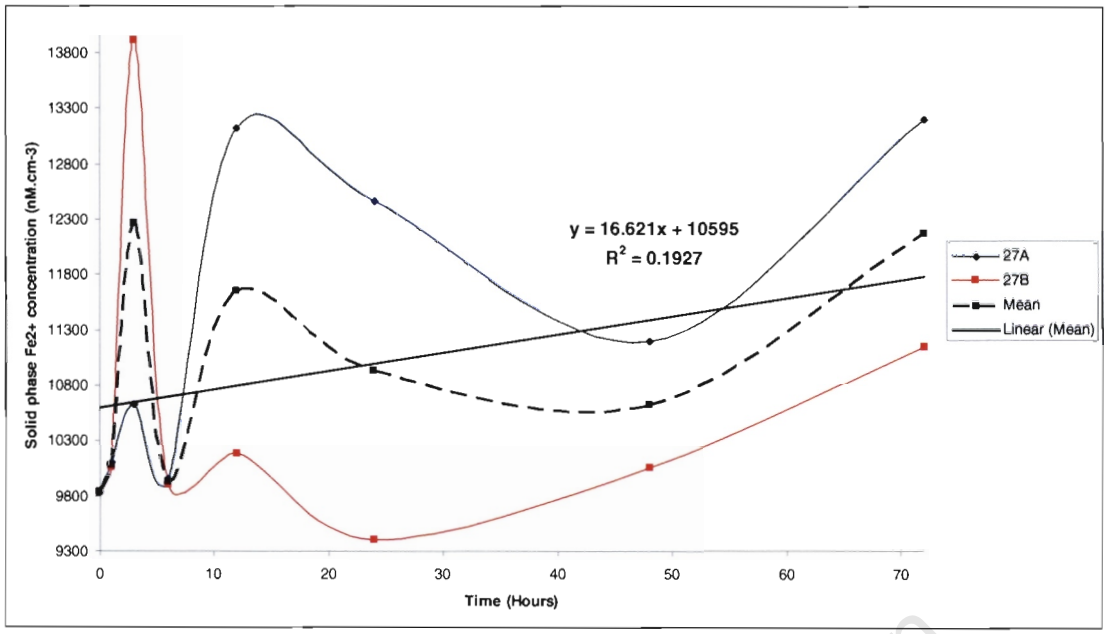

Figure 4.13: Solid phase Fe^{2+} concentrations measured over a 72-hour incubation period for sediment extracted from MW 27.

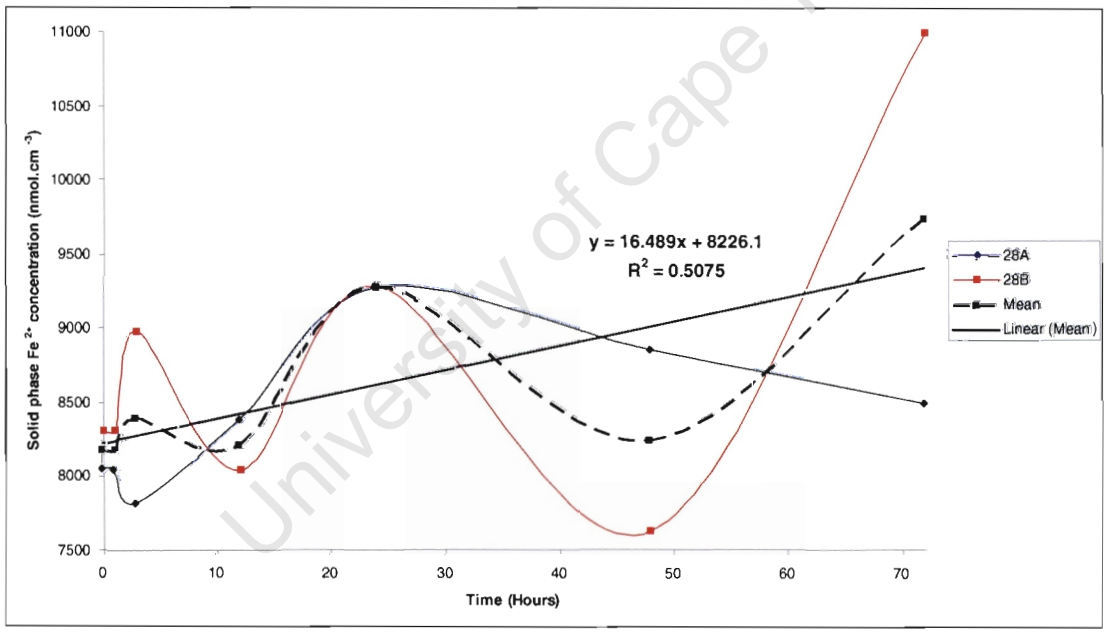

Figure 4.14: Solid phase Fe^{2+} concentrations measured over a 72-hour incubation period for sediment extracted from MW 28.

CHAPTER 5 – DISCUSSION

5.1 Groundwater chemistry

5.1.1 pH

The oxidation of organic materials within the contaminated plume consumes H^+ ions resulting in alkalinity (Table 2.1). However the analysis of background samples reveals pH values higher than those observed in the polluted groundwater environment. This observation is in agreement with the findings of Merrett (2003) and may best be explained by the precipitation of HCO_3^- along with iron thus reducing alkalinity in the plume. The narrow pH range for both the background and contaminated samples (6.6 – 7.2) can be explained by the buffering effect of calcareous shells present within the sands. This is in agreement with Chapelle (1993) who attributes these restricted ranges to the buffering capacity of the carbonate and silicate minerals that generally make up aquifers of this type. Generally speaking, anaerobes are sensitive to pH and operate efficiently in a narrow range. This range is observed to be between 6 and 8 (Norris *et al.*, 1994; Pepper and Josephson, 1996). Pfennig *et al.* (as cited in Fauque, 1995) suggests that for SRB the optimal pH is slightly alkaline (7 – 7.8). Of the contaminated samples, only MW 21, and MW 27, MW 28 falls within this range. All others fall within the range mentioned by Norris *et al.* (1993) and Pepper and Josephson (1996).

5.1.2 Alkalinity

Generally speaking, Alkalinity readings for the site are high, with average values for background and contaminant plume samples 8.2 mM and 8.5 mM respectively. One possible explanation for this may be the result of groundwater moving through the Langebaan (aeolian, calcrete capped calcareous sandstone) and Witzand (aeolian, calcareous, quartzose sand) Formations.

Additionally the production of CO_2 via microbial respiration, following iron and sulphate reduction, may also contribute to elevated alkalinity readings. The dissolution of CO_2 in aqueous environments will produce carbonic acid:

$$CO_2 + H_2O + \rightarrow H_2CO_3$$

Given the range of pH values at the site (between 6.6 - 7.2), the carbonic acid produced can be expected to dissociate to form H^+ and HCO_3^- via the following reaction:

$$H_2CO_3 \rightarrow H^+ + HCO_3^-$$

Thus the overall dissolution of CO_2 can be expressed as follows:

$$CO_2 + H_2O \rightarrow H^+ + HCO_3^-$$

Based on moles per mole stoichiometric turnover (Table 4.1), the processes of Fe^{3+}, and SO_4^{2-} reduction all contribute to the elevation of alkalinity.

Table 5.1: Contributions of alkalinity of redox processes involved in hydrocarbon mineralisation (Hunkeler *et al.,* 1999).

Process	**Contribution to alkalinity** [a]
Microbial hydrocarbon mineralisation [b]	
$0.17\ CH_{1.85} + FeOOH_{(s)} + 2\ H^+ \rightarrow 0.17\ CO_2 + Fe^{2+} + 1.66\ H_20$	+2
$1.37\ CH_{1.85} + SO_4^{2-} + 2\ H^+ \rightarrow 1.37\ CO_2 + H_2S + 1.26\ H_20$	+2

[a] Moles per mole stoichiometric turnover
[b] Average H/C ratio in diesel fuels of 1.85. All species given in the form in which they exist as the reference point of the alkalinity titration (pH=4.3). Thus the number of protons produced or consumed corresponds to alkalinity consumption or production.

Thus where the aforementioned processes are identified to take place within the contaminant plume, alkalinity levels should be greater than those recorded in background samples. Background alkalinity ranges between 7.6 mM and 9.2 mM and is associated with undetacble levels of Fe^{2+}, and low S^{2-}. Whilst alkalinity measurements in a number of polluted water samples are greater than those of background samples, this is not always observed to be the case, despite consistently higher Fe^{2+} and S^{2-} measurements. The reasons for this inconsistency are unknown.

5.1.3 Redox potentials

Redox potentials throughout the contaminated plume are negative, and are consistent with reducing conditions. Moreover, a comparative analysis of the oxygen and E_h contour plots suggests a positive correlation between measured values (Figures 4.1a and 4.1b). This is to be expected since oxygen concentrations are, as a rule, low in the presence of highly reducing environments.

The range of Eh values (-57 – (-302) mV) denotes mixed potentials (Figure 2.1). Fe^{3+} reduction tends to be associated with E_h values near -100 mV. The Fe^{2+} contour plot coincides with similar E_h values, which suggests that Fe^{3+} reduction is possibly taking place near the spillage point (Figure 4.1d).

The lowest values are found immediately to the north and north west of the point of discharge, and would suggest SO_4^{2-} reduction and or methanogenisis to be the dominant metabolic processes. Sulphide concentrations, indicative of SO_4^{2-} reduction, are greatest at MW 25, MW 26, and MW 35 and falls within the area of lowest Eh. It could therefore be argued that SO_4^{2-} reduction is the dominant process taking place in this part of the plume. It should be noted that the absence of detectable S^{2-} concentrations does not necessarily imply an absence of sulphate reducing conditions, since these anions may be precipitated out of solution in the presence of iron (Ulrich *et al.*, 1997). This further confirms the usefulness of E_h measurements in assessing metabolic pathways. However, as alluded to in section 2.9, Eh measurements should be looked at relative to each other rather than as absolute values, since natural waters are rarely at equilibrium (Lindberg and Runnels, 1984). Note that, parameters to account for the occurrence for methanogensis were not measured.

5.1.4 Temperature

An increase in temperature is associated with an increase in chemical reactions (Chapelle, 1993). Thus temperature plays an important role in microbial growth, and therefore impacts on the rates of bioremediation. Most natural groundwater systems exhibit a temperature range of 20 – 30 °C, and are dominated by microorganisms termed *mesophiles* (Chapelle, 1993). The temperature range, incorporating both background and contaminated samples, was found to exist between 17.5 and 22 °C, which is close to that of natural groundwater systems.

The optimum temperature range for growth of most microorganisms present in shallow aquifers is between 25 and 40 °C (Borden, 1994).

5.1.5 Concentrations of SO_4^{2-} , Fe^{2+}, S^{2-}

The spatial distribution of Fe^{2+} and S^{2-} indicates that Fe^{3+} and SO_4^{2-} reduction are taking place (Figure 4.1d and 4.1e). Interestingly the pattern of distribution suggests that these metabolic pathways dominate in isolation of each other. For example, Fe^{2+} is most concentrated near the spillage point (MW 4, MW 6, and MW 7) as well as at MW 28. By comparison, S^{2-} concentrations are at their lowest for the same monitoring stations. Conversely, at MW 19, MW 25, MW 26, MW 30, MW 31 and MW 40, Fe^{2+} is correspondingly low in the presence of elevated S^{2-}.

There are two possible explanations for this. Fe^{3+} reducers have been shown to inhibit the activity of SRB, thereby establishing areas of high Fe^{2+} concentrations (Chapelle and Lovely, 1992). The study showed that Fe^{3+} reducers were able to maintain substrate levels below the requirements for significant activity of SRB. Hoever this seems unlikely in this case since, certain parts of the plume are charaterised by low Fe^{2+} concentrations in the presence of SO_4^{2-}.

The alternative, and most likely explanation may be that in the presence of Fe^{2+}, the concentrations of detectable S^{2-}, is modulated through the precipitation of iron sulphide minerals either as FeS_2 or FeS (Ulrich *et al.*, 1997). Assuming this to be true, then concomitant Fe^{3+} and SO_4^{2-} reduction could be concluded. Moreover it would suggest that the rates of Fe^{3+} reduction exceed those of SO_4^{2-} reduction.

Figure 4.1c shows that SO_4^{2-} concentrations are detectable, however they are lowest nearer the spill site as well as west of this area. This is associated with elevated Fe^{2+} and low S^{2-} concentrations. This further adds weight to the idea that tandem Fe^{3+} and SO_4^{2-} reduction is likely taking place,

The highest recorded SO_4^{2-} concentrations are measured at MW 19 (1,107 µM), MW 25 (1,025 µM) and MW 27 (2,825 µM) which coincide with significantly low Fe^{2+} concentrations. S^{2-} concentrations for the same locations are some of the highest recorded (27, 25.5 and 18 µM). It is likely therefore that for these areas Fe^{2+} is the limiting factor during the formation iron sulphide precipitates during concomitant Fe^{3+} and SO_4^{2-} reduction, since the free sulphides suggest SO_4^{2-} reduction exceeds Fe^{3+} reduction.

5.1.6 BTEX concentrations

Hydraulic flow coupled to SO42- reduction may explain the observed spatial distribution for BTEX concentrations. Where hydraulic flow is reported, anaerobic TEA's are generally segregated into distinct zones (Lyngkilde and Christensen, 1992). From a thermodynamic sense, methanogenesis typically predominates up gradient near the source of contamination, since Fe^{3+} and SO_4^{2-} are depleted first. Thereafter the sequence moving away from the plume is Mn^{4+}, NO_3^- and finally O_2 (Figure 5.1).

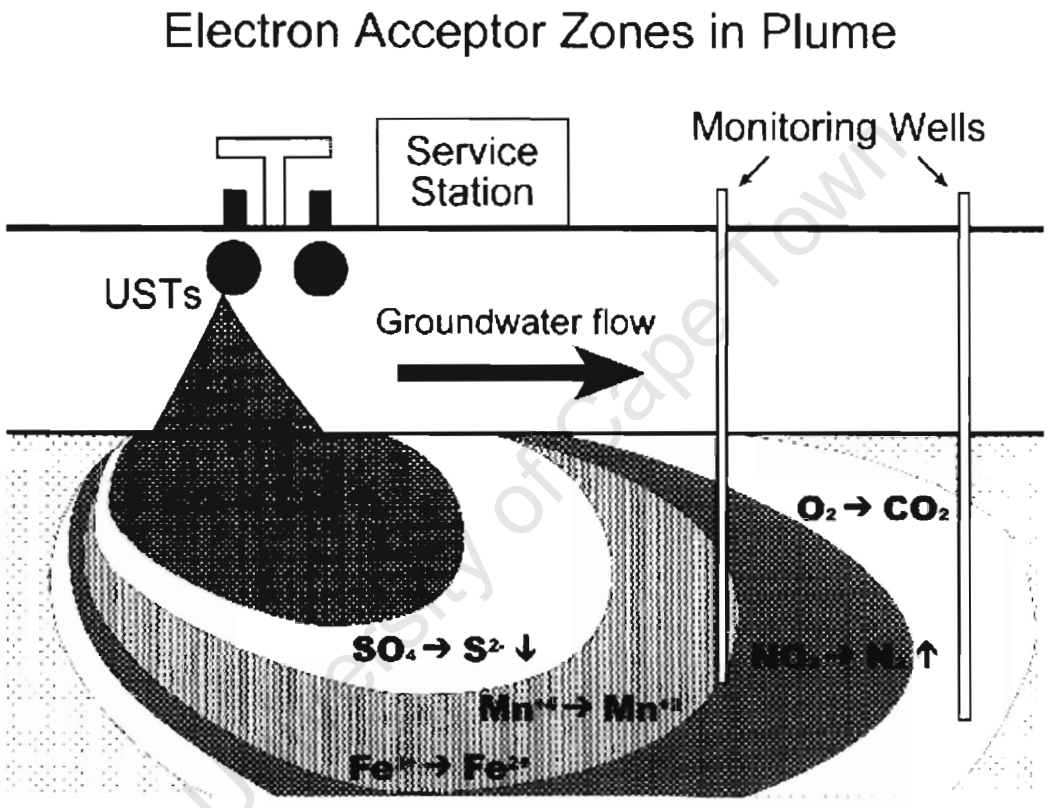

Figure 5.1: Typical distribution of TEA processes in a petroleum contaminated aquifer. (UST - underground storage tank)

This zonation pattern is typical of fast flowing groundwater, however in the absence of data, hydraulic flow is suspected to be slow at this site, since the topography of the Cape Flats region is characteristically flat. Slow moving groundwater tends to result in overlapping zonation patterns (Merrett, 2003). Generally speaking the flow appears to be in a westerly, and south westerly direction, relative to the spillage point

The distribution of SO_4^{2-}, S^{2-}, and Fe^{2+} concentrations indicates that SO_4^{2-} reduction is dominant process taking place north and north west of the point of

discharge, since this area is coincident with elevated SO_4^{2-} and S^{2-}. Additionally BTEX concentrations for the same area appear to be lowest, further suggesting that SO_4^{2-} reduction is acting efficiently along what appears to be the fringe of the plume.

Fe^{2+} concentrations, indicative of Fe^{3+} reduction, are coincident with high BTEX concentrations. Thus while Fe^{3+} reduction is taking place, it appears to be less efficient at BTEX removal compared to SO42- reduction. This is in agreement with the stoichiometry of the two species. For example, the ratio of the number of mol required to mineralize a single mol of Toluene is 0.22 for SO_4^{2-}, compared to 0.03 for Fe^{3+} (Table 2.1). This is an important observation since it may suggest that SO_4^{2-} is the predominant mechanism responsible for the fate of BTEX in this system. If this is believed than reduced SO_4^{2-} concentrations may be limiting the rate of BTEX removal which would suggest that amending the system with additional sulphate could prove to be useful in expediting bioremediation.

5.2 *In situ* sulphate reduction rates determined using radiotracer technique

Taking the two extremes for the samples, figure 4.2 shows that MW 27 recorded the highest calculated SRR (6,360 ±6,166 $nm.cm^{-3}.d^{-1}$; ±1σ, n = 3), whereas MW 28 was calculated to have the lowest SRR (116 ±31 $nm.cm^{-3}.d^{-1}$; ±1σ, n = 3). A comparison of SO_4^{2-} and BTEX concentrations for groundwater extracted from MW 27 and MW 28 reveals stark differences and likely explains this observation.

MW 27 has a high SRR in the presence of high SO_4^{2-} (2,825 µM), and low BTEX concentrations. Conversely, MW 28 has a low SRR where the concentrations of SO_4^{2-} (122 µM) and BTEX are respectively low and high. Thus despite limited substrate at MW 27, the SRR remains high, which suggests that SO_4^{2-} is the limiting factor controlling the SRR. Similar results were observed by Bordreau and Westrich (1984), who showed via SRB colonising marine sediments, that the SRR was limited by SO_4^{2-} concentrations below 3 mM. The measured SO_4^{2-} at the samples sites fall below this threshold.

The results for MW 24, however suggest that the substrate concentration may be limiting to a small degree. MW 24 with a SRR of 233 $nmol.cm^{-3}.d^{-1}$ is twice that of MW 28 at 116 $nmol.cm^{-3}.d^{-1}$, notwithstanding a lower SO_4^{2} concentration by comparison to MW 28. BTEX measurements show that for MW 28, the concentrations are comparatively lower (except for Ethylebenzene), thus the

system may be substrate limited at MW 24. Alternatively the resident SRB population may be reduced at MW 24, or perhaps phylogenetically different.

Previous work has shown that the reactivity of organic matter can control the overall SRR, (Jakobsen and Postma, 1999). In sediments taken from a shallow sandy aquifer, SRR were reported to be high, despite low SO_4^{2-} concentrations. Overall, BTEX concentrations at this site do not appear to be limiting.

Taking the *in situ* rates then, the predicted rates at which the various BTEX compounds will degrade can be calculated stoichiometrically (Table 5.2).

Table 5.2: Predicted rates of BTEX degradation coupled to sulphate reduction. The rates are predicted from the calculated *in situ* rates during radiotracer experiments and the reaction stoichiometry in Table 2.1.

Monitoring Well	Benzene Oxidation	Toluene Oxidation	Ethylebenze Oxidation	Xylene Oxidation
MW 19	526.50	0.08	0.03	0.01
MW 24	62.91	44.97	81.47	2.57
MW 27	1717.20	0.02	0.04	0.01
MW 28	31.32	28.49	47.93	3.87

All measured and predicted rates are given in $nmol.cm^{-3}.d^{-1}$

The efficiency at which Benzene removal is predicted to take place is noted. Benzene is a known carcinogen, and therefore its removal is of high importance. Indeed, Anderson and Lovley (2000) linked benzene removal to sulphate additions from samples taken from a petroleum contaminated aquifer located at Ponca City, Oklahoma. Studies with ^{14}C acetate and molybdate concluded that sulphate reduction was the primary TEA.

5.3 The effects on SRR determined by radiotracer experiments following sulphate amendments

Further evidence demonstrating the limiting effect of SO_4^{2-} concentrations was observed following sulphate amendments to sediments extracted from MW 27, and MW 28.

For MW 27, samples amended with increasing SO_4^{2-} concentrations correlated to a steady increase in the SRR (Figure 4.3), with perhaps a hint of an approaching threshold between 20 and 28 mM. BTEX concentrations at the start of the

experiment were assumed to be equal in all samples. Furthermore, by first incubating the samples for 24 hours, it was further assumed that starting SO_4^{2-} concentrations were minimal, if not completely reduced by the resident SRB. Thus, based on these assumptions, it is highly likely that the increased SRR are a direct consequence of SO_4^{2-} additions, and thus SO_4^{2-} is suspected to limit SRR's and therefore by proxy, the rate of hydrocarbon degradation.

The fluctuating SRR's following amendments to sediments at MW 28 did not fully reflect the results obtained from sediments at MW 27 (Figure 4.4). Although a similar trend was observed, SRR's showed a marked increase at 1 mM additions, whereas for 20 and 28 mM additions the SRR's decreased. These variations are likely the consequence of the scintillation counts recorded to detect the radioactive disintegrations following the addition of the radiotracer ($^{35}SO_4^{2-}$).

Samples 1 (b) and 1 (c) reported significantly high distillate counts, whereas for 20 (b), 20 (c), 28 (b) and 28 (c), the counts were low (Appendix B). High CPM distillate values are indicative of increased levels of radioactive sulphide which may be the result of a large SRB population increasing the overall SRR, or alternatively, accidental contamination of the distillate with excessive radiotracer. For low values, the converse is true. Given that the supernatant counts for the offending samples were typical values for the volume of tracer added, it seems more likely that microbial populations accounted for the discrepancies.

Discrepancies aside, and assuming the plot for MW 28 follows a similar trend to that of MW 27, then it appears as though SRR's calculated for MW 28, are greater than those following corresponding SO_4^{2-} additions. An inspection of BTEX concentrations indicates stark differences. Substrate at MW 27 is significantly depleted by comparison to the abundance at MW 28 (Appendix B). Given that the same SO_4^{2-} concentrations were added, it therefore appears as though substrate limitation may, to a lesser extent, impact on the overall SRR.

Chapelle (1993) suggests that indigenous microorganisms are often required to acclimate upon the addition of unfamiliar TEA's. However given that groundwater SO_4^{2-} concentrations are highest at MW 27, acclimation is unlikely to account for the observed differences in SRR.

The results of this experiment have shown that SO_4^{2-} additions correlate positively to an increase in SRR. Furthermore, although substrate concentrations

appear somewhat responsible for observed differences in the SRR's, SO_4^{2-} concentrations are suspected of being the major limiting factor in BTEX removal.

5.4 Monod kinetics

To reiterate, the basis for most microbial growth models is expressed in terms of the empirically derived Monod equation (Monod, 1949). An assessment of the half saturation constant, K_s, establishes the concentration at which a limiting substance corresponds to one half the specific growth rate of the microbial organism. In keeping with the theme of this study, K_s values are calculated based on limiting SO_4^{2-} concentrations. For a more detailed discussion as to how the parameters (K_s *and* R_{max}) of the Monod equation are calculated, the reader is referred back to section 2.8.

Linewaver-Burke plots show the R_{max} calculated for MW 28 (50,000 $nm.cm^{-3}.d^{-1}$) is double that of MW 27 (27,000 $nm.cm^{-3}.d^{-1}$; Figures 4.5 and 4.6). Since R_{max} is dependant on a number of variables e.g. reactivity of individual BTEX compounds (Roychoudhury, *per. comm.* 2005), which is beyond the scope of this study, the implications of R_{max} will not be discussed further.

The observations in respect of K_s shows MW 27 at 7.5 mM to be more than double that of MW 28 at 3.5 mM. Since K_s quantifies the concentration at which the specific growth rate, R, is half its maximum, a doubling of the K_s values yields concentrations indicative of maximum specific growth rates. Thus for MW 28, 7 mM SO_4^{2-} concentration is required, whereas for MW 27 the concentration is 15 mM.

Roychoudhury (2004), observed disparate K_s values for samples taken from different hydrothermal springs in Yellowstone National Park, U.S.A. In this study it was suggested that the substrate uptake mechanism of the microbes was possibly inefficient. If this argument is applied to this study, then it may point to phylogenetically different SRB populations between sampled sites. Uniformity in terms of organic matter will add weight to this theory, since microbes will be exposed to the same substrate, which for this site is BTEX. This is possible Given that the organic matter is believed to be uniform throughout the site, and may point to between the two sites.

Furthermore, the reactivity of the organic substrate may have influenced the value of K_s since higher values are coincident with lower reactivity. Given that organic matter is assumed to be uniform across the contaminated area, the reactivity is likely to be same, thus excluding this as a possibility. Moreover, if there

Relating this back to the comparable SRR's following corresponding SO_4^{2-} dilution amendments, the disparities observed suggest that the existing BTEX concentrations at each sample site influences the SRR. To reiterate, the SRR's for MW 27 with significantly reduced substrate concentrations were shown to be lower than comparable SRR's calculated for MW 28.

Bioremediation strategies that potentially involve SO_4^{2-} additions at this site are reliant on these calculated K_s values. A look at *in situ* SO_4^{2-} concentrations measured at the time the sulphate tracer experiments were conducted, shows that both the *in situ* concentrations for MW 27 (2.35 mM) and for MW 28 (0.13 mM) are significantly lower than the respective K_s values. This suggests that there is scope to significantly increase SRR's. Based on the two sampled sites, and assuming a homogeneous, ubiquitous network of SRB's, then the minimum concentration of SO_4^{2-} required to ensure the most efficient rate of bioremediation, would be based on the largest K_s value. Applying SO_4^{2-} in excess is not only wasteful, but also costly from a financial standpoint, since the maximum rate of reduction across the site, is limited by the smallest determined microbial growth rates It could therefore be argued, that for this particular study, amending the contaminant plume by applying SO_4^{2-} at 15 mM concentrations, would likely yield the most efficient rate of BTEX biodegradation.

5.5 Sulphate reduction rates determined by radiotracer experiments following sulphide amendments

The literature review has described the potential inhibitory effects of sulphide on the activity of SRB (section 2.3). An assessment of the ability of the system to buffer against free sulphide accumulation is therefore necessary, particularly when considering the use of sulphate as a potential solution to expedite BTEX removal.

The results shown in figure 4.7 illustrate that relative to *in situ* conditions, SRR's were significantly reduced following increasing S^{2-} concentrations. Surprisingly

however, the reduced rates appeared consistent even following 10 mM additions, which suggest that concentrations in excess of 0.5 mM have no further impact on inhibition. Previous studies have indicated that SRR's decrease with increasing S^{2-} amendments (Edwards *et al.*, 1992). Furthermore, at high concentrations (≥ 5 mM), reduction was reported to cease completely.

The consistency in SRR for this study could in part be explained by the oxidation of biogenetic H_2S in the presence of aqueous Fe^{2+}. This would then remove a portion of free S^{2-} and thereby reduce the inhibitory effect. The presence of black precipitate, probably iron sulphide, observed in some of the sediment provides evidence for this. Furthermore, it appears that since inhibition is taking place, S^{2-} cannot effectively be removed from the system and is likely the result of limiting Fe^{3+} reduction. The presence of elevated *in situ* S^{2-} at MW 27 provides further evidence for this.

Iron sulphide formation aside, consistencies with respect to SRR's following amendments cannot be explained, since if the inhibitory effects of increasing S^{2-} are to be believed, calculated SRR's should show decline with increasing S^{2-} additions, especially if Fe^{3+} reduction rates are limiting. Unless there is some other mechanism to buffer the increased S^{2-} levels, this observation cannot be explained.

5.6 Sulphate reduction rates determined by radiotracer experiments following organic substrate addition

Perusal of available literature has indicated that SRB have developed affinities for particular substrate types. Given limited resources available affinities with respect to individual BTEX compounds was not possible. By amending samples with organic salts, characterized by disparate complexities, it was possible to determine, by proxy, whether the resident SRB were capable to BTEX removal.

Figure 4.8 shows that following the addition of lactate, the SRR increased relative to the *in situ* rate. Thus even in the presence of sufficient BTEX, lactate was preferred by the resident SRB. Indeed, these results support Kleikemper *et al.*, (2002) who describe lactate as being the most generic carbon source for SRB. The results for less complex organic acids add further credence to this idea. The SRR calculated following formate and acetate addition fall below the *in situ* rate,

therefore suggesting that less complex organic salts are not the substrate of choice.

One likely explanation may be that the resident SRB's at MW 27 resemble more modern sulphate reducers, since they are believed to have developed affinities to more complex organic compounds (Roychoudhury, 2004). If this is the case then it may serve as a proxy for SRB that have developed mechanisms capable of degrading more complex compounds like BTEX. This can only be confirmed following a phyllogenetic study, which is beyond the scope of this investigation.

The observed inhibitory effects on the SRR's following less complex organic salt additions are not easily explained. Certainly, rates below the *in situ* rate are unexpected. In a study by Sajemann *et al*. (cited in Roychoudhury, 2004), decreases in SRR were observed in psychrophiles from the Arctic Ocean where a complex mixture of organic substrates was added. No explanation was proposed for that study. These decreases may be the result of dilutions of sulphate on addition of the substrate, in which case the actual SRR following lactate addition is greater than that which is being reported.

5.7 Fe^{2+} and SO_4^{2-} reduction via incubation experiments

In assessing the ability of a system to buffer the toxic effects of free S^{2-} accumulation, it is necessary to establish the rates of iron reduction, as the presence of Fe^{2+} is known to precipitate S^{2-} out of solution as iron sulphides. To this end incubation experiments were conducted during which pore water Fe^{2+} and SO_4^{2-} pore water concentration were established. To this end incubation experiments were conducted over a 72-hour period.

A comparison of Fe^{2+} and SO_4^{2-} pore water concentration plots (Figures 4.9, 4.10, 4.11, and 4.12) hints at the possibility of the tandem reduction of Fe^{3+} and SO_4^{2-} during incubation experiments. For MW 27, the Fe^{2+} concentrations tended to vary considerably over the 72-hour incubation period. Within the first 3 hours, the concentration showed a rapid increase, before dropping off significantly in the 21 hours that followed. These fluctuations can possibly be explained in conjunction with the SO_4^{2-} concentration plot for the same sample site. Initially Fe^{2+} concentrations are expected to increase as Fe^{3+} is reduced. Thereafter the observed decrease in SO_4^{2-} levels over the same time period is likely to

precipitate Fe^{2+} out of solution as iron sulphide forms. As SO_4^{2-} levels ease, and therefore reduction rates slow, precipitation of iron sulphide is likely to ease. The result is that Fe^{2+} is again expected to increase. This is observed over a 24-hour period (from 24 to 48 hours). However, the period between 48 hours and 72 hours indicates that Fe^{2+} concentrations once again decrease, suggesting further precipitation of iron sulphide. The rate at which Fe^{2+} decreases is unexpected given that SO_4^{2-} reduction rates appear similar to rates for the previous 24-hour period. A possible explanation may lie in the observed increase in the oxygen levels of the anaerobic chamber recorded when vials were sacrificed after 72-hours. This is likely to have resulted in the oxidation of Fe^{2+}. The reasons for the elevated oxygen levels could not be established, however, it may be that the catalysts responsible for maintaining oxygen levels were faulty, or a leak in the chamber developed during the final hours of the experiment. Given time and financial constraints the experiment could not be repeated.

The results for MW 28 appear to be more consistent with the notion that concomitant Fe^{3+} and SO_4^{2-} reduction is taking place (Figures 4.10 and 3.12). The first hour of incubation shows that as pore water Fe^{2+} increases, so SO_4^{2-} decreases. Thereafter Fe^{2+} decreases, probably as a result of iron sulphide formation. The apparent spike in the SO_4^{2-} readings after 3 hours could be the result of oxidation, however this is unlikely given that SO_4^{2-} concentrations consistently decrease in the hours that follow. It should be noted that cracked vials resulting from the centrifuge, account for the lack of data for the 6-hour mark. Furthermore, the observed yellow colour of the pore water used to measure SO_4^{2-} concentrations is likely to have interfered with absorbancy readings when using the spectrophotometer. This possibly explains the significant difference between the groundwater SO_4^{2-} concentration (4,335 μM) and pore water concentration (148 μM) determined at the start of the incubation (t=0). Given the clear disparities, the reliability of the data is called into question.

Sufficient sample was preserved in 0.05 M HCl in the hope that accurate SO_4^{2-} concentrations could be determined using a Dionex Ion Chromotograph, however IC-equipment located at the Department of Geological Sciences and Chemistry Department at the University of Cape Town were not functioning. Given time constraints, the incubation experiments could not be repeated.

5.8 Extractable Fe^{2+}

An increase in extractable Fe^{2+} over time implies that Fe^{2+} is being removed from pore water. The likely mechanism for this is via the precipitation of iron sulphides. The variable concentrations measured for MW 27 during the 72-hour incubation period, makes a trend difficult to distinguish (Figures 4.13). During 48-hour incubation experiments conducted by Merrett (2003), solid phase Fe^{2+} concentration for sediments taken from MW 27 was shown to increase. Increasing extractable Fe^{2+} with time confirms that concomitant reduction of SO_4^{2-} and Fe^{3+} is taking place.

Apart from concentrations measured after 24 hours, precipitated Fe^{2+} appears to remain stable for the first 48 hours for MW 28 (Figures 4.14). This is unexpected, given that SO_4^{2-} reduction for the same time period is most rapid. However, given experimental problems outlined above, conclusions are difficult to make.

CHAPTER 6 - CONCLUSIONS

Geochemical data emanating from groundwater samples has shown that the contaminated plume is dominated by anaerobic conditions, as confirmed by the measured redox potentials, depleted oxygen concentrations, and elevated concentrations of reduced species of Fe^{2+} and S^{2-}. The recorded temperature and pH ranges fell within optimal ranges for anaerobic microbial activity.

The presence of Fe^{2+} and S^{2-} shows that Fe^{3+} and SO_4^{2-} reduction is occurring. The reduced levels of S^{2-} in the presence of elevated Fe^{2+}, and conversely reduced Fe^{2+} coincident with high S^{2-} concentrations, are likely the result of the precipitation of iron sulphide. This further suggests that tandem Fe^{3+} and SO_4^{2-} reduction is taking place and that the rates of reduction are variable across the site. Although results emanating from the Fe^{3+} and SO_4^{2-} incubation experiments, were inconclusive, previous work by Merrett (2003) and Roychoudhury and Merrett (in review) suggests that tandem reduction of the two species is occurring.

The results following tracer experiments showed that *in situ* sulphate reduction is taking place. Furthermore monitored sites were shown to exhibit variable SRR's. These disparities were identified to be the result of limiting sulphate concentrations. In sulphate addition experiments spiked with $^{35}SO_4^{2-}$, increases in SRR's were correlated with increasing SO_4^{2-} concentrations. From these results, Monod kinetic parameters were calculated. By comparing the half saturation constants, K_s, with *in situ* SO_4^{2-} concentrations, it was confirmed that available SO_4^{2-} concentrations are limiting growth rates at the site. Moreover, it was calculated that SO_4^{2-} concentrations of 15 Mm would be sufficient to optimize microbial growth rates.

Tracer experiments involving sulphide additions concurred with previous findings that free sulphide accumulation in sediment is detrimental to microbial activity. Sulphide additions of 0.5 mM or more were sufficient enough to reduce SRR's to below *in situ* rates.

Following the addition of organic salts of varying complexity and molecular weight, the resident SRB were observed to have developed affinities towards higher molecular weight compounds, suggesting they have developed mechanisms necessary to mineralize BTEX.

6.1 Implications of findings

The main objective of this study was to assess the capacity of sulphate addition to act as an effective bioremediation strategy in removing BTEX hydrocarbons from the contaminated aquifer.

Perusal of the literature has indicated that sulphate can serve as an excellent TEA for BTEX removal *in situ*. To recap SO_4^{2-} is highly water-soluble, has a high electron-accepting capacity for its mass, and it does not sorb appreciably. Most importantly from a stoichiometric standpoint, SO_4^{2-} is highly efficient at degrading these hydrocarbons.

This study has indicated that while it appears as though SRB's, with the mechanisms to degrade BTEX exist at the site, current SO_4^{2-} concentrations are limiting their ability to effectively mineralize these compounds. Certainly, the calculated half saturation constants would suggest that concentrations could be substantially increased to optimize growth rates which would lead to more effective biodegradation.

While free sulphide accumulation was demonstrated to reduce SRR's, it seems apparent that iron minerals form a significant component of the aquifer matrix and thus serve to act as a buffer against the highlighted problems of sulphide toxicity. Regardless of the buffering capacity, there is evidence among the literature to indicate that where iron minerals are lacking these may be supplemented through amorphous amorphous $Fe(OH)_3$ or $FeSO_4$ additions.

Based on these findings then, initial indications are that increasing SO_4^{2-} concentrations could act as an effective strategy in removing BTEX from the aquifer. Whilst the experiments conducted in this study proved useful and provided a theoretical basis for amending the contaminated plume with sulphate to expedite BTEX removal, previous work has warned against the reliance on laboratory work to accurately predict the fate of BTEX hydrocarbons. For this reason, future work into assessing the feasibility of amending this contaminated aquifer with sulphate, should include studies in the field.

REFERENCES

Akagi, J.M. (1995). Respiratory sulfate reduction, p. 89-112. *In* L.L. Barton (ed.), Sulfate-reducing bacteria. Plenum Press, New York, N.Y.

Anderson, W.C. (1995). Innovative site remediation technology. Springer-Verlag. Berlin. 288pp.

Anderson, R.T., and Lovley, D.R. (2000). Anaerobic bioremediation of benzene under sulphate-reducing conditions in a petroleum-contaminated aquifer. *Environmental Science and Technology*, **34**, 2261-2266.

Anid, P.J., Alvarez, P.J.J., and Vogel, T.M. (1994). Biodagradation of monoaromatic hydrocarbons in aquifer columns amended with hydrogen peroxide and nitrate. *Water Research*, **27**, 685-691.

Barbaro, J.R., Barker, J.F., Lemon, L.A., and Mayfield, C.I. (1992). Biotransformation of BTEX under anaerobic, denitrifying conditions: field and laboratory observations. *Journal of Contaminant Hydrology*, **11**, 245-272.

Barton, L.L., and Tomei, F.A. (1995). Characteristics and activities of sulfate-reducing bacteria, p. 1-32. *In* L.L. Barton (ed.), Sulfate-reducing bacteria. Plenum Press, New York, N.Y.

Beckman Instruments (1988) LS 5000 TD and TA Liquid scintillation systems: Operating manual. Nuclear Systems Operations, California, 201pp.

Bellar, H.R., Grbić-Galić, D., and Reinhard, M. (1992). Microbial degradation of toluene under sulfate-reducing conditions and the influence of iron in the process. *Applied and Environmental Microbiology*, **58**, 786-793.

Brezonik, P.L. (1993) Chemical kinetics and process dynamics in aquatic systems. Lewis Publishers, Florida, 754 pp.

Brown, R. (1994). Treatment of petroleum hydrocarbons in ground water by air sparging. *In* R.D., Norris, R.E., Hinchee, R., Brown, P.L., McCarty, L., Semprini, J.T., Wilson, D.H., Kampell, M., Reinhard, E.J., Bouwer, R.C., Borden, T.M.,

Vogel, J.M., Thomas, C.H., Ward (ed.). Handbook of bioremediation. CRC Press Inc, Florida.

Canfield, D.E., Raiswell, R., Westrich, J.T., Reaves, C.M., and Berner, R.A. (1986). The use of chromium reduction in the analysis of reduced inorganic sulfur in sediments and shales. *Chemical Geology*, **54**, 149-155.

Casella, S., and Payne, W.J. (1996) Potential of denitrifiers for soil environment protection. *FEMS Microbiology Letters*, **140**, 1-8.

Chapelle, F.H. (1993). Ground-water microbiology and geochemistry. John Wiley and Sons, Inc, New York, 424pp.

Chapelle, F.H., Bradley, P.M., Lovely, D.R., and Vroblesky, D.A. (1996). Measuring rates of biodegradation in a petroleum contaminated aquifer using field and laboratory methods. *Groundwater*, **34**, 691-698.

Chapelle, F.H., and Lovley, D.R. (1990). Rates of bacterial metabolism in deep coastal plain aquifers. *Applied and Environmental Microbiology*, **56**, 1865-1974.

Chapelle, F.H., and Lovley, D.R. (1990). Competitive exclusion of sulphate reduction by Fe (III)-reducing bacteria: a mechanism for producing discrete zones of high-iron ground water. *Ground Water*, **30**, 29-36.

Chaudhuri, B.K., and Wiesmann, U. (1995). Enhanced anaerobic degradation of benzene by enrichment of mixed microbial culture and optimization of the culture-medium. *Applied Microbiology and Biotechnology*, **43**, 178-187.

Cline, J.D. (1969). Spectrophotometric determination of hydrogen sulfide in natural waters. *Limnology and Oceanography*, **14**, 454-458.

Dineen, D., Slater, J.P., Hicks, P., Holland, J., and Clandening, L.D., (1993). In situ biological remediation of petroleum hydrocarbons in unsaturated soils. p. 453-463. *In* E.J. Calabrese, and P.T. Kostecki (ed.), Principles and practices for petroleum contamination, Lewis Publishers, Baco Raton.

Edwards, E.A., and Grbić-Galić, D. (1992). Complete minerlization of benzene by aquifer microorganisms under strictly anaerobic conditions. *Applied and Environmental Microbiology*, **58**, 2663-2666.

Edwards, E.A., Wills, L.E., Reinhard, M., and Grbić-Galić, D. (1992). Anaerobic degradation of toluene and xylene by aquifer microorganisms under sulfate-reducing conditions. *Applied and Environmental Microbiology*, **58**, 794-800.

Englert, C.J., Kenzie, E.J., and Dragun, J. (1993). Bioremediation of petroleum products in soil. p. 111-129. *In* E.J. Calabrese, and P.T. Kostecki (ed.), Principles and practices for petroleum contamination, Lewis Publishers, Baco Raton.

Ensley, B.D. and Suflita, J.M. (1995). Metabolism of environmental contaminants, p. 293-332. *In* L.L. Barton (ed.), Sulfate-reducing bacteria. Plenum Press, New York, N.Y.

Fauque, G.D. (1995). Ecology of sulfate-reducing bacteria, p. 217-241. *In* L.L. Barton (ed.), Sulfate-reducing bacteria. Plenum Press, New York, N.Y.

Godsey, E.M., Warren, E., Cozzarelli, I.M., Bekins, B.A., and Eganhouse, R.P. (2004). Determining BTEX biodegrdation rates using in situ microcosms at the Bemidji site, Minessota: Trials and tribulations. Unpublished paper.

Gieg, L.M., Kolhatkar, R.V., McInerney, M.J., Tanner, R.S., Harris (jnr), S.H., Sublette, K.L., and Sulfita, J.M. (1999). Intrinsic bioremediation of petroleum hydrocarbons in a gas condensate-contaminated aquifer, *Environmental Science and Technology*, **33**, 2550-2560.

Goldhaber, M.B., and Kaplan, I.R. (1975) Controls and consequences pf sulphate reduction rates in recent marine sediments. *Soil Science*, **119**, 42-45.

Haag, F., Reinhard, M., and McCarty, P.L. (1991). Degradation of toluene and *p*-xylene in anaerobic microcosms: Evidence for sulfate as a terminal electron acceptor. *Environmental Toxicology and Chemistry*, **10**, 1379-1389.

Harris, C., Oom, B.M., and Diamond, R.E. (1999). A preliminary investigation of the oxygen and hydrogen isotope hydrology of the greater Cape Town area and

an assessment of the potential for using stable isotopes and tracers. *Water S.A.*, **25**, 15-24.

Hunkeler, D., Höhener, P., Bernasconi, S., and Zeyer, J. (1999). Engineered in situ bioremediation of petroleum hydrocarbon-contaminated aquifer: assessment of minerlization based on alkalinity, inorganic carbon and stable isotope balances. *Journal of Contaminant Hydrology*, **37**, 201-223.

Johnson, S.J., Woolhouse, K.J., Prommer, H., Barry, D.A., and Christofi, N. (2003). Contribution of anaerobic microbial activity to natural attenuation of benzene in groundwater. *Engineering Geology*, **70**, 343-349.

Jørgensen, B.B. (1978). A comparison of methods for the quantification of bacterial sulphate reduction in coastal marine sediments: I. Measurement with radiotracer techniques. *Geomicrobiology Journal*, **1**,11 –27.

Kleikemper, J., Schroth, M.H., Sigler, W.V., Schmucki, M., Bernasconi, S.M., and Zeyer, J. (2002). Activity and diversity of sulfate-reducing bacteri in a petroleum hydrocarbon-contaminated aquifer. *Applied and Environmental Microbiology*, **68**, 1516-1523.

Klemps, R., Cypionka, H., Widdel, F., and Pfennig, N. (1985). Growth with hydrogen, and further physiological characteristics of *Desulfotomaculum* species, *Archeological Microbiology*, **143**, 203-208.

Kuhn, E.P., Colberg, P.J., Schnoor, J.L., Wanner, O., Zhender, A.J.B., and Schwarzenbach, R.P. (1985). Microbial transformations of substituted benzenes during infiltration of river water to groundwater: Laboratory column studies. *Applied and Environmental Microbiology*, **19**, 961-968.

Knox, R.C., Sabatini, D.A., and Canter, L.W. (1993). Subsurface transport and fate processes. Lewis Publishers, Florida, 430pp.

Leahey, J.G., and Colwell, R.R. (1990). Microbiology Review, **54**, 305-315.

Linberg, R.D., and Runnels, D.D. (1984). Ground water redox reactions: an analysis of equilibrium state applied to Eh measurements and geochemical modelling. *Science*, **225**, 925-927.

Lovley, D.R. (1997) Potential for anaerobic bioremediation of BTEX in petroleum-contaminated aquifers. *Journal of Industrial Microbiology and Biotechnology*, **6**, 75-81.

Lovley, D.R., Coates, J.D., Woodward, J.C., and Phillips, E.J.P. (1995). Benzene oxidation coupled to sulfate reduction. *Applied and Environmental Microbiology*, **61**, 953-958.

Lovely, D.R., Woodward, J.C., and Chapelle, F.H. (1994). Stimulated anoxic biodegradation of aromatic hydrocarbons using Fe(III) ligands. *Nature*, **370**, 128-131.

Madsen, E.L. (1991). Determining in situ biodegradation: Facts and Challenges. *Environmental Science and Technology*, **25**, 1663-1673.

McAllister, P.M., and Chiang, C.Y. (1994) *Ground Water Monitoring and Remediation*, **14**, 161-173.

McInerney, M.J., Bhupathiraju, V.K., and Sublette, K.L. (1992). Evaluation of a microbial method to reduce hydrogen sulfide levels in a porous rock biofilm. *Journal of Industrial Microbiology*, **11**, 53-58.

Merrett, G.L. (2003). MSc Thesis. Groundwater redox conditions at a petroleum contaminated site, Kuils River, South Africa: Pathways for BTEX biodegradation.

Meyer, P.S. (2001). An explanation of the 1:500 000 general hydrogeological map Cape Town 3317. Department of Water Affrairs and Forestry. 59pp.

Monod, J. (1949). The growth of bacterial cultures. *Annual Reviews in Microbiology*, **3**, 371-394.

Nakagawa, T., Sato, S., Yamamoto, Y., Fukui, M. (2002). Successive changes in community structure of an ethylbenzene-degrading sulfate-reducing consortium. *Water Research*, **36**, 2813-2823.

Norris, R.D., Hinchee, R.E., Brown, R., McCarty, P.L., Semprini, L., Wilson, J.T., Kampell, D.H., Reinhard, M., Bouwer, E.J., Borden, R.C., Vogel, T.M., Thomas,

J.M, Ward, C.H. (1994). The handbook of bioremediation, Lewis Publishers, Boca Raton, Florida, 257pp.

O'Flaherty, V., Mahony, T., O'Kennedy, R., and Colleran, E. (1998). Effect of pH on growth kinetics and sulphide toxicity thresholds of a range of methanogenic, syntrophic and sulphate-reducing bacteria. *Process Biochemistry*, **33**, 555-569.

Oleszkiewitcz, J.A., Marstaller, T., and McCartney, D.M. (1989). Effects of pH on sulphide toxicity to anaerobic processes. *Environmental Technology Letters*, **10**, 815-822.

Pepper, I.L., and Josephson, K.L. (1996). Biotic activity in soil and water, p.31-44. *In* I.L. Pepper, C.P. Gerber, and M.L. Brusseau (ed.) Pollution science, Academic Press, Toronto.

Phelps, C.D., and Young, L.Y. (1999). Anaerobic biodegradation of BTEX and gasoline in various aquatic sediments. *Biodegradation*, **10**, 15-25.

Phelps, C.D., Kazumi, J., and Young, L.Y. (1996). Anaerobic degradation of benzene in BTX mixtures dependent on sulfate reduction. *FEMS Microbiology Letters*, **145**, 433-437.

Rabus R., Nordhaus, R., Ludwig, W, and Widdel, F. (1993). Complete oxidation of toluene under strictly anoxic conditions by a new sulfate-reducing bacterium. *Applied and Environmental Microbiology*, **59**, 1444-1451.

Reid, D.L., Rogers, J. and Hartnady, C.J. (1998). *International Volcanological Congress, Field excursion B2: Geology of the Cape Peninsula*. Department of Geological Sciences, University of Cape Town, Rondebosch, South Africa. 51pp.

Reinhard, M., Shang, S., Kitanidis, P.K., Orwin, E., Hopkins, G.D., and Lebron, C.A. (1997). In situ BTEX transformations under enhanced nitrate- and sulfate-reducing conditions. *Environmental Science and Technology*, **31**, 28-36.

Reis, M.A.M., Almeida, J.S., Lemos, P.C., Carrondo, M.J.T. (1992). Effect of hydrogen sulfide on growth of sulfate-reducing bacteria. *Biotehcnology and Bioengeneering*, **40**, 593-600.

Rosenberg E., and Ron E.Z. (1996). *In* R.L. Crawford and D.L. Crawford (ed.), Bioremediation of petroleum contamination. Bioremediation: Principles and practises, pp. 100-124, Cambridge University Press, Cambridge.

Roychoudhury, A.N. (2004). Sulfate respiration in extreme environments: A kinetic study. *Geomicrobiology Journal*, **21**, 33-42.

Roychoudhury, A.N., and Merrett, G.L. (2004). Petroleum contamination in a shallow sandy aquifer: Redox pathways for hydrocarbon degradation. *Environmental Science and Technology* (in review).

Sarazin, G., Michard, G., and Prevot, F. (1999). A rapid and accurate spectroscopic method of alkalinity measurements in sea water samples. *Water Research*, **33**, 290-294.

SAWB (South African Weather Bureau). (1996). The weather and climate of the extreme south-western cape. Department of Environmental Affairs and Tourism, South Africa.

Stackerbrandt, E., Stahl, D.A., and Devereux, R. (1995). Taxonomic relationships p. 49-88. *In* L.L. Barton (ed.), Sulfate-reducing bacteria. Plenum Press, New York, N.Y.

Stookey, L.L. (1970). Ferrozine – a new spectrophotometric reagent for iron. *Analytical Chemistry*, **42**, 779-781.

Stumm, W., and Morgan, J.J. (1996). Aquatic chemistry. 3rd edition. John Wiley and Sons, New York. 1022pp.

Speece, R.E. (1983). Anaerobic biotechnology for industrial wastewater treatment. *Environmental Science and Technology*, **17**, 416-427.

Tabatabai, M.A. (1974). A rapid method for the determination of sulphate in water samples. *Environmental Letters*, **7**, 237-243.

Theron, J.N., Gresse, P.G., Siegfried, H.P., and Rogers, J. (1992). *The Geology of the Cape Town Area*. Geological Survey, Republic of South Africa, Government Printers.

Ulrich, G.A., Krumholz, L.R., and Suflita, J.M. (1997). A rapid and simple method for estimating sulphate reduction activity and quantifying inorganic sulfides. *Applied and Environmental Microbiology*, 63, 1627-1630.

Villatoro-Monzón, W.R., Mesta-Howard, A.M., and Razo-Flores, E. (2003). Anaerobic biodegradation of BTEX using Mn(IV) and Fe(III) as alternative electron acceptors. *Water Science and Technology*, **48**, 125-131.

Ward, C.H., Loehr, R.C., Spain, J.C., Nyer, E.K., Wilson, J.T., Piotrowski, M.R., Norris, R.D., and Thomas, J.M. (1995). *In* W.C. Anderson (ed.). Innovative site remediation technology: Bioremediation. Springer-Verlag, New York.

Weiner, J., and Lovley, D.R. (1998). Anaerobic benzene degradation in petroleum-contaminated aquifer sediments after inoculation with a benzene-oxidizing enrichment. *Applied and Environmental Microbiology*, **64**, 775-778.

Widdel, F. (1988). Microbiology and ecology of sulphate- and sulphur- reducing bacteria, p.469-585. *In* A.J.B. Zehnder (ed.), Biology of anaeriobic microorganisms. Wiley, New York.

APPENDIX A

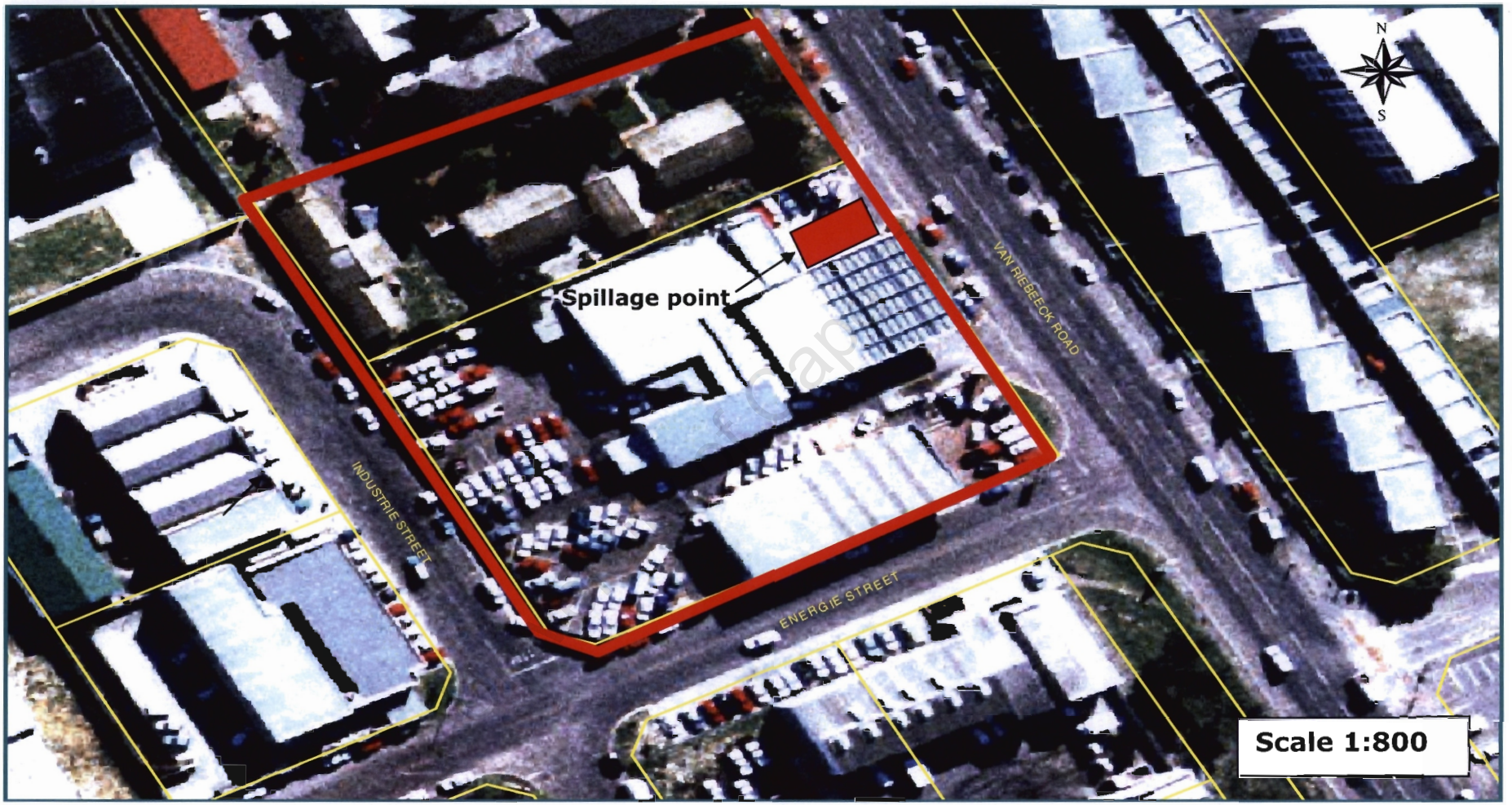

Aerial view of study area. The polygon shown represents the approximate coverage of the contaminated area. The solid rectangle depicts the approximate position of the spillage point. (Plan published with permission of Kantey & Templer Consulting Engineers).

APPENDIX B

Table B1: Results of groundwater parameters as measured in the field

Borehole	pH	EC (µs/cm)	Temperature (°C)	Eh (mV)	DO (%)	DO (mg/l)	Salinity	Alkalinity (mM)	SO_4^{2-} (µM)	S^{2-} (µM)	Fe^{2+} (µM)
4	6.7	1289	19.4	-135	4.1	0.39	0.6	12.7	116	0.7	2171
6	6.8	1270	22.0	-128	9.9	0.88	0.6	9.5	144	0.8	1024
7	6.7	1210	18.6	-108	7.8	0.71	0.5	11.1	398	1.6	890
8	6.7	1160	18.3	-98	9.5	0.88	0.5	10.9	337	1.6	378
13	6.8	1177	20.7	-117	16.3	1.46	0.5	6.9	133	1.4	389
14	6.8	1140	17.5	-85	9.5	0.9	0.5	9.7	179	1.7	362
19	6.7	1272	19.5	-172	5.1	0.47	0.6	4.4	1107	27.2	7
20	6.7	1285	19.5	-105	11.4	1.04	0.6	7.1	772	2.0	269
21	7.0	1432	19.8	-133	8.4	0.75	0.7	10.3	982	1.3	433
22	6.7	1096	21.0	-191	4.8	0.43	0.5	7.1	263	3.0	330
23	6.6	991	20.6	-119	8.4	0.75	0.4	8	697	3.0	527
24	6.7	1039	21.2	-302	9.9	0.89	0.5	8.1	342	3.8	280
25	6.9	1498	21.9	-299	0.1	0	0.7	9	1025	25.5	16
26	6.8	1426	21.3	-247	8	0.68	0.7	9.4	835	60.2	12
27	7.2	2160	20.0	-195	0.5	0.06	0.8	9.3	2825	18.4	4
28	7.1	1622	20.3	-292	3.5	0.3	1.1	12.1	122	1.0	749
30	6.8	1031	19.3	-277	1.3	0.08	0.5	7.2	127	18.4	11
31	6.8	1597	19.1	-269	3	0.26	0.8	9.5	125	32.0	31
32	6.8	1155	19.9	-138	10.7	0.98	0.5	9.5	267	2.0	537
34	6.6	1328	20.8	-113	12.6	1.13	0.6	8	913	1.9	1258
35 [a]	7.1	288	19.9	2	35.1	3.19	0	1.2	203	0.2	3
36	6.7	817	17.9	-85	13.3	1.09	0.3	7.3	103	1.9	544
37	6.6	1232	19.2	-57	11	1.07	0.6	7.4	371	1.0	117
38	6.8	1033	19.5	-130	9.3	0.86	0.5	8.3	223	2.0	315
39	6.9	1417	19.1	-153	10.9	1	0.7	10.9	313	10.0	75
40	6.9	1397	18.4	-243	8.7	0.84	0.7	9.4	521	19.2	6

Table B1 continued...

Borehole	pH	EC (µs/cm)	Temperature (°C)	Eh (mV)	DO (%)	DO (mg/l)	Salinity	Alkalinity (mM)	SO_4^{2-} (µM)	S^{2-} (µM)	Fe^{2+} (µM)
41	6.6	854	17.6	-62	18.6	1.95	0.4	6.6	97	0.5	547
44	6.8	1240	18.5	-207	9.8	0.95	0.6	5.8	809	4.0	138
45	6.7	1471	19.0	-246	7.2	0.66	0.7	9.6	123	10.9	33
48 [b]	7.1	1182	19.9	150	24.3	2.23	0.5	9.2	934	0.1	0
49 [b]	7.0	911	18.1	209	21.7	2.03	0.4	7.8	702	0.2	0
50 [b]	7.1	925	19	132	11.3	1.15	0.4	7.6	681	0.3	0

[a] Data excluded from results as it was thought that this monitoring well may exhibit backrground groundwater properties
[b] Background samples

Table B2: *In situ* sulphate reduction rates for MW 19, MW 24, MW 27, and MW 28

Sample	Vial Weigh t (g)	Vial/Sample Weight (g)	Sediment Incubated (g)	Sediment Distilled (g)	SO_4^{2-} Concentration (μmol/ml)	CPM Distillate	CPM Supernatant	SRR (nmol.cm^{-3}.d^{-1})	Average SRR (nmol.cm^{-3}.d^{-1})
19 (a)	6.918	15.154	8.236	1.028	799.000	151.000	26580.000	2095	
19 (b)	6.855	15.544	8.689	1.009	799.000	91.000	22060.000	1635	1950
19 (c)	6.892	14.968	8.076	1.014	799.000	145.000	25075.000	2119	
24 (a)	6.877	14.879	8.002	1.014	103.000	220.000	34803.330	296	
24 (b)	6.940	13.966	7.026	1.023	103.000	135.000	33573.330	164	233
24 (c)	6.901	14.928	8.027	1.030	103.000	173.000	33613.330	238	
27 (a)	6.886	14.737	7.851	1.009	2352.000	45.000	33850.000	1401	
27 (b)	6.861	14.168	7.307	1.018	2352.000	123.000	27087.000	4415	6360
27 (c)	6.890	15.193	8.303	1.008	2352.000	328.000	27590.000	13264	
28 (a)	6.891	15.317	8.426	1.029	127.000	41.000	30560.000	80	
28 (b)	6.894	14.879	7.985	1.011	127.000	116.000	52005.000	129	116
28 (c)	6.873	15.338	8.465	1.016	127.000	44.000	19452.730	138	

Table B3: ^{35}S Radiotracer experiment data following sulphate amendments for MW27

Sample	Vial Weight (g)	Vial/Sample Weight (g)	Sediment Incubated (g)	Sediment Distilled (g)	SO_4^{2-} Concentration (μmol/ml	CPM Distillate	CPM Supernatant	SRR (nmol.cm^{-3}.d^{-1})	Average SRR (nmol.cm^{-3}.d^{-1})
Control (a)	6.958	16.737	9.780	1.021	0.000	319.000	22631.110	0	
Control (b)	6.941	17.948	11.007	1.063	0.000	0.000	0.000	0	0
Control (c)	6.925	17.347	10.423	1.015	0.000	207.000	21934.000	0	
100 (a)	6.885	16.711	9.826	1.034	100.000	151.000	21898.000	377	
100 (b)	6.888	15.898	9.010	1.025	100.000	185.000	22222.220	421	316
100 (c)	6.852	15.806	8.954	1.015	100.000	80.000	27312.500	149	
250 (a)	6.861	15.597	8.736	1.026	250.000	143.000	27747.500	632	
250 (b)	6.881	15.992	9.111	1.023	250.000	115.000	17301.670	852	693
250 (c)	6.852	14.613	7.761	1.020	250.000	130.000	23973.330	594	
500 (a)	6.898	16.172	9.274	1.003	500.000	137.000	26157.500	1394	
500 (b)	6.883	15.897	9.014	1.029	500.000	86.000	30648.570	708	1333
500 (c)	6.845	16.015	9.170	1.012	500.000	146.000	20090.000	1896	
1 (a)	6.894	15.961	9.067	1.024	1000.000	172.000	26875.000	3263	
1 (b)	6.876	16.217	9.341	1.010	1000.000	142.000	23664.440	3196	3023
1 (c)	6.916	16.526	9.610	1.003	1000.000	93.000	19667.270	2609	
3 (a)	6.900	15.646	8.746	1.035	2000.000	137.000	31425.710	4243	
3 (b)	6.877	16.383	9.506	1.017	2000.000	93.000	28035.000	3571	3907[a]
3 (c)	6.868	15.679	8.811	1.010	2000.000	0.000	0.000	0.000	
5 (a)	6.882	16.412	9.530	1.014	5000.000	86.000	22928.890	10150	
5 (b)	6.859	16.493	9.634	1.019	5000.000	210.000	25695.000	22249	16025
5 (c)	6.868	15.530	8.662	1.031	5000.000	143.000	22070.000	15675	

Table B3 continued...

Sample	Vial Weight (g)	Vial/Sample Weight (g)	Sediment Incubated (g)	Sediment Distilled (g)	Concentration (μmol/ml)	CPM Distillate	CPM Supernatant	SRR (nmol.cm^{-3}.d^{-1})	Average SRR (nmol.cm^{-3}.d^{-1})
10 (a)	6.835	15.600	8.765	1.012	10000.000	100.000	26682.500	18693	
10 (b)	6.878	16.043	9.165	1.005	10000.000	111.000	29214.290	19954	36993
10 (c)	6.893	15.470	8.577	1.005	10000.000	307.000	20860.000	72332	
15 (a)	6.896	16.766	9.870	1.023	15000.000	242.000	22935.550	87937	
15 (b)	6.891	15.194	8.303	1.001	15000.000	128.000	21940.000	41802	57215
15 (c)	6.894	15.724	8.830	1.005	15000.000	101.000	18292.730	41905	
20 (a)	6.852	15.659	8.807	1.027	20000.000	119.000	21080.000	55757	
20 (b)	6.859	15.924	9.065	1.015	20000.000	170.000	19018.180	91949	82760
20 (c)	6.858	16.292	9.434	1.022	20000.000	195.000	20614.000	100573	
28 (a)	6.884	16.088	9.204	1.016	28000.000	173.000	26942.500	93796	
28 (b)	6.870	16.465	9.595	1.006	28000.000	237.000	30085.710	121151	95482
28 (c)	6.900	16.506	9.606	1.015	28000.000	134.000	28600.000	71500	

[a] Sample excluded from SRR calculation dues to cracked vial following centrifuge.

Table B4: ^{35}S Radiotracer experiment data following sulphate amendments for MW 28

Sample	Vial Weight (g)	Vial/Sample Weight (g)	Sediment Incubated (g)	Sediment Distilled (g)	SO_4^{2-} Concentration (µmol/ml	CPM Distillate	CPM Supernatant	SRR (nmol.cm^{-3}.d^{-1})	Average SRR (nmol.cm^{-3}.d^{-1})
Control (a)	6.905	14.698	7.793	1.002	0.000	666.000	32920.000	0	
Control (b)	6.891	15.144	8.253	1.044	0.000	91.000	1830.000	0	0
Control (c)	6.905	16.010	9.105	1.014	0.000	935.000	21502.000	0	
100 (a)	6.846	15.749	8.903	1.016	100.000	887.000	33520.000	1335	
100 (b)	6.888	15.269	8.381	1.022	100.000	954.000	30985.710	1454	1447
100 (c)	6.856	15.112	8.256	1.036	100.000	133.000	3934.000	1552	
250 (a)	6.874	15.644	8.770	1.019	250.000	570.000	27790.000	2541	
250 (b)	6.874	15.611	8.737	1.001	250.000	756.000	24546.670	3870	2968
250 (c)	6.879	15.294	8.415	1.007	250.000	676.000	32625.710	2493	
500 (a)	6.865	15.977	9.112	1.037	500.000	546.000	26680.000	5178	
500 (b)	6.900	15.805	8.905	1.014	500.000	482.000	13344.000	9134	6503
500 (c)	6.881	15.456	8.575	1.035	500.000	737.000	33823.330	5198	
1 (a)	6.847	15.929	9.082	1.005	1000.000	113.000	1837.000	32012	
1 (b)	6.888	16.015	9.127	1.033	1000.000	3065.000	30208.570	51625	43871
1 (c)	6.848	15.765	8.917	1.001	1000.000	2088.000	22326.670	47976	
3 (a)	6.893	15.266	8.373	1.006	2000.000	474.000	27207.500	16701	
3 (b)	6.849	15.036	8.187	1.032	2000.000	227.000	34026.660	6096	12379
3 (c)	6.855	15.047	8.192	1.017	2000.000	408.000	26395.000	14341	
5 (a)	6.887	15.458	8.571	1.006	5000.000	305.000	19812.730	37765	
5 (b)	6.867	15.681	8.814	1.030	5000.000	154.000	7015.000	54092	39976
5 (c)	6.899	15.230	8.331	1.021	5000.000	421.000	35237.330	28071	

Table B4: continued…

Sample	Vial Weight (g)	Vial/Sample Weight (g)	Sediment Incubated (g)	Sediment Distilled (g)	Concentration (μmol/ml)	CPM Distillate	CPM Supernatant	SRR (nmol.cm^{-3}.d^{-1})	Average SRR (nmol.cm^{-3}.d^{-1})
10 (a)	6.867	16.909	10.042	1.033	10000.000	508.000	32757.140	86819	
10 (b)	6.891	15.368	8.477	1.015	10000.000	323.000	26962.500	57617	55467
10 (c)	6.901	16.341	9.440	1.014	10000.000	110.000	26850.000	21964	
15 (a)	6.876	15.363	8.487	1.028	15000.000	304.000	27790.000	78014	
15 (b)	6.851	15.275	8.424	1.024	15000.000	332.000	31262.860	75466	84347
15 (c)	6.879	16.318	9.439	1.001	15000.000	306.000	25035.000	99562	
20 (a)	6.896	16.662	9.766	1.019	20000.000	388.000	26555.000	161284	
20 (b)	6.838	16.027	9.189	1.021	20000.000	146.000	35003.330	43237	35579
20 (c)	6.879	14.977	8.098	1.027	20000.000	111.000	36103.330	27922	
28 (a)	6.905	15.810	8.905	1.033	28000.000	319.000	34620.000	128083	
28 (b)	6.890	15.263	8.373	1.040	28000.000	41.000	30440.000	17486	36103
28 (c)	6.881	16.141	9.260	1.003	28000.000	78.000	32162.860	36103	

Table B5: ^{35}S Radio tracer experiment data following sulphide amendments for MW 27

Sample	Vial Weight (g)	Vial/Sample Weight (g)	Sediment Incubated (g)	Sediment Distilled (g)	SO_4^{2-} Concentration (µmol/ml)	CPM Distillate	CPM Supernatant	SRR (nmol.cm^{-3}.d^{-1})	Average SRR (nmol.cm^{-3}.d^{-1})
Control (a)	6.899	16.000	9.101	1.010	2484.000	167.000	45496.000	4730	
Control (b)	6.973	16.000	9.027	1.011	2484.000	145.000	45824.000	4042	4511
Control (c)	6.969	16.000	9.031	1.011	2484.000	135.000	36233.330	4759	
Insitu (a)	6.977	16.655	9.678	1.013	2484.000	282.000	43144.000	8933	
Insitu (b)	6.664	15.420	8.756	1.017	2484.000	566.000	44232.000	15760	11836
Insitu (c)	6.993	15.487	8.494	1.019	2484.000	378.000	41680.000	10814	
500 (a)	6.929	15.643	8.714	1.035	2484.000	22.000	42056.000	630	
500 (b)	6.950	15.655	8.705	1.032	2484.000	47.000	37073.330	1530	8019
500 (c)	6.951	16.035	9.084	1.034	2484.000	259.000	40592.000	8019	
1 (a)	6.821	16.185	9.364	1.005	2484.000	383.000	40660.000	12555	
1 (b)	6.932	16.097	9.165	1.026	2484.000	295.000	40908.000	9215	8992
1 (c)	6.828	16.185	9.357	1.006	2484.000	148.000	37823.330	5206	
3 (a)[a]	6.961	16.032	9.071	1.022	2484.000	31.000	16.000	2459984	
3 (b)	6.944	15.981	9.037	1.003	2484.000	174.000	21926.000	10228	9661
3 (c)	6.620	15.879	9.259	1.011	2484.000	314.000	45236.000	9094	
5 (a)	6.908	16.369	9.461	1.025	2484.000	287.000	36260.000	10451	
5 (b)	6.970	16.919	9.949	1.037	2484.000	206.000	39650.000	7130	8779
5 (c)	7.004	15.912	8.908	1.007	2484.000	57.000	8237.000	8757	
10 (a)	6.999	16.650	9.651	1.010	2484.000	56.000	6414.000	11934	
10 (b)	6.941	15.907	8.966	1.008	2484.000	159.000	39573.000	5112	8318
10 (c)	6.917	16.072	9.155	1.022	2484.000	272.000	44072.000	7909	

[a] Sample excluded from SRR calculation dues to anomalous CPM count

Note: *Insitu* as well as sulphide amendment SRR's as reported in the text are values calculated by subtracting the mean SRR calculated for the control (4,511nmol.cm^{-3}.d^{-1})

Table B6: ^{35}S Radio tracer experiment data following organic salt additions for MW 27

Sample	Vial Weight (g)	Vial/Sample Weight (g)	Sediment Incubated (g)	Sediment Distilled (g)	SO_4^{2-} Concentration (µmol/ml)	CPM Distillate	CPM Supernatant	SRR (nmol.cm^{-3}.d^{-1})	Average SRR (nmol.cm^{-3}.d^{-1})
Control (a)	6.899	15.682	8.783	1.010	2484.000	167.000	45496.000	4565	
Control (b)	6.973	16.120	9.147	1.011	2484.000	145.000	45824.000	4096	4484
Control (c)	6.969	16.058	9.089	1.011	2484.000	135.000	36233.330	4790	
Insitu (a)	6.977	16.655	9.678	1.013	2484.000	282.000	43144.000	8933	
Insitu (b)	6.664	15.420	8.756	1.017	2484.000	566.000	44232.000	15760	11836
Insitu (c)	6.993	15.487	8.494	1.019	2484.000	378.000	41680.000	10814	
Lactate (a)	7.002	16.184	9.182	1.008	2484.000	441.000	40880.000	14057	
Lactate (b)	6.656	15.854	9.198	1.009	2484.000	391.000	34333.330	14851	14623
Lactate (c)	6.914	16.187	9.273	1.008	2484.000	285.000	25068.890	14961	
Formate (a)	6.973	15.782	8.809	1.003	2484.000	0	0	0	
Formate (b)	6.969	15.453	8.484	1.008	2484.000	286.000	34693.330	9925	9988 [a]
Formate (c)	6.913	15.631	8.718	1.018	2484.000	319.000	38883.330	10050	
Acetate (a)	6.969	16.807	9.838	1.011	2484.000	352.000	40356.000	12142	
Acetate (b)	6.907	16.180	9.273	1.001	2484.000	274.000	41284.000	8795	10468
Acetate (c)[b]	6.889	15.372	8.483	1.015	2484.000	32.000	40932.000	935	

[a] Sample excluded from SRR calculation due to cracked vial following centrifuge

[b] Low CPM distillate counts may not truly reflect the SRR

Note: *Insitu* as well as organic acid SRR's as reported in the text are values calculated by subtracting the mean SRR calculated for the control (4,484 nmol.cm^{-3}.d^{-1})

Table B7: Solid phase Fe^{2+} concentrations calculated for samples 27-A during the 72-hour incubation period

Time (Hours)	Vial/Sample Weight (g)	Vial Weight (g)	Sample Weight (g)	Volume (cm^{-3})	Concentration ($\mu mol.l^{-1}$)	Concentration ($nmol.cm^{-3}$) [a]
0	121.47	14.51	106.96	50.93	501	9832
1	120.34	13.88	106.46	50.70	512	10101
3	121.69	14.55	107.14	51.02	542	10626
6	123.56	14.38	109.18	51.99	518	9958
12	123.93	14.64	109.29	52.04	683	13127
24	126.06	12.27	113.79	54.19	676	12469
48	121.43	14.54	106.89	50.90	570	11206
72	128.49	12.99	115.50	55.00	726	13208

[a] Concentrations reported as $nM.cm^{-3}$ based on a calculated density of 2.1 $g.cm^{-3}$ (Merrett, 2003)

Table B8: Solid phase $Fe2^{+}$ concentrations calculated for samples 27-B during the 72-hour incubation period

Time (Hours)	Vial/Sample Weight (g)	Vial Weight (g)	Sample Weight (g)	Volume (cm^{-3})	Concentration ($\mu M.l^{-1}$)	Concentration ($nM.cm^{-3}$) [a]
0	124.06	13.53	110.53	52.63	518	9836
1	122.36	13.92	108.44	51.64	520	10062
3	123.32	14.56	108.76	51.79	721	13917
6	125.73	13.56	112.17	53.41	529	9904
12	123.64	14.54	109.10	51.95	529	10182
24	130.13	12.82	117.31	55.86	525	9402
48	125.13	12.30	112.83	53.73	540	10056
72	125.61	13.94	111.67	53.17	593	11150

[a] Concentrations reported as $nM.cm^{-3}$ based on a calculated density of 2.1 $g.cm^{-3}$ (Merrett, 2003)

Table B9: Solid phase Fe^{2+} concentrations calculated for samples 28-A during the 72-hour incubation period

Time (Hours)	Vial/Sample Weight (g)	Vial Weight (g)	Sample Weight (g)	Volume (cm^{-3})	Concentration ($\mu mol.l^{-1}$)	Concentration ($nmol.cm^{-3}$) [a]
0	127.28	12.79	114.49	54.52	439	8048
1	123.12	14.45	108.67	51.75	416	8042
3	127.30	12.90	114.40	54.48	426	7812
6[b]	0.00	0.00	0.00	0.00	0.00	0.00
12	123.88	14.43	109.45	52.12	437	8382
24	125.11	13.48	111.63	53.16	493	9279
48	121.69	14.57	107.12	51.01	452	8859
72	124.12	14.78	109.34	52.07	443	8499

[a] Concentrations reported as $nM.cm^{-3}$ based on a calculated density of 2.1 $g.cm^{-3}$ (Merrett, 2003)
[b] Sample excluded from calculation due to cracked vial following centrifuge

Table B10: Solid phase $Fe2^{+}$ concentrations calculated for samples 28-B during the 72-hour incubation period

Time (Hours)	Vial/Sample Weight (g)	Vial Weight (g)	Sample Weight (g)	Volume (cm^{-3})	Concentration ($\mu M.l^{-1}$)	Concentration ($nM.cm^{-3}$) [a]
0	127.33	12.22	115.11	54.81	456	8313
1	128.44	12.76	115.68	55.08	458	8306
3	121.69	14.55	107.14	51.02	458	8968
6[b]	0.00	0.00	0.00	0.00	0.00	0.00
12	125.06	14.40	110.66	52.69	424	8041
24[c]	0.00	0.00	0.00	0.00	0.00	0.00
48	123.35	14.48	108.87	51.84	395	7629
72	123.80	14.40	109.40	52.10	572	10984

[a] Concentrations reported as $nM.cm^{-3}$ based on a calculated density of 2.1 $g.cm^{-3}$ (Merrett, 2003)
[b] Sample excluded from calculation due to cracked vial following centrifuge
[c] Sample excluded from calculation due to cracked vial following centrifuge

Table B11: Pore water Fe^{2+} concentrations calculated for 72-hour incubation experiments

Time (Hours)	27-A	27-B	Average 27	28-A	28-B	Average 28
0	290	493	392	1144	719	931
1	600	463	532	5072	2202	3637
3	1604	1110	1357	1960	2821	2390
6	550	1533	1041	*	*	*
12	958	617	788	1952	4590	3271
24	582	668	625	5177	3849	4513
48	1828	1277	1553	5771	1289	3530
72	976	1351	1164	5867	5884	5875

All pore water Fe^{2+} concentrations reported as $\mu M.l^{-1}$
* Concentration could not be determined as vial cracked during centrifuge

Table B12: Pore water SO_4^{2-} concentrations calculated for 72-hour incubation experiments

Time (Hours)	27-A	27-B	Average 27	28-A	28-B	Average 28
0	2616	2830	2723	4296	4373	4335
1	2907	2677	2792	2952	3716	3334
3	2525	2708	2616	4235	3792	4014
6	2586	2509	2547	*	*	*
12	2082	2341	2211	2051	1975	2013
24	2250	2204	2227	875	799	837
48	2036	2143	2089	539	600	570
72	1776	1914	1845	539	478	509

All pore water SO_4^{2-} concentrations reported as $\mu M.l^{-1}$
* Concentration could not be determined as vial cracked during centrifuge

APPENDIX C

Table C1: BTEX concentrations measured using the purge and trap method. Published with permission of Kantey & Templer Consulting Engineers.

Borehole	Benzene	Toulene	Ethylbenzene	Xylenes
MW 4	12354	29091	3326	18832
MW 6	16223	29303	2415	15623
MW 7	2612	11464	2611	8276
MW 8	6214	14590	1205	4068
MW 13	2815	3679	154	1660
MW 14	4490	20449	2250	7960
MW 19	22	10	2	1
MW 20	3444	20752	847	7156
MW 21	1851	4206	565	5527
MW 22	6167	27322	1334	6870
MW 23	2441	6563	354	1992
MW 24	13010	27807	1011	11300
MW 25	6160	29162	2130	11198
MW 26	7715	17522	1293	4254
MW 27	7	15	2	7
MW 28	8242	16360	1523	8347
MW 30	4	3	BDL	1
MW 32	3329	29322	1181	11165
MW 36	BDL	3	BDL	1
MW 37	6081	5610	49	4211
MW 38	7346	25218	2310	8027
MW 39	4556	2540	24	2810
MW 40	3038	25374	2639	10055

Concentrations reported as $\mu g.l^{-1}$
BDL – below detection limit of $1\mu g.l^{-1}$